Carbon based conductive thin film : fabrication, properties and application

Tantang, Hosea

2011

Tantang, H. (2011). Carbon based conductive thin film : fabrication, properties and application. Doctoral thesis, Nanyang Technological University, Singapore.

https://hdl.handle.net/10356/48043

https://doi.org/10.32657/10356/48043

NANYANG TECHNOLOGICAL UNIVERSITY

SCHOOL OF MATERIALS SCIENCE & ENGINEERING

Carbon Based Conductive Thin Film:

Fabrication, Properties and Application

A thesis submitted to Nanyang Technological University in fulfilment of the requirement for the degree of Doctor of Philosophy of Materials Science and Engineering

By

Hosea Tantang

G0602400C

2011

Abstract

Transparent conductors are increasingly becoming important components in electronic devices due to the growing demand for devices such as LED, LCD, and touch screens. In particular, the common transparent conductor, Indium tin oxide (ITO), has become increasingly expensive due to limited supplies of the raw material, thus creating the need for an alternative to this material. Carbon nanotubes (CNT) were thoroughly studied in this research to determine if they could be the replacement material for ITO.

In this research, two types of sample were used: CNT solution and CNT thin films. Three kinds of material property were investigated from the samples: electrical (conductivity), optical (raman spectra or UV-vis absorption spectra) and physical properties (morphology).

The first investigation was dedicated to optimization of transparent conductive film fabrication method. The focus of the first investigation were on feedstock quality, composition formula, deposition methods and solutions properties. Afterwards, a study of the correlation between electrical property and optical property was carried out. Out of several reported mathematical models that could describe the correlation between conductivity and transmittance of conductive films, one model, namely the thin metallic film model was verified to be a suitable mathematical model for CNT films. That model could describe the behavior of CNT films well except in certain conditions where semiconducting nanotubes content in solution exceeds 90 %. Apart from that, a study on the effects of different metallic and semiconducting nanotube mixture was also presented, as it was believed previously that metallic semiconducting junctions are the crucial factor in CNT films, although our results proved otherwise.

The next topic of investigation was on how to improve carbon nanotube films conductivity through doping, as the present state of carbon nanotube film conductivity is still far inferior compared to Indium Tin Oxide (ITO). A new doping mechanism and new doping agents were presented in this research. Acid treatment of carbon nanotubes, which was previously thought to be a chemical attachment or surfactant removal, proved to be a proton attachment instead. With that argument, a new dopant, the piranha mixture, was found to be a stronger dopant.

Finally, after studying the film fabrication, investigating the film physics, improving the conductivity of CNT films by doping, and obtaining a highly conductive carbon nanotube films, these films were tested by some simple devices. Dye Sensitize Solar Cell (DSSC) with carbon nanotube electrodes was made and a decent performance of ~1-2% efficiency was obtained. Although the result was still lower than 3-4 % efficiency from FTO/Pt electrodes it showed that integration into these devices was not a problem. Similarly, all CNT transistors made of CNT electrodes and channels showed that the device is in proper operation with 2.5 order of on/off ratio and mobility of ~1, even though its mobility is still lower than the conventional device. These preliminary results open new possibilities for using CNT in various optoelectronic devices.

Acknowledgement

It has been a long and tough journey. This thesis would not have been produced if not for these special people who have supported me right from the start of my candidature. From the bottom of my heart, I would like to sincerely thank the following people for their support and encouragement.

First and foremost, I would like to thank Asst. Prof. Li Lain Jong and Asst. Prof. Zhang Qichun , my supervisor of this project for believing in me and giving me this rare opportunity to further my studies. Their invaluable advices, encouragements and support have kept me going until I reached the finish line. This experience has nurtured me to be more mature and better person, ready to face future challenges.

Secondly, I would like to thank Prof. Mary Chan, Dr. Wei Jun, Aung Ko Ko Kyaw for the valuable collaboration, advices and financial support throughout the project. I really appreciate the collaboration that has been performed throughout my PhD study.

Thirdly, I would like to thank Dr. Chan Soon Keng and Mr. Chang Tsung Han, Damian for the enormous help in grammar and language structure revision of my thesis.

I would also take this opportunity to thank my family, my mother especially who encouraged me to further my study. Their love and support has kept me going through the ups and downs in my life.

There are many occasions that I felt like giving up but the support that I got from these special people gave me renewed strength to carry on till the end : Dr Yudi Setiawan, Dr. Johnson Kasim, Dr. Peter Darmawan, Dr. Lee Chun Wei, Dr. Shi Yumeng, Dr. Dong Xiaochen, Han Xuanding, Hendro Mario, Fu Dongliang, Chen Fuming, Donny Lai, Steve Ong Hock Guan, Dalton Tay Chor Yong, Xu Yanping and many others. Thank you for your encouragement, support and most importantly for your priceless friendship.

Last but not least, I would like to extend my gratitude to all staff in the School of Materials Science and Engineering for their assistance and technical support in the use of various equipment.

This work is dedicated to all of you. Thank you so much.

Table of Contents

List of Figures

List of Tables

Publication List

1. **H. Tantang**, A. K. K. Kyaw, Y. Zhao, M. B. Chan-Park, A. I .Y. Tok, Z. Hu, L. J. Li, X. W. Sun, Q. Zhang
   Nitrogen-Doped Carbon Nanotube-based Bilayer Thin-Film as Transparent Counter Electrode for Dye Sensitized Solar Cell (DSSC),
   Chem. Asian J. 2011 (accepted)

2. **H. Tantang** , J. Wei, J. Xiao, Q. Zhang, M. B. Chan-Park, and L. J. Li, Low Cost and Ultra Strong p-type Dopant for Carbon Nanotube Transparent Conductive Films.
   Eur.J.Inorg. Chem **2011**, 4182 (2011)

3. **H. Tantang** , E.S. Ang, J. Wei, M. B. E. Chan, Q. Zhang, and L. J. Li, Stable and Reversible Solid State Protonation Effect on Carbon Nanotube Transparent Conductive Film.
   (2011- Submitted to Thin Solid Films)

4. **H. Tantang** , J. Wei (2010), Stabilization Effect of Surfactant and Functional group on Highly Concentrated Carbon Nanotube Conductive Ink.
   Proceedings of The ASME 2010 International Mechanical Engineers Congress and Exposition 38562 (2010).

5. **H. Tantang**, J.Y. Ong, C.L. Loh, X. Dong, P. Chen, Y. Chen, X. Hu, L.P. Tan and L. J. Li, Using oxidation to increase the electrical conductivity of carbon nanotube electrodes
   Carbon **47**, 1867 (2009)

Co-authored Publication

6. A. K. K. Kyaw, **H. Tantang**, T. Wu[2], L. Ke, C. Peh, Z. H. Huang, X. T. Zeng, H. V. Demir, Qichun. Zhang and X. W. Sun
   Dye-Sensitized Solar Cell with a Titanium Oxide Modified Carbon Nanotube Transparent Electrode
   Appl. Phys. Lett. **99**, 021107 (2011)

7. H. G. Ong, J. W. Cheah, X. Zou, B. Li, X. H. Cao, **H. Tantang**, L-J Li, H. Zhang, G. C. Han and J. Wang
   Origin of hystteresis in the transfer characteristic of carbon nanotube transistor
   Journal of Physics D : Applied Physics **44**, 285301 (2011)

8. Y.-Y. Lee, S.-H. Goh, Karen S. L. Chong, C.-L. Hee, Andrew M. H. Ng, Y. Xu, H. Tantang, C.-Y. Su, L.-J. Li, M. V. Kunnavakkam
   Scalable, Nanoimprint Patterning of Thin Graphitic Oxide Sheets and In-Sito Reduction
   J. Vac. Sci. Technol. B **29 (1)**, 011023-1-5 (2011)

9. C. Y. Tay, H. Gu, W. S. Leong, H. Yu, H. Q. Li, B. C. Heng, **H. Tantang**, S. C. J. Loo, L-J. Li and L. P. Tan, Cellular behavior of human mesenchymal stem cells cultured on single-walled carbon nanotube film
   Carbon **48**, 1095 (2010)

10. Y.M. Shi, X. Dong, **H. Tantang**, F. Chen, C.W. Lee, K. Zhang, Y. Chen, J.L. Wang, and L. J. L , Photoconductivity from Carbon Nanotube Transistors Activated by Photosensitive Polymers
    J. Phys. Chem. C **112**, 18201 (2008)

11. H.G. Ong, J. Cheah, L. Chen, **H. Tantang**, Y.P. Xu, B. Li, H. Zhang, L.-J. Li and J. Wang. Charge Injection at Carbon Nanotube-SiO2 Interface
Appl. Phys. Lett. **93**, 093509 (2008)

12. Y. Shi , **H. Tantang** , C. W. Lee , C-H Weng , X. Dong, L. J. Li, P. Chen Effects of Substrates on Photocurrents from Photosensitive Polymer Coated Carbon Nanotube Networks
Appl. Phys Lett. **92**, 113310 (2008*)*

13. B. Li, C. F. Goh, X. Zhou, G. Lu, **H. Tantang**, Y. Chen, C. Xue, F. Y. C. Boey, H. Zhang Patterning Colloidal Metal Nanoparticles for Controlled Growth of Carbon Nanotubes
Adv. Mater. **20**, 4873, (2008).

14. C. W. Lee , K. Zhang, **H. Tantang**, A. Lohani, T. Nagahiro, K. Tamada, Y. Chen, S. G. Mhaisalkar, L. J. Li
Tuning of Electrical Characteristics in Networked Carbon Nanotube Field-Effect Transistors Using Thiolated Molecules
Appl. Phys. Lett. **91**, 103515 (2007)

Conferences

1. **H. Tantang**, S. Lim ,J. Y. Ong, C. L. Loh, L.-J. Li
Simple solution based method for the making of carbon nanotube transparent electrodes for ITO replacement
Asia Nano 2008 Conferences, 3-7 November 2008, Singapore – poster presentation

2. **H. Tantang**, J.Y. Ong, J. Wei, L.J. Li
Conductivity enhancement of carbon nanotube networks thin film by means of oxidation
International Conference on Materials for Advanced Technology, 28 June – 3 July 2009, Singapore - presented orally on 30 june 2009 -Symposium J : Nanodevices and Nanofabrication.

3. **H. Tantang**, S. Lim, J.Y. Ong, J. Wei, L. J. Li
Low Cost and Scalable Fabrication of High Conductivity Carbon Nanotube Electrodes with Various Transparencies
ASME 2009 International Mechanical Engineering Congress and Exposition, 13-19 November 2009, Lake Buena Vista, Florida, USA – presented orally on 16 November 2009

4. **H. Tantang,** J. Wei
Stabilization Effect of Surfactant and Functional group on Highly Concentrated Carbon Nanotube Conductive Ink
ASME 2010 International Mechanical Engineering Congress and Exposition, 12-18 November 2010, Vancouver, British Columbia, Canada – presented orally on 16 November 2010

CHAPTER 1 – INTRODUCTION

1.1 Transparent Conductor in Optoelectronic Devices

Transparent conductors over the years have gained importance in optoelectronic devices, as they are commonly used for electrodes in flat panel displays such as liquid crystal displays (LCDs), plasma display panels, electronic paper displays and organic light-emitting-diodes (OLEDs), thin-film solar cells, and touch panels. [1-7]

At present, most transparent electrodes are made of indium-tin-oxide (ITO) prepared by magnetron sputtering deposition and the indium used in ITO for LCDs constitutes the largest use of this material, which is approximately 80% of the total amount [8]. The consumption of indium is not just limited to the expanding market of ITO used in the transparent electrode applications. There is also increasing use of the material in $CuInGaSe_2$ thin-film solar cells significantly in recent years[9]. As a result, there are serious problems associated with the huge demand for indium, especially ITO, as a stable supply may be difficult to obtain because of the high cost and scarcity of indium.

Besides the availability issue, indium compound (including ITO) powder has been reported to be toxic [10]. Therefore, it is important to develop substitute materials and technology for reducing indium usage in transparent electrodes [11-14]. In order to eliminate the requirement for ITO as thin-film transparent electrodes used in flat panel displays, it is essential to develop an alternative material that contains no indium.

Currently, CNTs have been identified to be a viable replacement for ITO because they have been demonstrated to exhibit the mechanical, electrical and optical properties that surpass that of many frequently used conducting

polymers [15,16]. In addition, carbon is plentiful in supply and is much cheaper compared to indium.

However, the challenge is to match the performance of CNT electrodes to those of ITO. ITO has been reported to have a sheet resistance as low as 15 Ohm/sq with 90% transmittance in the 550 nm region, which corresponds to the maximum sensitivity of the human vision whereas the best CNT films resistance is ~200 Ohm/sq with 85% transmittance at 550 nm wavelength. [17]

Since the current method and technology is unable to fabricate CNT films with high throughput and good electrical properties, more research has to be done. A thorough study from CNT solution preparation and alternative methods to improve its conductivity is crucially needed to solve this problem.

1.2 Aim of Research

The aim of this research is to fabricate CNT electrodes with electrical and optical properties that are comparable to ITO, and to study the physics behind the conductivity of the CNTs in thin films, and the chemistry behind carbon nanotube doping.

1.3 Objectives

The objectives of this research are to

- Identify the key parameters in CNT transparent conductive film fabrication.
- Investigate the parameters that affect the dispersion of the CNT solutions to the conductivity of the respective CNT thin films.
- Study and understand the conductivity models of the CNT transparent conductive thin films.

- Investigate and understand the chemistry of post treatment on the electrical properties of CNT thin films.
- Demonstrate the possible usage of carbon nanotube transparent conductive films in some simple devices.

1.4 Scope of Research

This research heavily emphasizes the characterization of electrical and optical properties of CNTs, as these two material properties are the key performance index of transparent conductors. Electrical property were characterized by a 4-point probe sheet resistance measurement, while the optical properties were characterized by UV-vis-NIR (Ultraviolet – visible - near infrared wavelength) spectroscopy. Chemistry and morphology of carbon nanotubes characterized by Raman Spectroscopy, Atomic Force Microscopy (AFM), Scanning Electron Microscopy (SEM), and Fourier Transform Infra Red Spectroscopy (FTIR) have been used as supplementary data.

Chapter one presents background information, motivation and scope of the thesis. Chapter two summarizes the current technologies of carbon nanotube transparent films, and the gap that prevents carbon nanotube films from being used in applications. Chapter three elaborates on the experimental methods that were adopted in this project. Chapters four to seven present the results of this project. Chapter four presents the optimization of solution process was adopted to fabricate the film of CNTs. Chapter five focuses on the physics of CNT thin films; investigations on how transmittance changes with the change in conductivity and thickness were carried out. Chapter six discusses the doping process that was used in improving carbon nanotube film conductivity. The last

part of this thesis demonstrates some simple devices fabricated using transparent conductive film of CNTs, such as carbon nanotube transistors and CNTs based dye-sensitized solar cells.

CHAPTER 2 : LITERATURE REVIEW

In the following chapter, results from different research groups are presented and commented on for their benefits or problems. A summary is included at the end of the chapter to highlight the problems present in current techniques, and why they need to be solved.

2.1. Background

As previously mentioned, there are demand and supply problems with transparent conductors. The use of transparent conductors is becoming more and more prevalent in display application, electrostatic sealing, solar cells, transparent circuit, touch screen panels and so on. However, the supply of Indium metals to be used in fabrication of Indium Tin oxide (ITO) is limited.[8] The only solution for this problem is to find a possible replacement for ITO which is abundant in supply.

Carbon nanotubes (CNTs) are being considered as a potential replacement. Carbon is an abundant material, hence it has a potentially much lower cost compared to ITO since CNTs fabrication cost has continually decrease over the years. CNTs also have extraordinary electrical and mechanical properties. They can be fabricated to form thin films through various techniques, such as dip coating, spray coating, filtration methods, etc. These methods can be carried out in ambient conditions, unlike ITO.

2.2. Indium Tin Oxide (ITO) as a Transparent Conducting Oxide

Generally, Indium tin oxide (ITO) is used as the transparent conducting oxide for applications in optoelectronics. This is because ITO possesses excellent electrical conductivity as well as high optical transparency, which falls within the visible wavelength region. Other properties that make ITO the choice material are its chemical stability, excellent adhesion to substrates and ease of patterning[18].

2.2.1 Electrical Properties

ITO is a solid solution made up of both Indium (III) Oxide (In_2O_3) and Tin (IV) Oxide (SnO_2). The conductivity of ITO depends on the doping level of tin because the carrier concentration increases with increasing tin concentration until the saturation level. Above this saturation level, the amount of active free carriers present begins to decrease, due to the higher probability of having adjacent tin cations.[19]

The solid solubility of Tin in Indium Oxide, which is around 8%, can also be the other cause. When the solubility limit is exceeded, a secondary tin oxide phase will form and distort the lattice structure. As a result, it leads to an increase in resistivity. Hence, the optimum doping level of Tin to give the lowest sheet resistance is about 8-10%.[20]

Degenerative ITO will be produced if the doping level of Tin is about 8-10%. [21] Figure 2-6 below shows the energy diagram of In_2O_3 and ITO. With a carrier concentration of around 10^{20} to 10^{21} cm^{-3}, ITO exhibits electrical properties similar to that of a metal.

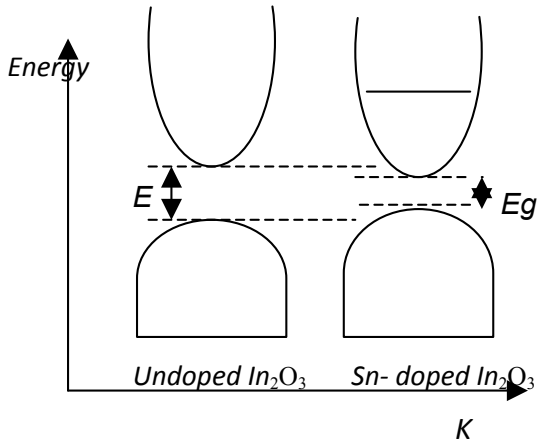

Figure 2-1. Energy diagram of In_2O_3 and ITO (Reproduced with permission from ref. [21]. Copyright 2008 Elsevier)

2.2.2 Optical Properties

The optical properties of ITO are related to the position of the plasma frequency and the magnitude of the electronic scattering time. The Drude model was used to derive the dielectric function for ITO film to obtain the respective plasma frequencies and electronic scattering times of the films [22].

ITO is regarded as an n-type degenerate semiconductor and has an optical band gap of 3.6 eV. The plasma frequency of ITO occurs in the near-IR spectral region, which makes it reflective in the mid- IR region and transparent in the visible region.[23]

2.2.3 Fabrication of ITO

ITO is widely fabricated into thin films for optoelectronic applications. Several types of deposition techniques have been established to produce the thin ITO films. These techniques are thermal evaporation deposition [23], magnetron sputtering [24,25], electron beam evaporation [26], spray pyrolysis [27], chemical vapour deposition (CVD) [28], dip-coating method [29,30] and pulsed-laser deposition (PLD) [31,32]. Among them, the direct current (DC) or radio frequency

(RF) magnetron sputtering method is the more commonly practiced technique. Typically, the magnetron sputtering method uses a low oxygen partial pressure in the sputtering gas along with the alloy and oxidized targets [33, 34].

Different deposition techniques will produce ITO films with a significant variance in properties, which are illustrated in Table 2-1 below. The best electrical properties of ITO is obtained through a radio frequency (RF) sputtering process. However despite all the variations, all the ITO properties obtained by various methods, are sufficient for usage in many optoelectronics devices.

Table 2-1. Properties of ITO synthesized using different deposition technique. (Reproduced with permission from ref. [12]. Copyright 2008 Elsevier)

Deposition Technique	Thickness (Å)	Carrier concentration (cm^{-3})	Resistivity ($\rho \cdot cm$)	Transmittance (%)	Ref.
r.f. Sputtering	7500	6.0×10^{20}	3.0×10^{-4}	90	[14]
r.f. Sputtering	5000	1.20×10^{21}	4.0×10^{-4}	95	[15]
Pulsed laser deposition	14000	$1.0\text{-}1.2 \times 10^{21}$	8.0×10^{-4}	90	[16]
Magnetron Sputtering	800	6.0×10^{20}	4.0×10^{-4}	85	[17]
d.c. Sputtering	1000	9.0×10^{20}	2.0×10^{-4}	85	[18]
Reactive evaporation	2500	5.0×10^{20}	4.0×10^{-4}	91	[19]
Ion Beam sputtering	600	2.0×10^{20}	1.2×10^{-3}	-	[20]
Spray Pyrolysis	3000	5.0×10^{20}	3.0×10^{-4}	85	[21]

However, there are still some drawbacks of ITO usage such as its brittleness, which make it unsuitable for printable applications, and the high cost of

processing and raw materials. All ITO fabrication methods involves high vacuum processes that increase its cost.

2.3. Requirements for replacement material

Various applications often impose specific restraints on the properties of the transparent conducting electrodes. For most optoelectronic applications, the display's size and type as well as the manufacturing process will greatly affect the nature of the properties of the material that are initially suitable. Generally, low temperature deposition results in high electrical resistance and poor optical transparency. Thus, it is important that the selected material, aligned to the specific processing conditions of these devices, still acquires the desired sheet resistance.

An example is the current conventional thin film transistors - LCDs (TFT-LCD) operating in either a vertical alignment (VA) or in-plane switching (IPS) mode. The transparent electrodes used in these TFT-LCDs must be deposited below 200 °C and still acquire 30 -120 Ω/sq listed in Table 2-1.

Glass is generally used as the substrate for most applications. Certain physical parameters also have to be considered, such as the VA-type LCDs application, and touch panels transparent electrodes require their thickness to be below 50 nm. Therefore, all these constraints have to be taken account for in the selection of the alternative material to replace ITO.

Table 2-2. Various transparent electrode applications requirements (Reproduced with permission from ref. [36]. Copyright 2002 Elsevier)

Applications		Substrate material	Deposition temperature [°C]	Film thickness [nm]	Resistivity [Ω cm] (sheet resistance [Ω/□])
LCD	TFT side	Glass	≈200	35–140	$4–5\times10^{-4}$ (30–120)
	CF side	Glass	<200	120–160	$1.6–3.6\times10^{-4}$ (16–30)
PDP		Glass	≈200 after 550	150–200	$2.0–3.0\times10^{-4}$ (<20)
OLED		Glass plastic film	<200	100–150	$2.0–4.0\times10^{-4}$ (<40)
Touch panel		Plastic film	150–180	10–30	(250–500)
CIGS solar cell		Glass	<200	1000–2000	on the order of 10^{-4} (<10)
a-Si solar cell		Glass	500–600	800–1000	on the order of 10^{-4} (<10)

2.4. Other Potential materials for the replacement of ITO

Several materials have been intensively researched on to replace ITO as transparent electrodes. Among these, Al-doped ZnO (AZO), Poly(3,4-ethylenedioxythiophene) (PEDOT) and CNTs are promising candidates.

2.4.1 Al-doped ZnO (AZO)

AZO appears to be a promising alternative to ITO because of its use of ZnO or Zn, which is inexpensive, non-toxic and has the ability to exhibit resistivity comparable to ITO indicated in Table 2-3. [12]

Table 2-3. Comparison of the properties of AZO and ITO as thin-film transparent electrodes (Reproduced with permission from ref. [12]. Copyright 2008 Elsevier)

	Doped ZnO	ITO
Low resistivity (Ω cm)	10^{-5}	10^{-5}
Practical resistivity (Ω cm)	$2–3\times10^{-4}$	1×10^{-4}
E_g (eV)	3.3	3.7
Index of refraction	2	2
Work function	4.6	4.8–5.0
Cost	Inexpensive	Very expensive
Stability		
Acid solution		<Good (stable)
Alkali solution		<Good (stable)
Oxidizing atmosphere at high temperature (or oxygen plasma)		<Good (stable)
Reducing atmosphere at high temperature (or hydrogen plasma)	Good (stable)>	

However, there are two major problems [12,36]: the difficulty of development of high deposition rate techniques that fabricate low resistivity AZO films on large substrates and the stability of the thin films in a humid environment.

Difficulties associated with AZO depositions especially lies in controlling of film thickness on large area substrates. These problems have to be resolved before techniques such as vacuum arc plasma evaporation (VAPE) with a high deposition rate can be of practical use [37-39]. But the preparation of AZO films by VAPE has proved to be difficult because of the extremely low vapor pressure of Al_2O_3[40]. In addition, VAPE systems are not popular. For these reasons, magnetron-sputtering deposition is the only current practical deposition technique suitable for applying transparent conducting AZO thin films in LCDs [11-18]. However, even with the use of magnetron sputtering depositions, there are problems associated with the thickness dependency of the resistivity and the spatial distribution of resistivity of the thin films. This is because increased thickness will decrease resistivity at the expense of the optical properties and the non-uniform resistivity distribution, causing in the resistivity of the deposited AZO thin films to increase. The properties of these magnetron sputtered thin films are also greatly affected by the apparatus, the deposition conditions and the sintered oxide target used. In particular, most commercially available oxide targets are unsuitable in obtaining AZO thin films with low resistivity and uniform resistivity distribution on the substrate [14].

The other major problem is the instability of the resistivity in a high humidity environment. It is of great importance that the transparent electrodes used, in optoelectronic devices, must be stable under such conditions, especially

in LCDs and touch panels applications. It was reported that the resistivity of transparent conducting AZO thin films fabricated with a thickness in the range of 20 to 200 nm on glass substrates at a temperature below 200 °C increased with exposure time when tested in a high humidity environment (air at 90% relative humidity and 60 °C) [13,14,41]. Minami et al. stated that this instability of impurity-doped ZnO thin films is due to the decrease of both the carrier concentration and the Hall mobility that results from the grain boundary scattering because of oxygen adsorption on the surface of the grain boundary and the thin film. Thus, the resistivity worsens in an oxidizing environment [14,41]. Although better film crystallinity and optimized chemical composition by varying the type and amount of doped impurity [42,43] can improve the stability, it is still not sufficient to provide the required stability of the AZO thin films in LCD and touch panel applications.

In addition, it is difficult to obtain good etched patterns compared to amorphous ITO films with the current photolithography process that uses wet treatments. It is because AZO films are more easily etched by both acid and alkaline solutions than ITO films listed in Table 2-3.

The above major problems and disadvantages stated show that the use of AZO thin films as the replacement for ITO in optoelectronics applications may not be the best option.

2.4.2 Poly (3, 4-ethylenedioxythiophene) (PEDOT)

PEDOT was studied intensively as an alternative because of its flexibility and high conductivity. An important advantage of conducting polymers is that they can be easily fabricated by inkjet printing, screen-printing, roll-to-roll

coating or other economical solution processes[44-46]. Furthermore, PEDOT, which is a polythiophene derivative, also has a relatively higher conductivity and better environmental stability among numerous conducting polymers. However, it is insoluble in many solvents.

The addition of PSS (polystyrenesulfonate) would make a water-dispersible PEDOT: PSS complex, which is extensively used as a hole-transport layer in organic optoelectronic devices because of its ease of processing and suitable work function [47]. PEDOT: PSS exhibits a significant optical transparency to visible light of 80% [48] and its conductivity can be improved by the addition of polyalcohols or high dielectric solvents[49-55]. However, its highest conductivity is still about 20 times lower than that of ITO (15Ω/sq, 3800 S/cm) [54]. The main reason for its low conductivity is the existence of the insulating PSS component.

Apart from its low conductivity, there are also downsides to PEDOT:PSS such as its degradation in ultraviolet light and high temperature / humid environments. The ease of removal of Na ions of the films by rinsing with hydrochloric solution also indicates that interfacial chemistry problems may occur in the presence of the acids in certain device fabrication processing steps.

To address the problems of using PEDOT:PSS, Y. M. Chang et al.[55] has reported PEDOT films with average conductivity of 500S/cm that exceeds the doped PEDOT:PSS conductive materials presented in previous works [49-55]. These PEDOT films obtained are as-synthesized that prevent dissolution of PEDOT in subsequent device fabrication process and have better surface roughness compared to ITO. Thus, PEDOT is made a better option than PEDOT:PSS. However, its conductivity is still much lower than ITO. Figure 2-2 below shows the influence of the thickness of PEDOT films on its

transmittance and sheet resistance, which is an important parameter in the requirements of transparent conducting electrode [55]. From Fig. 2-2, it can be seen that film thickness is a key factor in determining the device performance of PEDOT. The trend observed is also similar to the thickness dependency of resistivity in AZO.

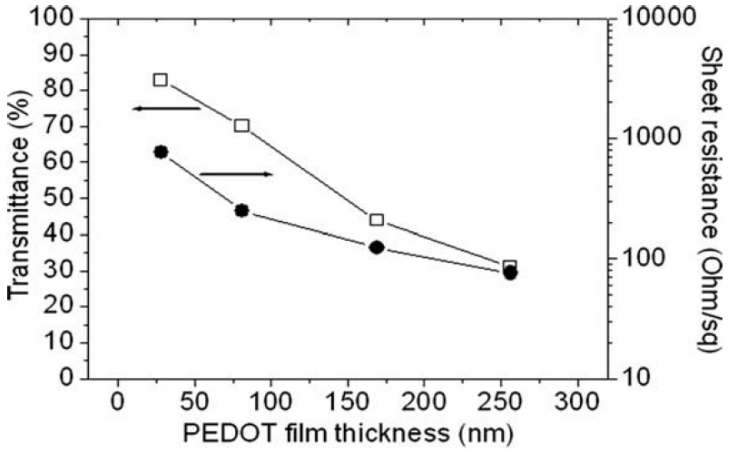

Figure 2-2. The influences of the thickness of PEDOT film on its sheet resistance and transmittance.(Reproduced with permission from ref. [48] Copyright 2008 Elsevier)

As a result, PEDOT may not be a suitable replacement for ITO as transparent electrodes in the optoelectronics applications because of its relatively lower conductivity.

2.5. Carbon Nanotubes as a Potential Substitute of Indium Tin Oxide

Since both Al-doped Zinc Oxide and PEDOT are problematic, many researchers are eyeing another potential material for replacing ITO, carbon nanotubes.

Carbon Nanotubes (CNTs) was first observed by Endo [56] in late 1970 as hollow carbon structure, and as a minor by-product of fullerene synthesis by Sumio Iijima in 1991 [57-59]. Since their discovery, research on CNTs growth,

characterization and application development has boomed due to their unique electronic and extraordinary mechanical properties. A CNT consists of carbon atoms bonded in a tubular arrangement. Figure 2-3 and Table 2-4 shows the polymorphs and properties of various stable forms of carbon, respectively.

CNT is a candidate likely to replace TCO thin films in optoelectronic applications because of its ability to overcome many shortcomings of ITO, due to CNT film's flexibility and potentially low cost.

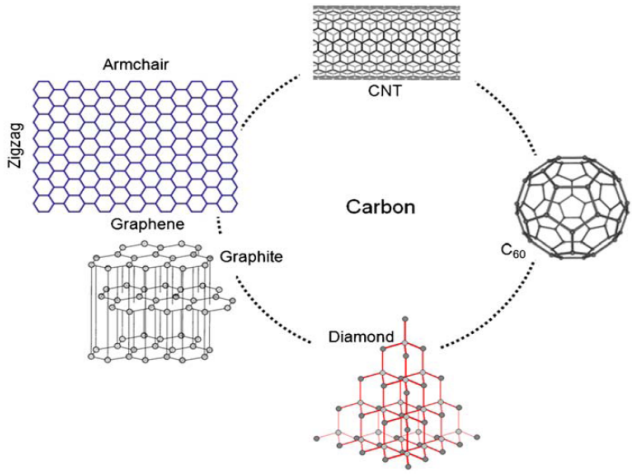

Figure 2-3. Polymorphs of Carbon (Reproduced with permission from ref. [60] Copyright 2006 Taylor and Francis Group)

Table 2-4. Properties of carbon allotropes (Reproduced with permission from ref. [60] Copyright 2006 Taylor and Francis Group)

	Crystal structure	Hybridization	Conduction type	Band gap (eV)	Work function (eV)
a-C	–	sp^3+sp^2	Semiconductor	0.2–3.0	4.9
Diamond	Cubic	sp^3	Insulator	5.5	5.45
Graphite	Hexagonal	sp^2	Conductor	0	5.0
Fullerene (C_{60})	Cubic	sp^2+sp^3	Semiconductor	1.6	4.6–5.0
CNT	Cylindrical	sp^2+sp^3	Metallic/semi-conducting	0.3–2.0	4.5–5.1
Graphene	–	sp^2	Semi-metallic/semi-conducting	0–0.3	5.0

2.5.1 Types of Carbon Nanotubes

There are basically two types of CNTs: single-walled nanotubes (SWNT) and multi-walled nanotubes (MWNT). SWNT can be described as a graphene sheet, which is a monolayer of sp^2-bonded carbon atoms, rolled into a cylinder. A typical SWNT can be several micrometers long and only a few nanometers in diameter. A SWNT can be either metallic or semiconducting, depending on the CNT chirality, or the degree of twist [58]. MWNT, on the other hand, is composed of concentric cylinders of graphene sheets[58]. As such, MWNT has a larger diameter than SWNT.

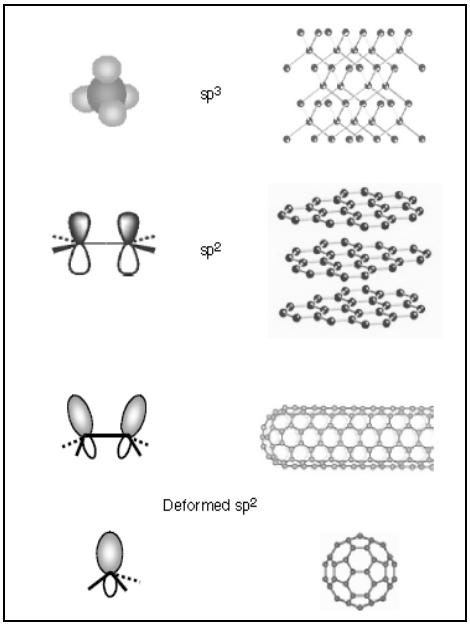

Figure 2-4. Bonding structures of diamond, graphite, nanotubes, and fullerenes (Reproduced with permission from ref. [60] Copyright Taylor and Francis Group).

2.5.2 Properties of Carbon Nanotubes

Electrical

The chirality of a CNT can greatly affect its electrical properties. The chiral representation of CNTs is in the vector form (n,m). When n=m, the nanotubes

are known as armchair nanotubes, and they are metallic. On the other hand, when n≠m and n-m is a multiple of 3, the nanotubes are known as zig-zag and chiral nanotubes. These nanotubes are semimetallic, that is, they have electrical and thermal conductivity between that of metals and semiconductors. In these cases where n-m is not a multiple of 3, those nanotubes are semiconductors. Theoretically, metallic nanotubes can carry an electrical current density of 4×10^9 A/cm^2. This is more than 1,000 times greater than metals such as copper. [60]

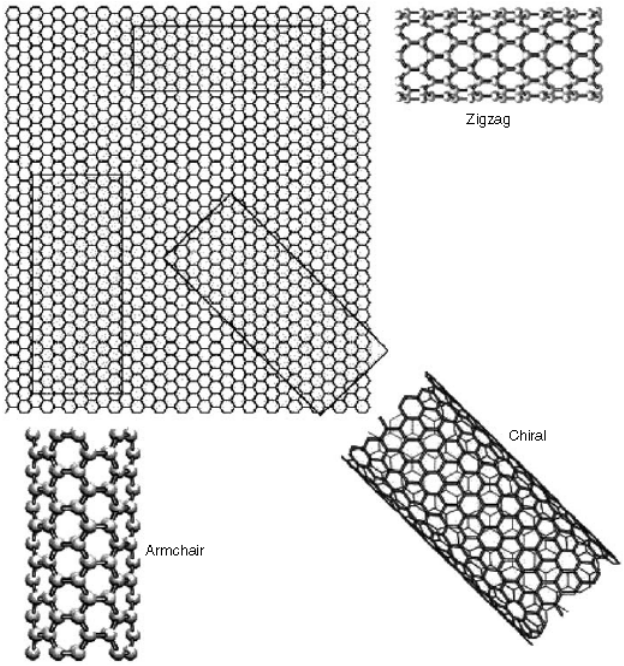

Figure 2-*5*. Schematic representation of the relation between nanotubes and graphene. (Reproduced with permission from ref. [60] Copyright Taylor and Francis Group)

In a random network of SWNTs, the conductivity of the SWNT network is affected by the inter-tubes junctions. There are essentially three types of inter-tubes junctions, namely, metallic-metallic, metallic-semiconducting and semiconducting-semiconducting. Metallic-metallic intertube junctions will give higher conductivity although ohmic contacts are formed (shown in figure 2-6). In contrast, metallic-semiconducting and semiconducting-semiconducting

intertube junctions will result in lower conductivity due to the high Schottky barriers formed. [59]

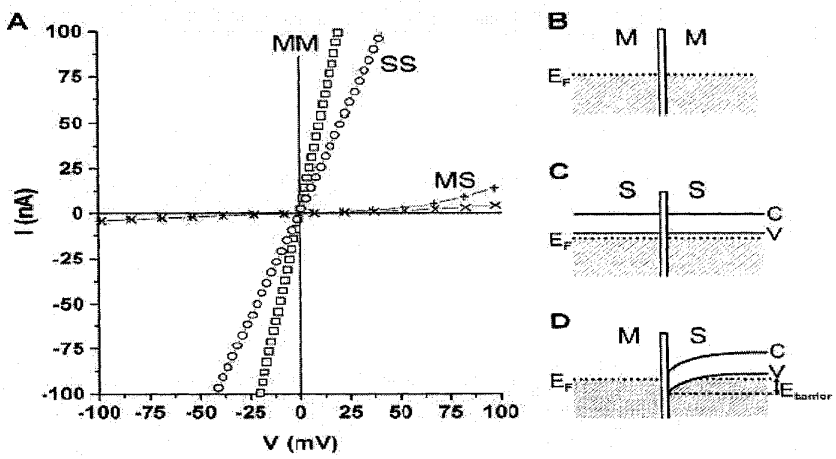

Figure 2-6. Junction resistance between metallic – metallic, metallic – semiconducting and semiconducting – semiconducting carbon nanotube. (Reproduced with permission from ref. [62] Copyright 2000 AAAS)

Mechanical

Both SWNT and MWNT have high elasticity and excellent mechanical properties due to the 2D arrangement of the carbon atoms in the graphene sheet, which enables large out-of-plane distortions. In addition, the strength of the carbon-carbon in-plane bonds causes the graphene sheet to be remarkably strong against any in-plane shear distortion or fracture.[61]

Table 2-5. Mechanical Properties of Nanotubes. (Reproduced with permission from ref. [61]. Copyright 2004 Marcel Dekker Inc)

	Young's modulus (GPa)	Tensile Strength (GPa)	Density (g/cm^3)
MWNT	1200	~150	2.6
SWNT	1054	75	1.3
SWNT bundle	563	~150	1.3
Graphite (in-plane)	350	2.5	2.6
Steel	208	0.4	7.8

Kaempgen et al. [63] reported that a CNT-coated plastic foil was able to remain conductive (Figure 2-7) even after being crumpled severely. Clearly, ITO substrates were not able to show such flexibility. This result made CNTs more promising in soft electronic industry such as touch panels where electrodes have to be conductive, transparent and highly flexible.

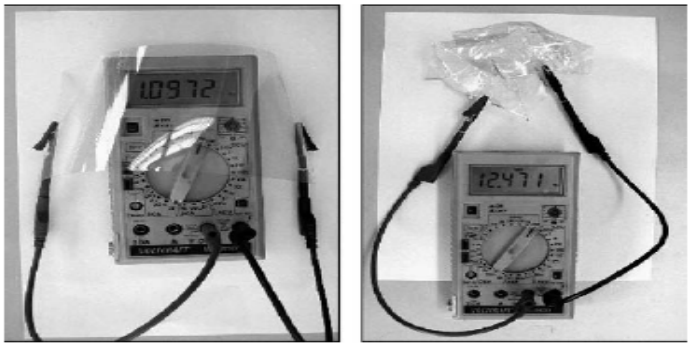

Figure 2-7. Foil on left is slightly bent while on the right is same sample heavily crumpled. The sheet resistance of the film is 1 MΩ (left) and 12 MΩ (right). (Reproduced with permission from ref. [63]. Copyright 2005 Elsevier)

Thermal

CNTs are very good thermal conductors along the tube. Such a property is also known as "ballistic conduction". However, CNTs are thermally insulating along the lateral tube axis. It was estimated that CNTs are able to transmit up to 6000 watts per meter per Kelvin at room temperature. This figure is much better than copper, which can only transmit 385 watts per meter per Kelvin. In addition, the temperature stability of CNTs is found to be up to about 2800^{o}C in vacuum and 750^{o}C in air.[61]

Optical

The diameter of a nanotube is in the nanometer range, which is much smaller than the wavelength of light. However, its length is usually in the same range or even greater than the optical wavelength. Therefore, both microscopic and macroscopic views of the nanotubes can coexist within a single nanotube. Such unique optical property will lead to new optical applications in the near future.[61]

2.6. Progress towards Carbon Nanotube Electrodes

Despite a significant amount of work done on carbon nanotube electrodes, the reported properties of these carbon nanotube electrodes were still inferior to ITO. The fabrication of carbon nanotube film involves several steps. The key step is how to disperse CNTs evenly in solution

Commercially available carbon nanotubes for transparent conductor applications are HiPCO CNTs by Carbon Nanotechnologies Inc (CNI) [64-66], Arc Discharge CNT by Carbon Solution Inc [69], Arc Discharge CNTs by Iljin Nanotech Co. Ltd [68], Laser Ablation CNTs by Rice University [64] , CNTs by Nanocyl Inc. [66], and many others from non commercial lab productions.[64] Laser ablation CNTs have been shown to be the best carbon nanotube feedstock, however only scientific institutions can afford the high cost laser ablation process. Arc-discharge CNTs by Iljin Nanotech have also been used by several researchers and have shown remarkable results [65]. Unfortunately, Iljin Nanotech no longer supplies CNTs. Out of all the possible sources left, only CNI, Carbon Solution and Nanocyl still supply carbon nanotube powder commercially.

Carbon nanotubes are only soluble in some organic solvents, such as dimethylformamide [64], dichloroethane,[65] or dichlorobenzene,[66] These solvents

are toxic and have high boiling points. Water or ethanol would be a suitable benign solvent, however a covalent functionalization of carbon nanotubes with some hydrophilic groups like –OH or –COOH is necessary to dissolve NTs in this solvent. With 3-6 wt%, this functional group could make CNTs soluble in hydrophilic solvents without degrading its electrical property.[64] Excessive amounts of this hydrophilic group are known to degrade the electrical conductivity of carbon nanotubes due to the opening of π bonding between each carbon molecule in the nanotube structure.[65] Hence the functionalization reaction need to be carefully controlled.

The other option is to use a surfactant to dissolve carbon nanotubes. Surfactants do not change carbon nanotube electrical properties because there is no covalent bonding on it. However its presence affects the electrical conductivity of the film, because surfactants are electrically insulating. So the surfactants need to be removed before a highly conducting film can be obtained. The removal of surfactants is a very difficult process. It needs either a strongly oxidizing acid [68], or rigorous washing with water.

There are also several common surfactants that are used to dissolve CNTs. The most popular surfactants are SDS (sodium dodecyl suphate)[68-71], SDBS (Sodium dodecyl benzene sulphonate) [64] and Triton-X. [72]

The deposition methods of carbon nanotube solutions into films can be performed with many different methods, such as vacuum filtration followed by transfer printing [70], spin coating [68], air spraying[71], dip coating[70, 72], electrophoretic deposition.[73]. In the work of M. J. de Andrade et al.,[74] a comparison among the fabrication techniques used for CNT films was made as shown in Figure 2-8. [74]

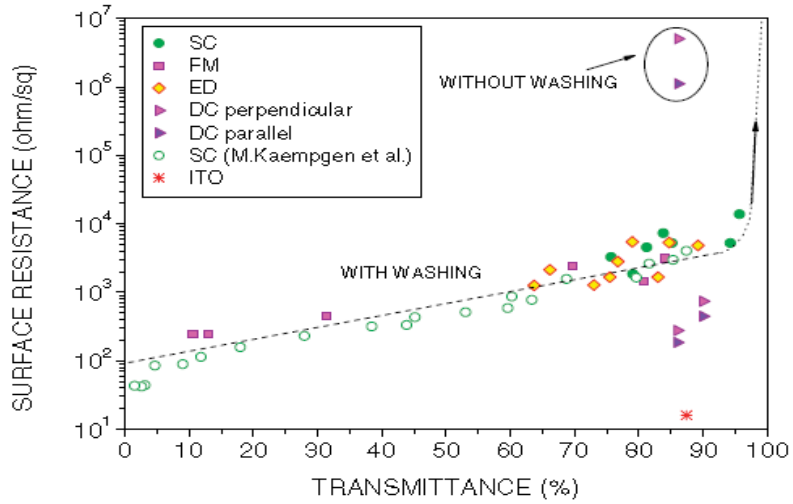

Figure 2-8. Comparison of SWNT films properties prepared using different techniques; SC - Spray Coating, FM - Filtration Method, ED - Electrophoretic Deposition, DC - Dip Coating. (Reproduced with permission from ref. [74]. Copyright 2007 Wiley-VCH)

In Figure 2-8, the sheet resistances and transparencies of the CNT thin films fabricated by different techniques were compared. Among the techniques, the dip-coating method gave the best quality CNT thin films. It should also be mentioned that the better properties obtained by dip-coating are a result of the as-prepared CNT networks being much smoother and the CNTs in films being relatively well-aligned, resulting in the improvement of the conductance along the tubes. However dip coating process is time consuming and hard to reproduce.

The filtration method process shown in figure 2-9 is another popular process used to fabricate carbon nanotube thin film. The advantage of the filtration method is that it does not require a post deposition process to remove the surfactant. Instead, they will be removed during the vacuum filtration process. [58] However, this method also carries some drawbacks such as poor scalability, low utilization yield of carbon nanotubes, a limited substrate for stamp area, and a time-consuming fabrication process. The filtration method process consists of vacuum filtering a CNT solution through a filtration membrane followed by

transferring CNT from the filtration membrane to PDMS, then clamping the PDMS into the substrate at 100 ^{o}C for 30-60 minutes to transfer the CNT film from the PDMS stamp into the substrate.

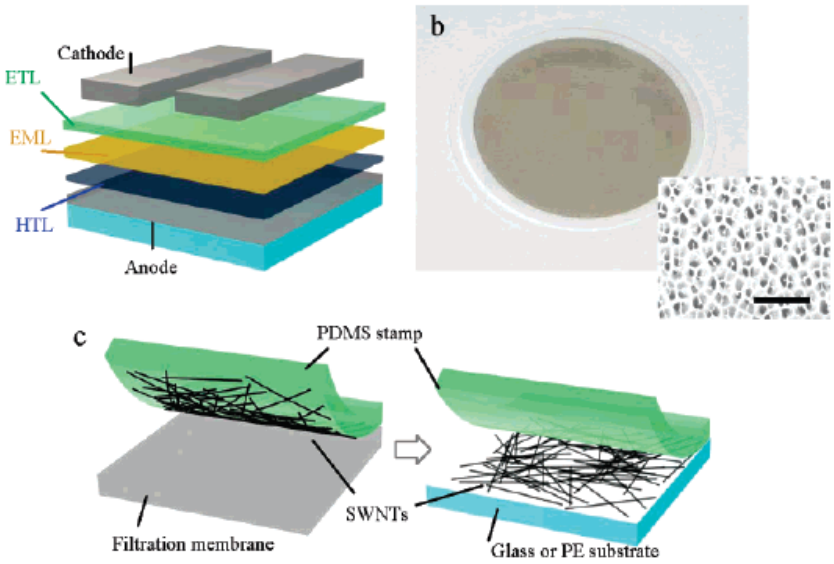

Figure 2-9. Vacuum Filtration followed by Transfer printing method (Reproduced with permission from ref. [75] Copyright 2006 American Chemical Society)

The dip-coating method was also employed by Ng et al. [72] to fabricate CNT thin film electrodes. Their best film had a resistivity of 130 Ohm/square for 69% transparencies, which is lower compared to the other method. Such poor results might be due to the double-sided-coating of the CNTs.

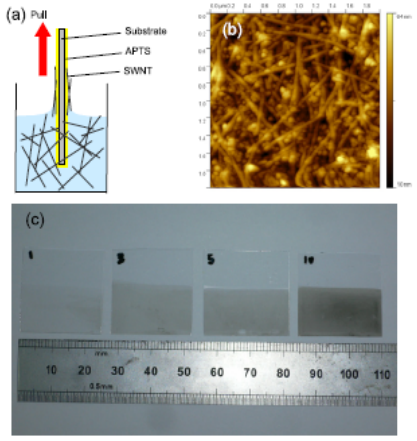

Figure 2-10. Dip coating Method and the resulting carbon nanotube film (Reproduced with permission from ref. [72]. Copyright 2008 IOP Publishing)

Airgun spraying (shown in figure 2-11) is another method adopted by many other researchers [76-79]. This method directly uses an airgun to spray a carbon nanotube solution containing a SDS or SDBS surfactant, followed by acid treatment to remove the surfactants. Among all the deposition methods, airgun spraying is the only method that is scalable. However, this method is not well explored yet.

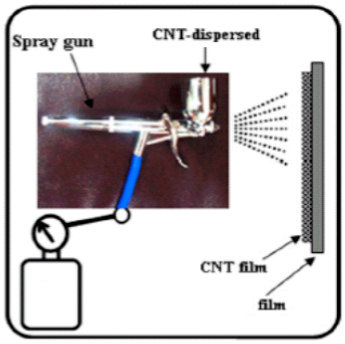

Figure 2-11. Spray Coating Method (Reproduced with permission from ref. [74]. Copyright 2007 Wiley-VCH)

The lowest sheet resistance of ITO films that can be obtained is less than 10 ohms/sq at a transmittance greater than 80%. However, if we want to further increase its transmittance to 90%, it will cause the sheet resistance of ITO to be greater than 100 ohm/sq.[80] Although the current sheet resistance of CNT films is about 80 ohms/sq at a transmittance of 80%, research has been ongoing to find ways to decrease the sheet resistance of CNT films while retaining high transmittance.

The fabrication of CNT thin films is normally followed by acid post treatment. The purpose of this acid treatment is to remove surfactants from the films. In order to further improve the electrical conductivity, a chemical doping method such as acid, $SOCl_2$[81,82] or $AuCl_3$[83,84] is employed. For example, Geng et al.[71] reported that the as-prepared SWNT films have sheet resistances of about

40 and 80 Ohms/sq at corresponding transmittances of 70% and 80% after acid treating the films in 12 M of nitric acid (HNO_3). The CNTs used here are arc discharge carbon nanotubes from Iljin Nanotech. Figure 2-12 shows the sheet resistance and corresponding transmittance of the treated SWNT films, indicated by the solid-circle line. After the BrØnsted acid treatment, the CNT sheet resistance was reduced by more than 50%, which indicates the increasing possibility and feasibility to replace conventional ITO with CNT. However, it is still very difficult to obtain CNT films with similar sheet resistance value to that of ITO at the same transmittance.

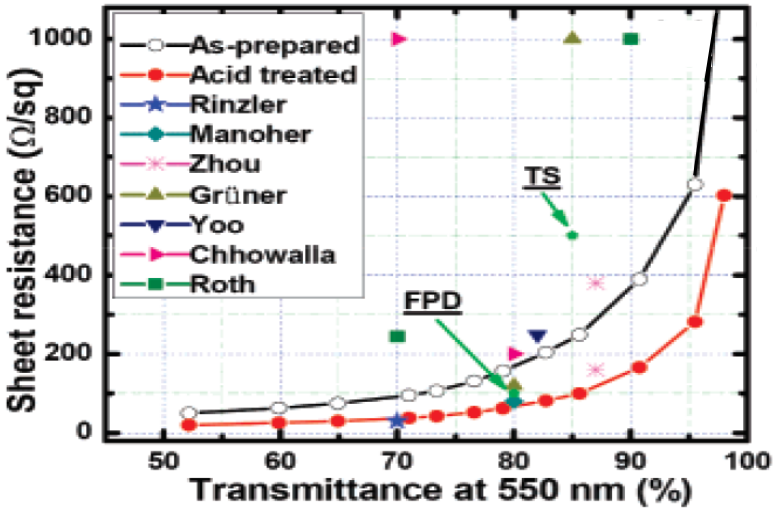

Figure 2-12. Sheet resistance versus transmittance at 550 nm before (open circle) and after (solid-circle) nitric acid treatment with previously reported values for comparison. (Reproduced with permission from ref. [71]. Copyright 2009 American Chemical Society)

More recently, Miyata et al.[85] showed that the sheet resistance of the SWNT films could be reduced from 6.2 to 0.99 kOhm/sq after the treatment of H_2SO_4. They explained that the reduction was due to the shift in the Fermi level after doping (Figure 2-13). The disappearance of the S11 optical absorption peak after doping further proposed that the Fermi level shift is between 0.4-0.7 eV. However, no mechanism is proposed in this report.

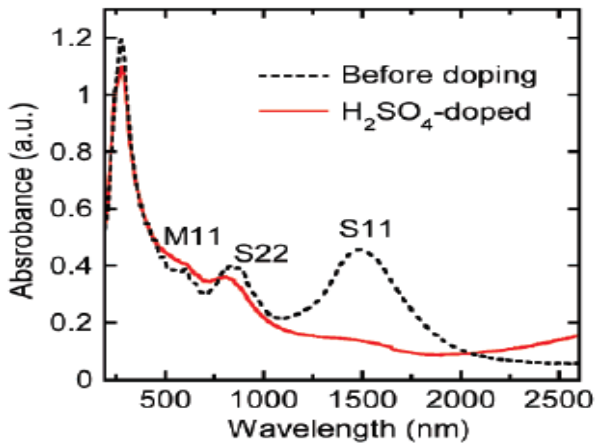

Figure 2-13. Optical absorption spectra of SWCNT thin films before and after hole-doping by H_2SO_4 (Reproduced with permission from Ref. [85] Copyright 2008 American Chemical Society).

Another way to improve CNT film conductance is by obtaining a uniform population of carbon nanotube in the solution precursor.[83-86] The main idea for this work originated from the fact that dissimilar species junctions, i.e. semiconducting-metallic carbon nanotube are much more resistive compared to similar species junctions. The film made of separated metallic CNTs [83,84] and the separated double walled carbon nanotubes [85] was observed to show significant improvement compared to the film made of its mixture. However, this process suffers from a low utilization yield of carbon nanotubes.

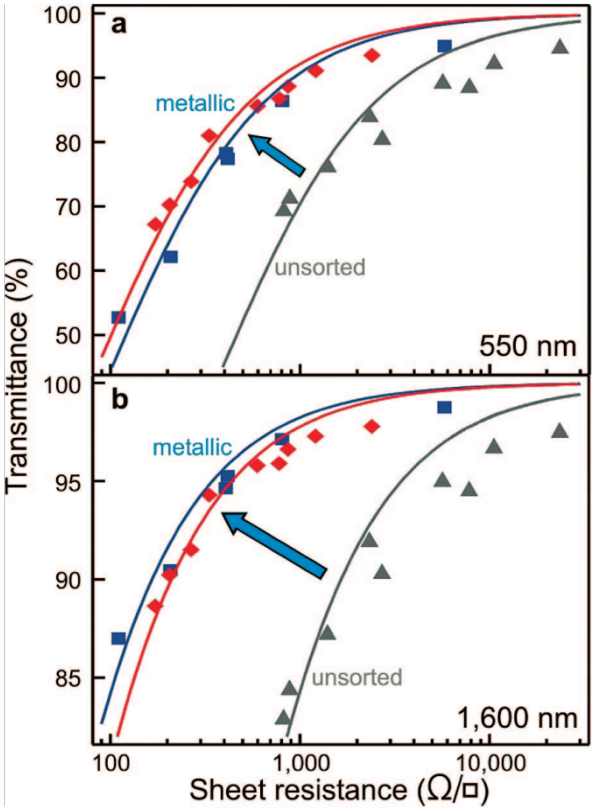

Figure 2-14. Sheet resistance and transmittance of sorted metallic carbon nanotube film (Reproduced with permission from ref. [83] Copyright 2010 ACS Publishing Group).

2.7. Devices Fabricated with Carbon Nanotube Thin Film

Zhang et al [72] from University of Southern California used the filtration method to fabricate carbon nanotube electrodes for Organic Light Emitting Display (OLED) applications. The best result that they obtained was a CNT film with 380 Ohm/sq at 87% transparencies. The sheet resistance was further improved by $SOCl_2$ doping, and they finally obtained a value of 160 Ohm/square. Figure 2-9 is the schematic diagram of the filtration method.

P3 and HiPCO CNTs were used in the OLED fabrication. The P3 carbon nanotube film showed better surface roughness (7 nm) compared to the HiPCO carbon nanotube film (11 nm). Later on, it was found that the surface roughness of carbon nanotube is very important for the performance of OLEDs. OLEDs

made with P3 films show a stable performance of up to 4-5 hours. However, OLEDs using HiPCO CNTs as electrodes started to fail after 30 s because of either short or open circuits. The current density and brightness of CNT film OLEDs is still inferior compared to Indium Tin Oxide by about 1-2 orders of magnitude. The suggested reason was the higher resistance of CNT films and a higher work function.

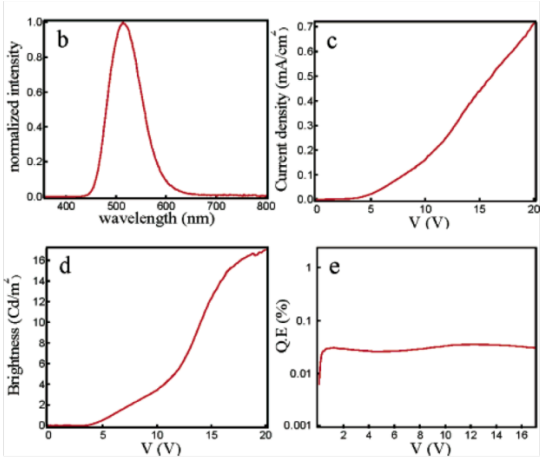

Figure 2-15. OLED with carbon nanotube electrodes device characteristic. (Reproduced with permission from Ref. [75]. Copyright 2006 American Chemical Society)

In other reports, CNT films continued to prove its capability compared to ITO. In solar cell applications, Du Pasquier et al.[86] reported that the CNT thin films were able to obtain a higher efficiency than ITO films (25 Ohm/sq). These thin films were fabricated from different amounts of SWNT solution and the lowest sheet resistance measured was 282 Ohm/sq. The SWNT films were then used as transparent conducting electrodes in photovoltaic devices along with ITO films to show the feasibility of CNTs in OPV applications. Table 2-6 below shows the comparison of the photovoltaic characteristics of both devices.

Table 2-6. Solar cell parameters at 100 mW/cm^2 illumination for both ITO and SWNT on glass substrate. (Reproduced with permission from ref. [89] Copyright 2009 AIP Publishing Group)

Values@100 mW/cm^2	ITO-glass drop cast reference	Best SWNT-glass drop cast
% efficiency	0.69	0.99
FF	0.32	0.3
I_{sc}(mA/cm^2)	5	6.65
V_{oc}(mV)	426	500

From table 2-6, it was evident that the photovoltaic performance of SWNT devices was much better than those with ITO. The suggested explanation was the 3D network of the SWNT thin films that allows 3D connection with the photoactive composite in the device. The authors believed that the work function of SWNT between 4.5 eV and 5eV might be another reason, since it was reported by other researchers to be in the same range as ITO. These promising results made the authors believe that SWNT is highly suitable to be used for hole collection.

There is much work that has been done in the field of carbon nanotube transparent conductive films, and some groups have been able to obtain highly conductive carbon nanotube fims, with the filtration method, separation method or $SOCl_2$ doping. However all these methods are still not perfect. The filtration method process is very time consuming. The separation method process will waste most of the raw carbon nanotubes feedstock. And the $SOCl_2$ process is very hazardous. Therefore a new method which is scalable, less hazardous, and has high utilization yield of carbon nanotubes need to be researched and obtained to enable the applications of carbon nanotube films.

CHAPTER 3 : MATERIALS AND EXPERIMENTAL PROCEDURES

3.1. Fabrication Roadmap and Parameters Involved

In this project, different diameters of carbon nanotubes were deposited as transparent conducting thin films for comparison. The preparation steps for the CNT solutions, which were the same for all SWNTs, DWNTs and MWNTs, are as follows:

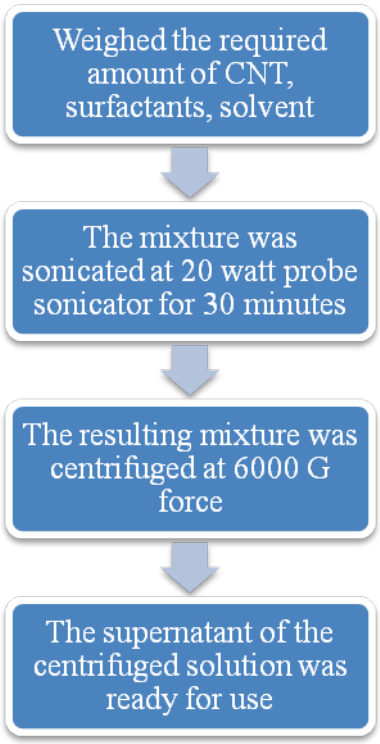

Figure 3-1. Flowchart for preparation of CNTs solution

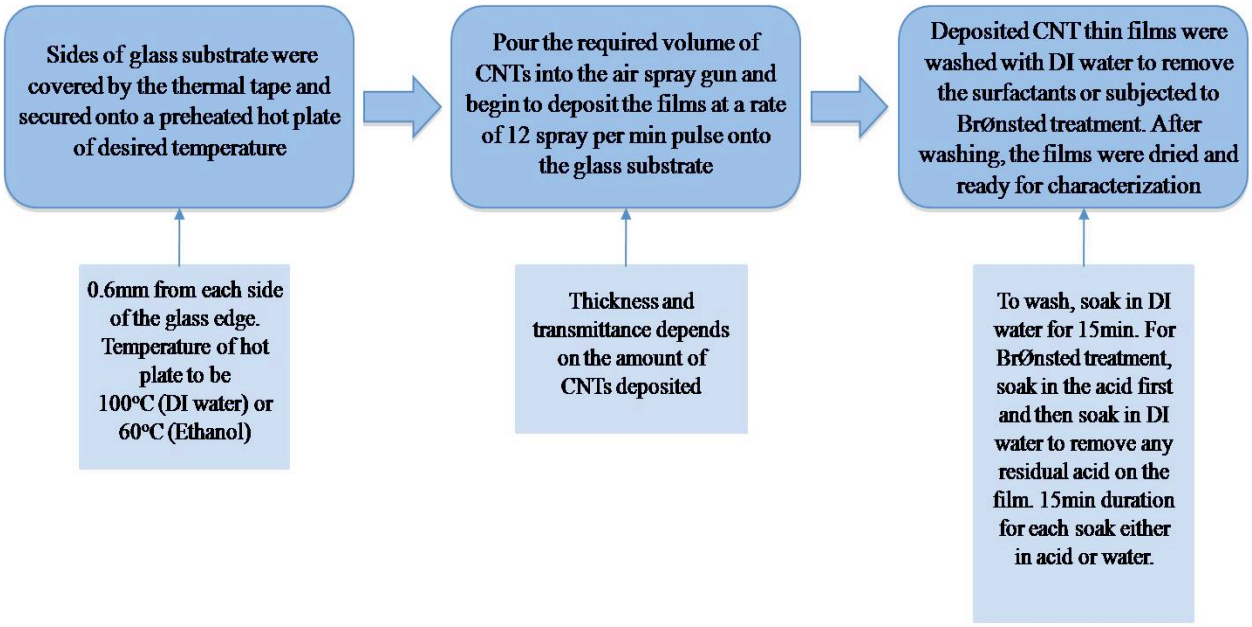

Figure 3-2. Flowchart for the deposition and post-treatment of the CNTs thin films

Due to its high rate of deposition (85% transmittance film could be fabricated in less than 5 minutes) and its ease of handling, the air pulsed spraying technique was selected. Although it did not provide the desired high-density networks of CNTs, the resistivity of CNT thin films obtained on the glass substrate was still acceptable. The deposition steps and conditions are shown in figure 3-2.

3.2. Characterization of CNT thin films

The CNT thin films deposited were then characterized by the use of a Four-point Probe meter, UV-Vis-NIR Spectrometer, Raman Spectrometer, Scanning Electron Microscopy (SEM) and Atomic Force Microscopy (AFM). The four-point probe meter was used to retrieve the sheet resistances of the thin films. Measurements were taken from five different points for each film followed by the tabulation of individual thin film average sheet resistance. The transmittance of the thin films on the glass substrate also had to be collected by using UV-Vis-

NIR Spectrometer so as to allow the comparison between different diameters of CNTs with their respective sheet resistance.

AFM was used to provide information on the morphology of the thin films. A Raman spectrometer was not only used to identify the chemistry of carbon nanotube but also to understand the phenomenon behind the post treatment effect on the CNT films by obtaining the respective D and G bands of various CNTs thin films.

CHAPTER 4 : FABRICATION AND OPTIMIZATION OF CARBON NANOTUBE TRANSPARENT CONDUCTIVE FILM

This chapter will discuss the parameters of carbon nanotube film fabrication comprehensively. It starts with laying down the fabrication steps, listing down all the parameters involved, and then testing it out and observing it. This work is carried out first to ensure that fabrication parameters have been optimized, before continuing to post-fabrication process experiments.

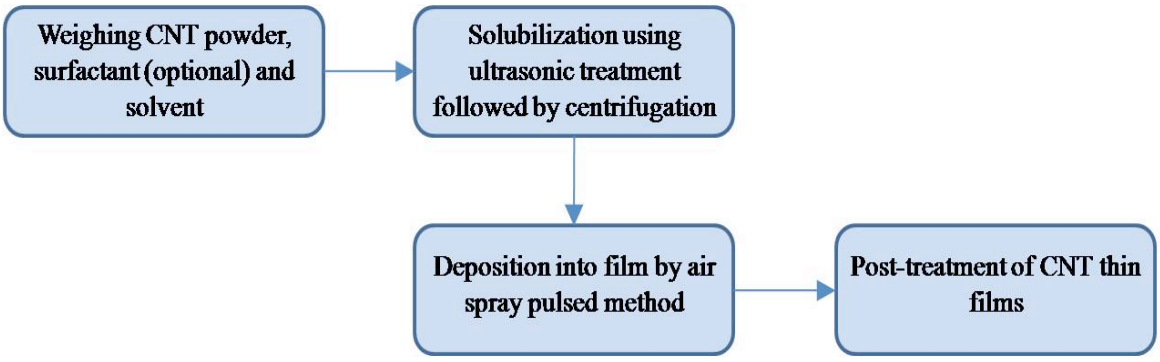

Figure 4-1. Main preparation steps for the fabrication of the CNTs thin films

Table 4-1. Parameters involved in the various steps of CNT films fabrication

STEPS	*PARAMETERS*
Raw materials preparation	• Selection of raw materials and concentration • Selection of surfactant and concentration • Selection of solvent
Solubilization by ultrasonic treatment followed by centrifugation	• Ultrasonic type (bath/probe), power and duration

Deposition into film	• Centrifugation speed and duration • Deposition method, pressure used for airspraying • Deposition temperature • Substrate used
Post-treatment of CNT films	• Post-treatment chemicals • Doping / simply surfactant removal

4.1 Selection of Carbon Nanotube Raw Materials

The selection of carbon nanotube raw materials for transparent thin film electrodes is a crucial step. There are many CNTs from different manufacturers with different properties and product specifications are based on the limited resolution of characterization tools. Raman spectroscopy measurement can provide some information on the quality of carbon nanotubes. The G/D ratio shown in Raman spectroscopy would indicate the ratio of sp^2 bonds and other defects in CNT powders. Residual mass at high temperature (800 ^oC) for TGA measurement indicates the remains of refractory metal catalyst / catalyst support.

There are many kinds of impurities and defects in carbon nanotube powders, which cannot be fully characterized with only one characterization tool. Although catalyst and catalyst-support impurities might not be characterized by Raman spectroscopy, these impurities could greatly affect the properties of carbon nanotubes. Some defects on carbon nanotube walls cannot be easily characterized through TGA (Thermo-Gravimetric Analysis). In addition, the D band of Raman spectroscopy can lead to several different possibilities, such as attachment of foreign chemicals, intrinsic defects or impurities.

Since there are many factors or possibilities involved in carbon nanotube characterization, it may be difficult for us to rely fully on characterization data. Thus, in this project, our approach was to directly investigate 14 different carbon nanotube films from four manufacturers.

Table 4-2 List of carbon nanotube product investigated

Pristine Carbon Nanotube

Type	Manufacturer
HiPCO Single walled CNT	Carbon Nanotechnologies
P2 Arc Discharge Single walled CNT	Carbon Solution
Double Walled CNT	Nanocyl
Short Double Walled CNT	Nanocyl
Multi walled CNT	Nanocyl
Short multi walled CNT	Nanocyl
CoMoCAT 65 Single walled CNT	Southwest Nanotechnology
CoMoCAT 76 Single walled CNT	Southwest Nanotechnology
CoMoCAT CG200 Single walled CNT	Southwest Nanotechnology

Functionalized Carbon Nanotube

Type	Manufacturer	Functional group
P3 arc discharge CNT	Carbon Solution	-COOH functionalized
DWNT-COOH	Nanocyl	-COOH functionalized
MWNT-COOH	Nanocyl	-COOH functionalized
DWNT-NH2	Nanocyl	-NH_2 functionalized
MWNT-NH2	Nanocyl	-NH_2 functionalized

All other fabrication parameters are maintained constant:

- probe ultrasonication of 20 watt 90% power for 15 minutes followed by 6000 g force centrifugation
- Constant carbon nanotube concentration : 0.1 mg/ml
- SDBS surfactant 1% wt for pristine and $–NH_2$ functionalized carbon nanotube, no surfactant for – COOH functionalized,
- 10 psi airpspray pressure, with rate 0.5 ml/ mins
- 68% concentrated Nitric acid post-treatment

The resulting sheet resistance and transmittance is then tabulated into graphs.

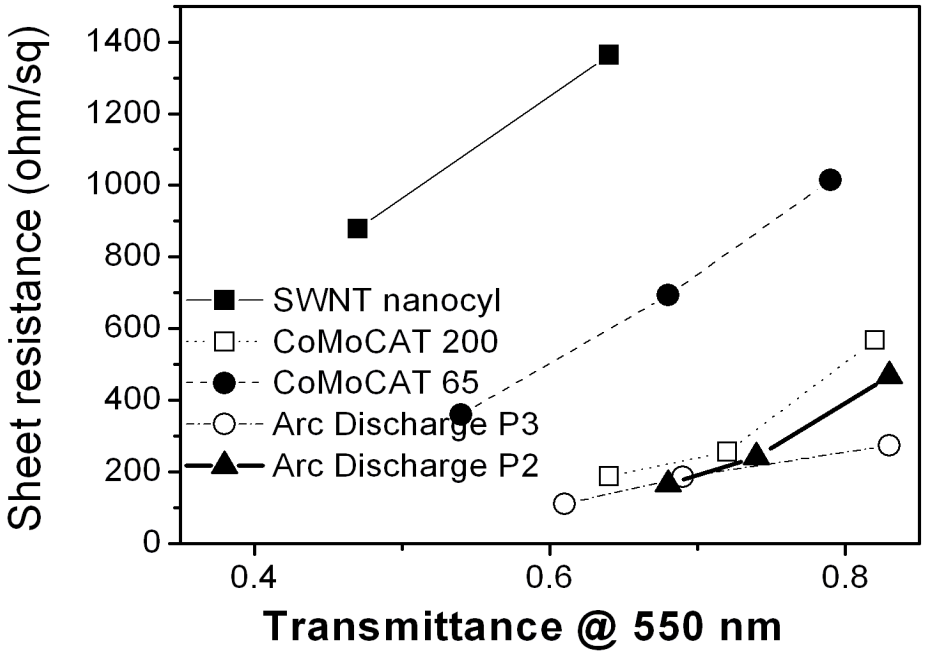

Figure 4-2. Sheet resistance-transmittance curve of different single walled carbon nanotubes

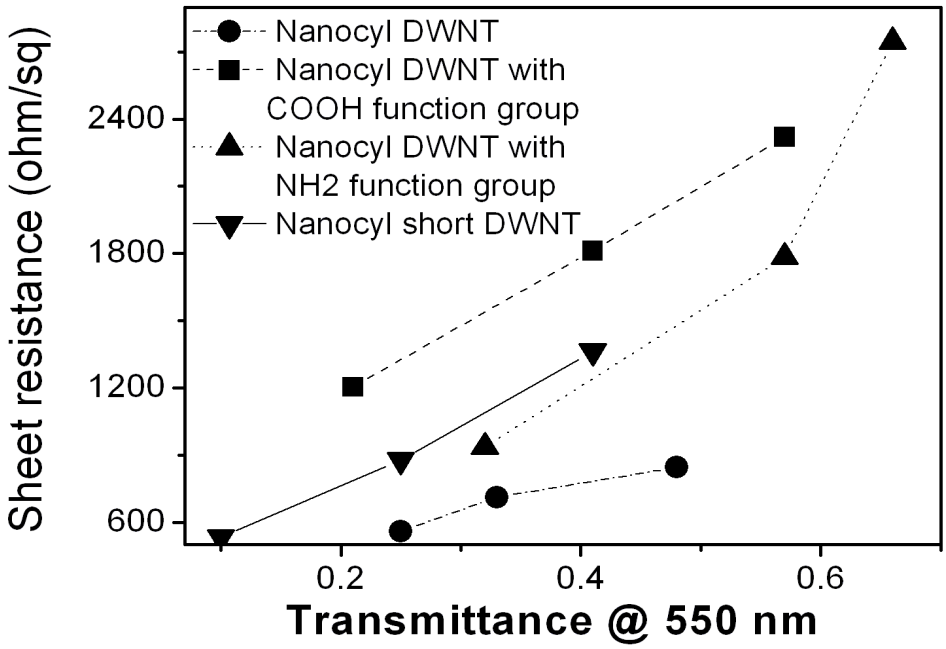

Figure 4-3. Sheet resistance-transmittance curve of different double walled carbon nanotube

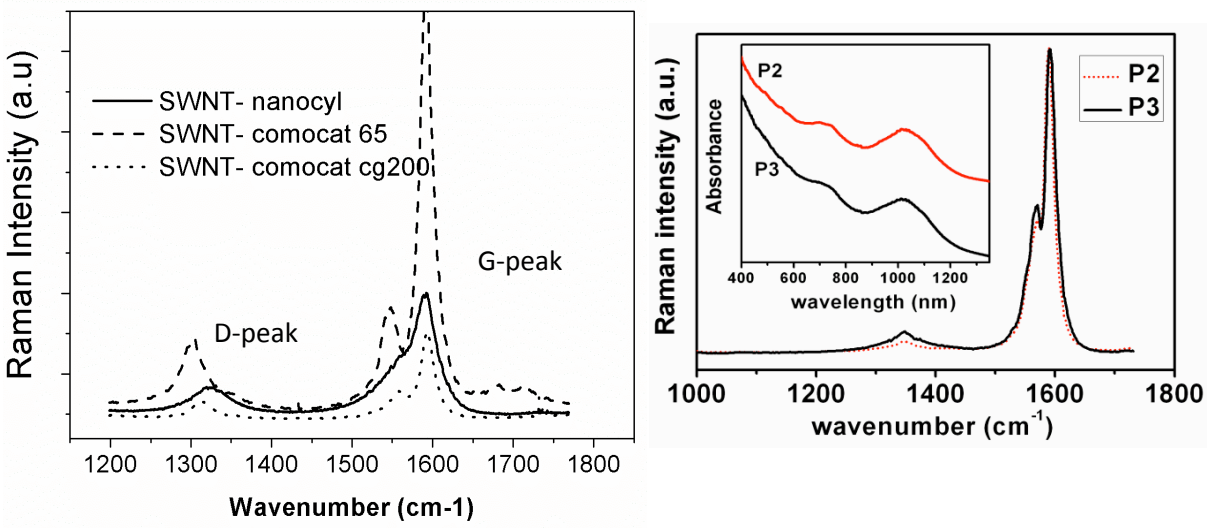

Figure 4-4. Raman spectra of different single walled carbon nanotubes, CoMoCAT SWNT (left) and Arc Discharge SWNT (right)

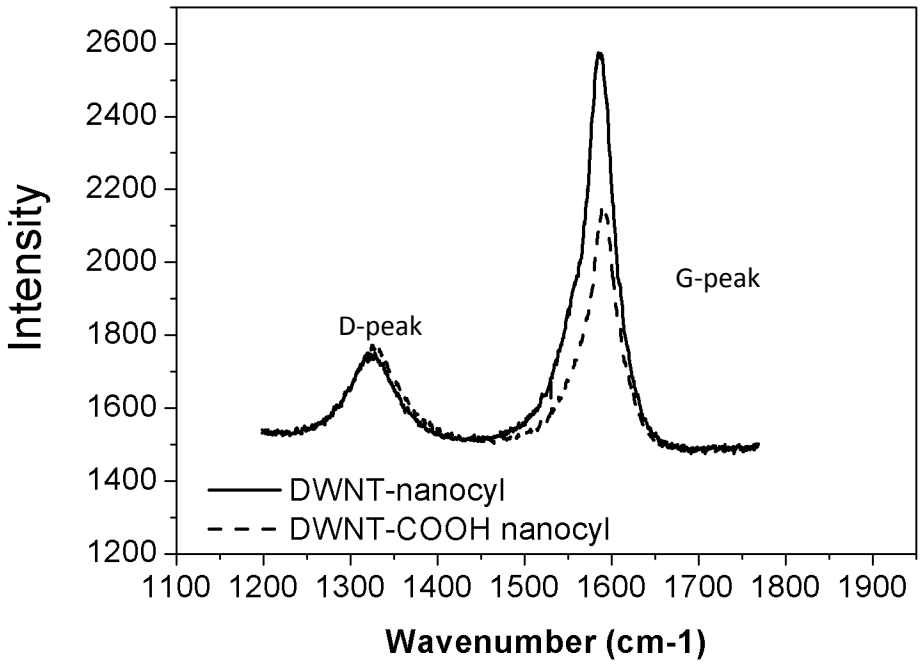

Figure 4-5. Raman spectra of pristine and carboxyl DWNT carbon nanotubes from Nanocyl

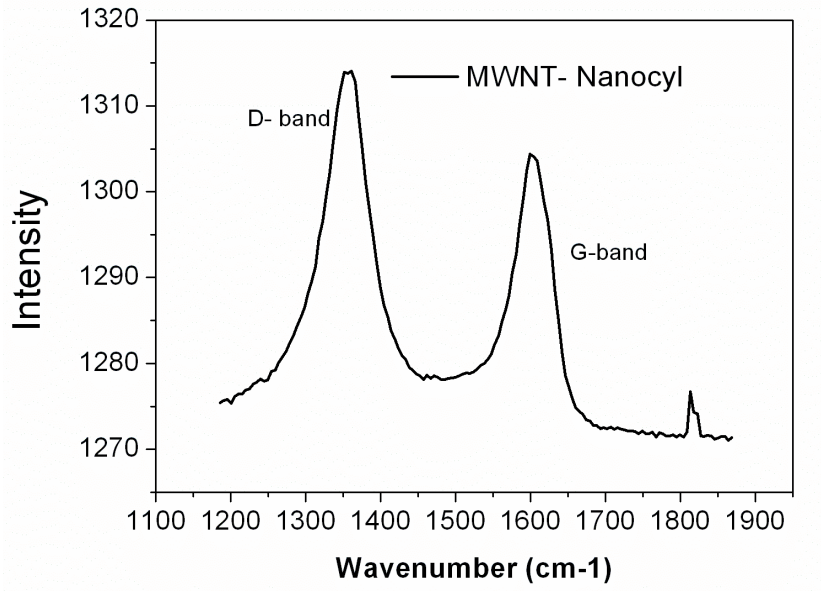

Figure 4-6. Raman Spectra of Nanocyl multiwalled carbon nanotubes

The data in figure 4-2 to 4-6 showed that the properties of CNT from different sources are dramatically different and will affect the conductivity of the resulting thin films significantly. CNTs with a high G/D Raman spectroscopy ratio would make lower resistance films, whereas carbon nanotubes with high D peaks would normally give poor conductivity films. Single-walled nanotubes in this case showed better conductivity compared to double walled or multi walled carbon nanotubes due to their low D peak, which means SWNT have fewer impurities or defects. From figure 4-4, P3 CNTs showed a G/D ratio of more than 20, whereas the other showed a G/D ratio starting from 4 (nanocyl) to 8 (CoMoCAT).

For the SWNT series, it was shown that both P3 and P2 arc discharge CNT thin films attained the best conductivity. From the absorption spectra, two broad peaks were observed that indicated the dispersion of the SWNTs to be in bundles and the presence of many different species of CNTs. The S11 absorption peak at around 1800 nm shown in figure 4.8, suggests that the diameter of carbon nanotube is large (about 1.4 nm).[88]

The CNTs with the second best conductivity was CoMoCAT CG200, and was followed by CoMoCAT 76 CNT. All the CoMoCAT CNTs had absorption spectra with sharp and distinct peaks as shown in Figure 4-7 that indicated the CNTs consisted only of a few CNT species. From the RBM spectra and S11 absorption peak of CoMoCAT CNTs, most of the nanotubes were shown to possess smaller diameters. CoMoCAT CG 200 (S11 at 1200 nm-1400 nm) had a larger diameter compared to CoMoCAT 76 (S11 at 1100-1200 nm), and CoMoCAT 76 had a larger diameter than CoMoCAT 65 (S11 at 1000 nm). [88]

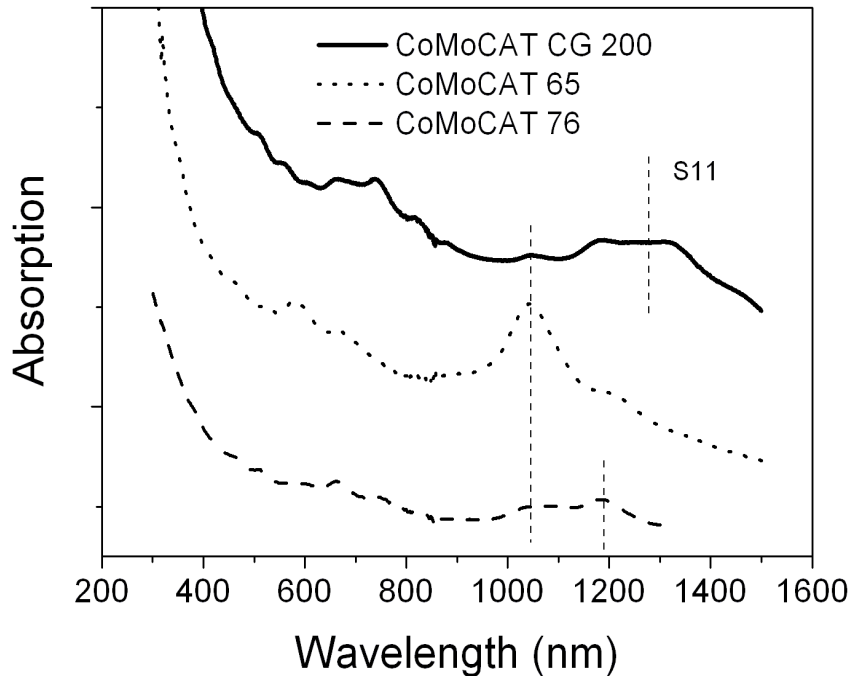

Figure 4-7. Absorption spectra of CoMoCAT CNT

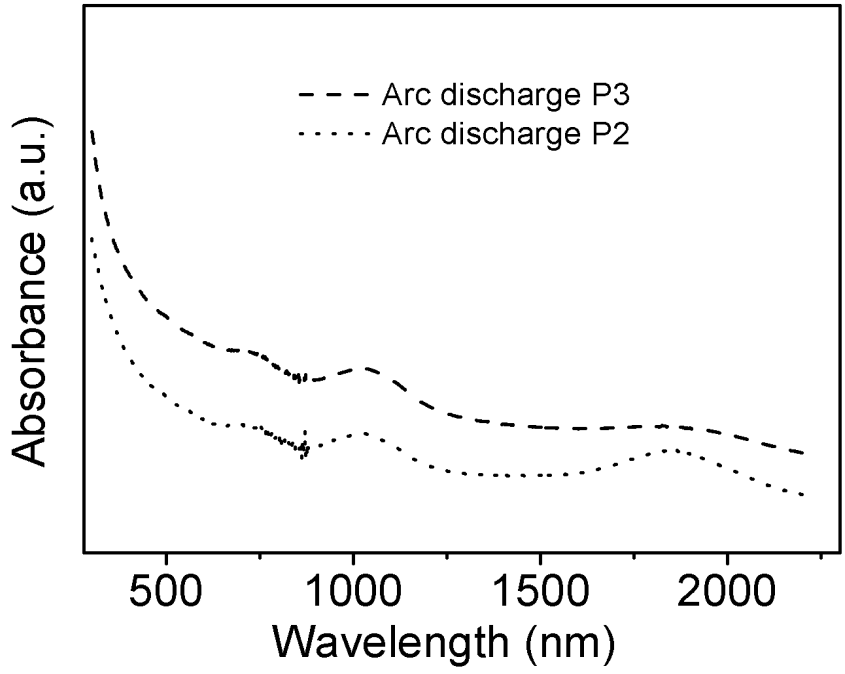

Figure 4-8. Absorption spectra P2 and P3

Surprisingly, CNT diameters correlated directly to their conductivity. This shows that CNT diameter is an important factor in obtaining high conductivity films.

Among all SWNTs used, Nanocyl SWNT, the only one with 80% of purity instead of over 90% purity, had the lowest conductivity. This observation is in line with Raman Spectroscopy data showing the lower G/D ratio of Nanocyl SWNT compared to P3 and CoMoCAT CNTs. From the data gathered, several conclusions can be drawn on the effect of CNT feedstock on the properties of conductive CNT films:

- Larger diameter CNT favour better conductivity. There were several advantages of large diameter carbon nanotubes: greater carrier concentration, greater elasticity to endure forces applied so as to retain its length during solubilization, lower tendency to chemical reaction (chemically more stable), and a smaller bandgap for the semiconducting species.
- The purity of CNTs was important as the presence of amorphous carbon degrades its conductivity (shown in the case of 80% purity Nanocyl SWNT)
- CNTs with similar chirality did not yield any advantages in the fabrication of conductive CNT films. CoMoCAT 65 had a 95% population of (6,5) chirality carbon nanotubes, yet its conductivity was inferior compared to P2, P3 and CG200, which were a mixture of several carbon nanotubes. CoMoCAT CG 200, which had metallic selectivity, also did not give a better performance than P3 arc discharge CNTs with a totally random population. Hence, it was clear that a better approach to improve CNT film properties was to get larger diameter carbon nanotubes with improved quality (better purity) rather than to perform separation of CNTs.

From the Double Walled Carbon Nanotube (DWNT) data, it could be seen from the Raman Spectra that the G/D ratio of the Nanocyl DWNT was not as

high as that of the SWNTs as shown in figure 4-5. Pristine DWNT showed a G/D ratio of 4 and –COOH functionalized DWNT showed a G/D ratio of 2.5. High D peaks may have resulted from impurities or defects. Defects could have been introduced by some treatments in purification or non-optimized synthesis conditions. The benefit of DWNT was its ease of fabrication that allows it to be fabricated on a large scale by the floating catalyst method, [81] but the quality of carbon nanotubes needs to be improved before it can be used as conductive films.

The Raman Spectra of Nanocyl Multiwalled Carbon Nanotubes (MWNT) was observed to have the lowest G/D ratio. This indicates that there were many dangling bonds, amorphous carbon and defects present in the carbon nanotubes. From this data analysis, the reason for the low quality of the as-prepared conductive MWNT films became clear.

In conclusion, there are two key parameters for good carbon nanotube precursors. The first is high G/D ratio obtained from Raman spectroscopy. This data assures us that the carbon nanotubse have fewer defects or impurities and this affects film conductivity a lot. The second is that larger diameter carbon nanotubes will yield better conductivity films.

4.2 Solubilization of Carbon Nanotubes

The concentration of dissolved carbon nanotubes in solution needs to be optimized to achieve optimum dispersion and yield for the fabrication of carbon nanotube films. There are several factors to be considered for this optimization. The yield of carbon nanotube being utilized, fabrication time, and the resulting conductivity of films are three most important parameters. The yield of carbon

nanotubes is characterized by observing how much of the carbon nanotubes could be dispersed in solution after centrifugation, and this factor is limited by the maximum solubility of carbon nanotubes inside the solvent.

The higher the carbon nanotube concentration inside the solution, the faster the deposition time, because a smaller number of coatings is needed. However there is a limit on how concentrated we can make a solution of carbon nanotubes, and different concentrations might affect the properties of the fabricated thin films. There are several ways to increase carbon nanotube concentrations inside solution: increase the initial carbon nanotube mass on the solution, put the solution under more rigorous ultrasound mixing, incorporate surfactants, functionalize carbon nanotubes with –COOH groups, and select a better solvent.

4.2.1 Mass of carbon nanotube powder inside solution

Since carbon nanotubes with the functional group (P3) have a certain solubility limit in water, a study in this section will determine the optimum upper limit of carbon nanotube solubility. The yield of carbon nanotubes inside solution was characterized by comparing the absolute UV-vis-NIR absorption of the carbon nanotube solution. Figure 4-9 shows an absorption spectroscopy for P3 carbon nanotubes in water.

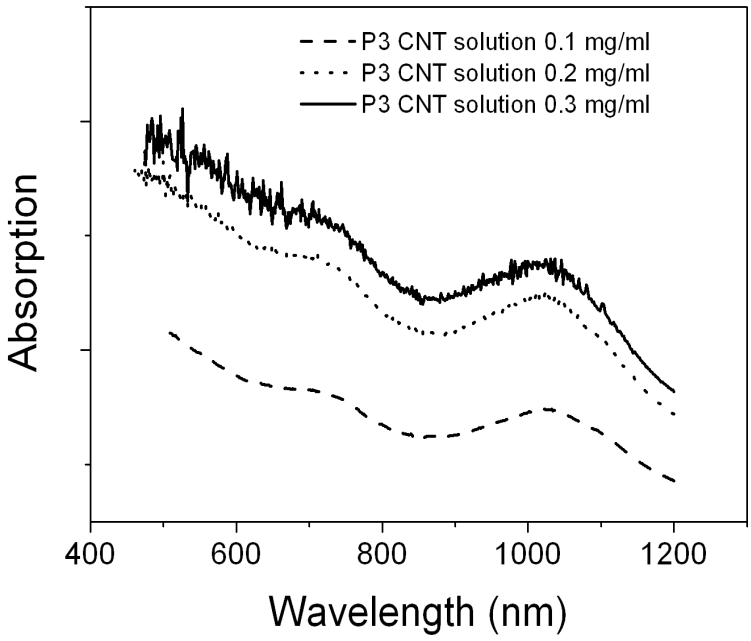

Figure 4-9. UV- vis spectroscopy of P3 solution in different concentration

It was observed that when CNT concentration is increased from 0.1 mg/ml to 0.2 mg/ml there was significant increase in carbon nanotube absorption signal, which was proportional to the amount of carbon nanotube inside the solution. At 0.2 mg/ml to 0.3 mg/ml, there was only a slight increase in the absorption signal. This indicated that the maximum concentration of carbon nanotubes inside solution was reached at a concentration between 0.2 to 0.3 mg/ml.

The sheet resistances of the resulting conductive films made by all these carbon nanotube solutions are shown in Table 9, and at below 0.1 mg/ml concentration, decent conductive films could not be produced. A possible reason for this is that at low concentrations it is difficult to form conductive networks of nanotubes by using the airspraying method. 0.2 mg/ml was observed to be the optimum concentration, since it showed the similar conductivity to 0.1 mg/ml and a lower volume needed to fabricate similar transparent films. A lower volume consumed would translate to faster film fabrication.

Table 4-3. Correlation between carbon nanotube concentration and the solution quality

Initial concentration	Rs average value	Transmittance	Volume used
0.2 mg/ml	294 Ohm/sq	65%	2ml
0.1 mg/ml	592 Ohm/sq	79%	2ml
0.1 mg/ml	273 Ohm/sq	63%	4ml
0.05 mg/ml	14200 Ohm/sq	94%	2ml
0.05 mg/ml	1302 Ohm/sq	82%	8 ml

4.2.2. Selection of Surfactant and Concentration

Carbon Nanotubes are made up of π-conjugated and highly hydrophobic sidewalls, making them very insoluble in water, and are only soluble in several specific organic solvents, such as dichlorobenzene, dimethyl formamide, tetrahydrofurane, n-methyl pyrrolydone. [90-93] However, in order to disperse CNT as a thin film onto substrates, it is more effective to dissolve it in a solvent first. It is then necessary to add in surfactants or aromatic compounds which will have a strong π- π interaction with the tubes. [94-96]

Many studies are focused on finding an option that will fully dissolve CNTs without chemically reacting with the CNT. It has been discovered that the surfactants are able to break up the CNT bundles, and stabilize each individual CNT tube. [96] Amongst the choice of surfactants, the most popular candidate for dissolving CNTs in water is the anionic surfactant sodium dodecylbenzenesulfonate (SDBS). [97-100]

Therefore, in this section, we carried out a series of investigations on the different types of surfactants with different concentrations. In our experiment, we only focused on one type of carbon nanotube.

In addition to SDBS, we also tried four different surfactants: Sodium Dodecyl Sulphate (SDS), Sodium Cholate (SC), Triton X-100, initially tested with a fixed concentration of 1 wt%.

Table 4-4. Summary of 4 different common surfactants used for film fabrication

Surfactant	***CNT***	***Sheet resistance***	***Trans-mittance***	***Remarks***
SDS 1%	P3	-	-	Not able to measure readings as film peels off when water washed.
Sodium Cholate 1%	P3	-	-	Not able to measure readings as film peels off when water washed
SDBS 1%	P3	978 ohm/sq	85%	
Triton X 1 %	P3	8581 ohm/sq	83%	Shows low affinity to water, hence ineffective washing

The results in Table 4-4 show that even though there were many surfactants that could be used to disperse carbon nanotubes, only SDBS was suitable for conductive film fabrication because it can be removed easily. The interaction between the SDS surfactant and carbon nanotube is much weaker than that between the SDBS surfactant and carbon nanotubes, due to the presence of the

benzene ring in SDBS that is able to form π- π interaction with carbon nanotube sidewalls [91]. These weak interactions of SDS leave a gap between one carbon nanotube and another, hence resulting in weak van der walls forces between each nanotube in the film. Therefore, during the water rinsing, these van der walls forces can easily be broken by mechanical forces of flowing water during the removal of surfactants. On the other hand, SDBS surfactants attached strongly to the carbon nanotubes and increase the packing density of the film, which is very helpful in forming stronger van der waals forces between each tubes. Clearly, stronger van der waals forces would allow it to stay intact even though the surfactant is being dissolved in water. SDS surfactants could only be used in hydrophobic substrates such as PET (Poly ethylene terephtalate), as the interaction between the carbon nanotubes and substrate can help the carbon nanotube film to stay intact during the removal of the surfactant. For Triton X, this is a non-ionic surfactant, which has less affinity to water. That means for Triton X, water rinsing could not be used to remove it and several cycles of acid rinsing was needed to remove Triton X from the carbon nanotube film.

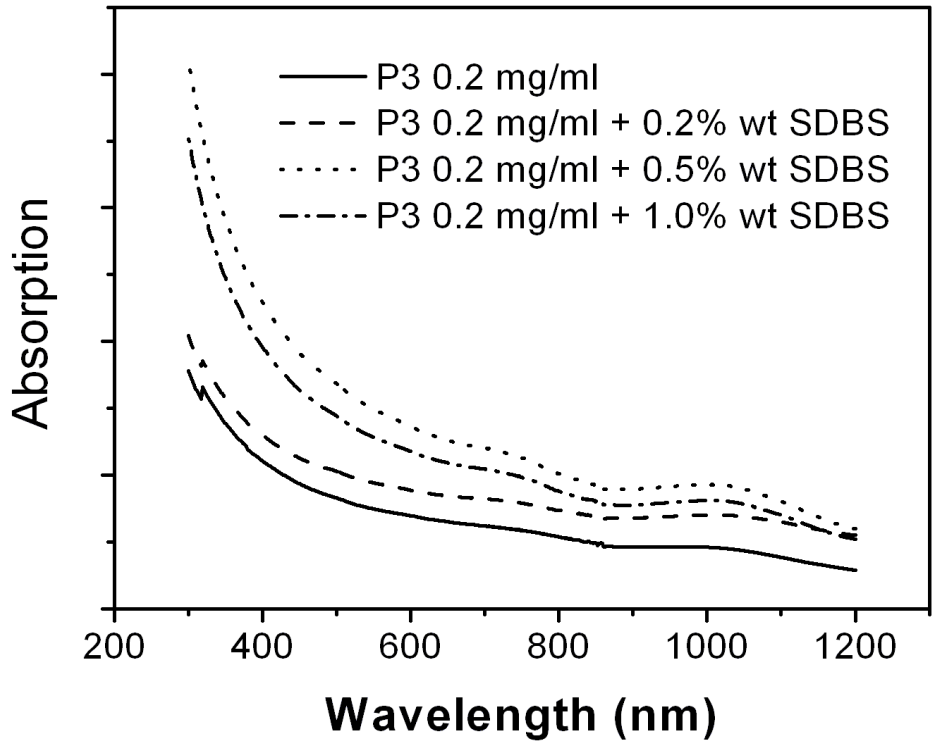

Figure 4-12. UV- Vis Spectroscopy of P3 solution with different surfactant concentration

Figure 4-12 shows that a 0.5wt% of SDBS could dissolve the most carbon nanotubes, which suggests that it is the optimum concentration that should be used. It is important to note that adding surfactants beyond 0.5 wt% did not increase the solubility of carbon nanotubes in the solvent. Excessive surfactants inside the solution would reduce CNT solubility and cause difficulties in surfactant removal.

Table 4-5. Sheet resistance of different carbon nanotube surfactant formulation

Surfactant	CNT	Resistivity	Transparencies
SDBS 0.25%	P3	912 Ohm/Sq	82%
SDBS 0.5%	P3	642 Ohm/Sq	80%
SDBS 1 %	P3	837 Ohm/Sq	80.9%

In table 4-5, it is shown that an optimum concentration of surfactant also results in better conductivity of carbon nanotubes. Optimum surfactant contents gave a better dispersion of nanotubes, both in solution and substrate. Excess surfactant present between nanotubes will be detrimental as the spaces, initially occupied by the surfactant, would be voids after its removal. However insufficient surfactants would cause the inadequate dispersion of CNTs in the solvent.

4.2.3 Selection of Solvent

Using organic solvents, it is possible to formulate a carbon nanotube solution without usage of surfactants. Dimethyl formamide (DMF) was chosen due to its lower toxicity compared to other solvents.

Normal thin film fabrication was carried out. An organic solvent was used to replace water. Due to high boiling point of organic solvents, a higher temperature deposition was necessary and hence the deposition temperature was increased to 120^{o}C.

Our investigation suggested that the sheet resistances of these films are usually high, in the range of ~8000 ohm/sq @ 70% transmittance. Similar carbon nanotubes (P3) dissolved in water could generate a much better sheet resistance of ~ 300 ohm/sq @70% transmittance. Though other sources mentioned that DMF solutions were able to obtain relatively good sheet resistance films (i.e 380 Ohm/sq at 80% using laser ablation CNT) [70], our experiment showed different results. Some possible reasons are:

- A difference in the type of CNT used : laser ablation CNTs are believed to have longer length, better purity and less defects due to fewer purification steps needed.
- The contamination of the DMF solvent: since all of our experiments were conducted in an ambient environment, contamination could not be avoided.
- Since the DMF solvent can cause N-doping, it may counteract oxygen p-doping from the atmosphere.

The CNTs formulation by DMF solvent was drop-casted into the substrate and was characterized using FE-SEM. We found many glue-like structures in the films and the network density was very low as shown in figure 4-13. It was suspected that there were contaminants trapped between the junctions of the CNT bundles, causing the junction resistance to be very high. CNT films from water solution, shown in figure 4-14, showed better density and cleaner morphology.

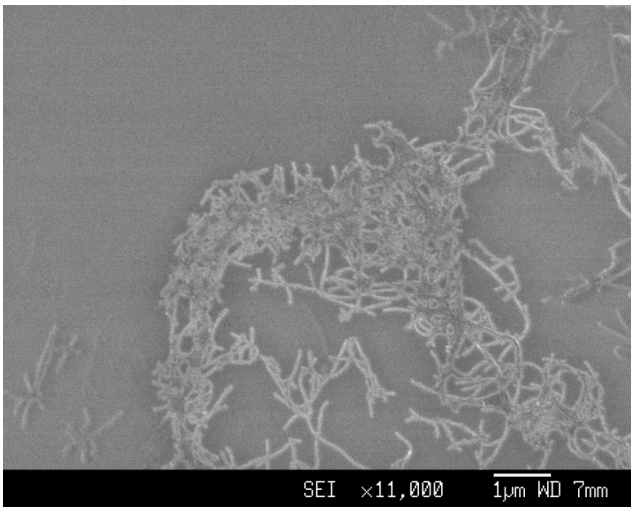

Figure 4-13. FE-SEM Image of samples deposited from DMF solution, with some glue-like features

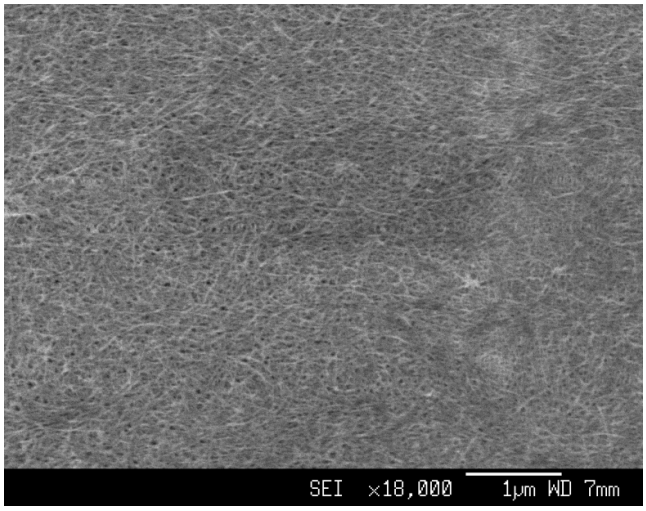

Figure 4-14. FE-SEM images of drop casted CNT solution dissolved in water, showing clean CNT networks.

A low temperature deposition is desirable for the solution deposition process because the condition will be compatible to many different substrates; on the other hand, faster drying is also necessary to provide a higher deposition throughput process.

The current temperature that was applied during deposition (100 ^{o}C) was considered too high for flexible substrate deposition. PET, a common flexible substrate undergoes glass transition at 70 ^{o}C. A lower temperature like 70 ^{o}C could be used for the same solution, however the fabrication throughput will decrease substantially because we need to wait until all the droplets evaporate after each spray. A lower boiling point solvent (i.e. alcohol) was needed for flexible substrate deposition. Due to alcohol hydrophilicity, it could only dissolve carbon nanotubes with a –COOH functional group.

A P3 Carbon nanotube solution with ethanol and methanol solvent was produced and characterized. The UV-vis-NIR spectroscopy of these solutions can be observed in Figure 4-15. It is shown that alcohol could not dissolve as many carbon nanotubes as water did.

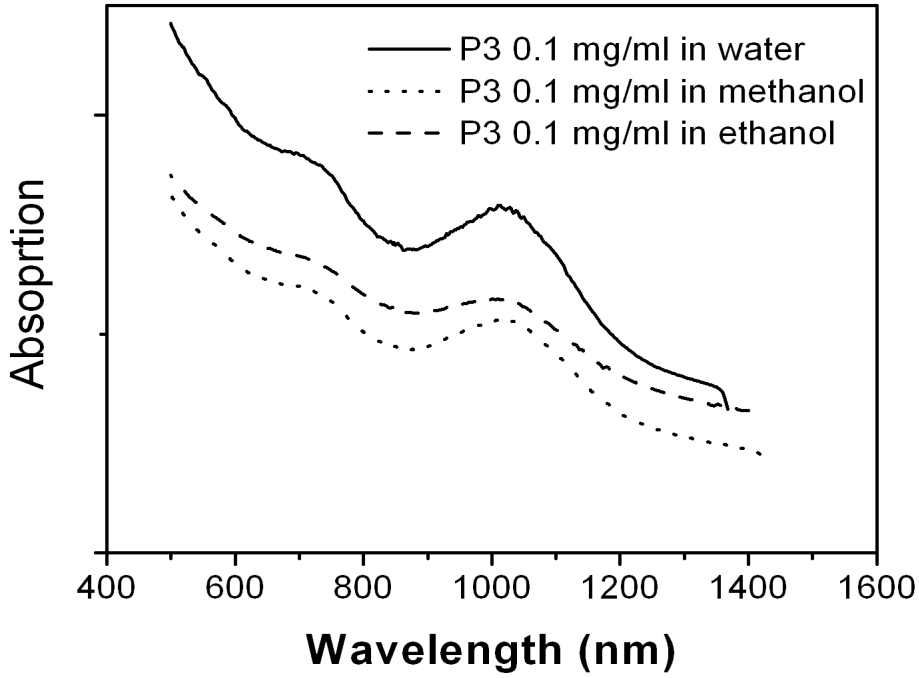

Figure 4-15. UV-Vis Absorption for P3 carbon nanotube in different solvent

The figure 4-16 below shows the sheet resistance of CNT films deposited from solutions of different solvents.

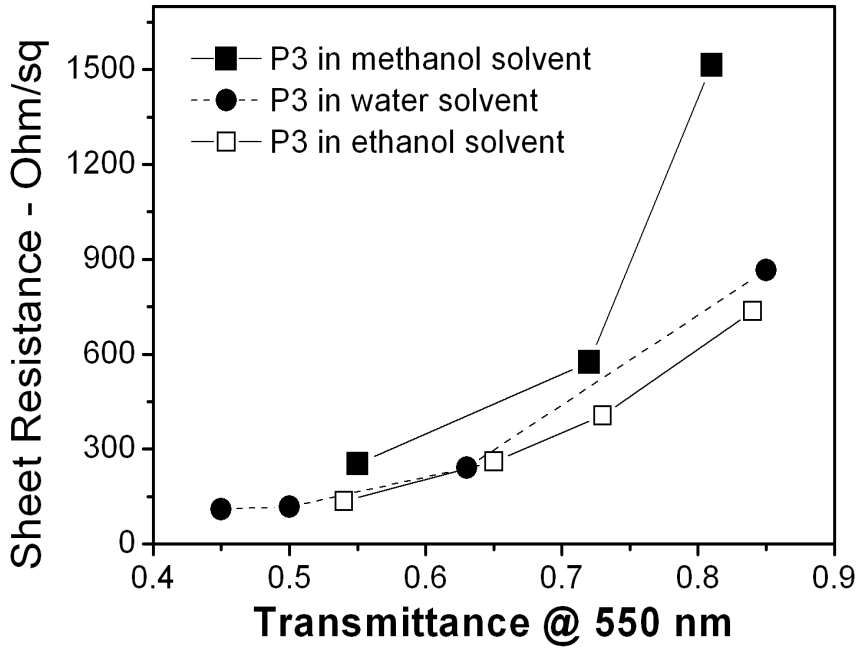

Figure 4-16. Effect of different solvents on P3-SWCNT films

Solvents are found to be crucial especially at the high transmittance ranges. At this range, CNTs coverage on the substrate is extremely important. The CNT solution might not have adequate time to wet the surface with fast evaporating solvents like methanol. However, with too slow a solvent evaporation speed, i.e. with water, CNTs tend to agglomerate to form non-uniform films. Therefore, the evaporation rate must be controlled in order to get a good dispersion. At 60% transparencies and below, all the three solvents give a similar performance. However, at higher transparencies, ethanol yielded better sheet resistance.

Although water gives a similar range of resistance values, it tends to cause non-uniformity of the film at higher transmittance films, due to the slower evaporation rate. Also, some features such as coffee ring patterns also appear in water based CNT solutions. However, this morphology was not shown in CNT ethanol solutions. This may be the reason why at higher transmittance the ethanol-based solution could give a lower sheet resistance. Its uniform coverage without the presence of coffee ring patterns would make forming interconnecting percolating networks easier. However as the deposition continues, even samples with coffee ring pattern (water solvent) would be able to form similar degrees of interconnecting percolating networks, hence it is observed that both solutions eventually could yield good sheet resistance films at transmittance level below 60%.

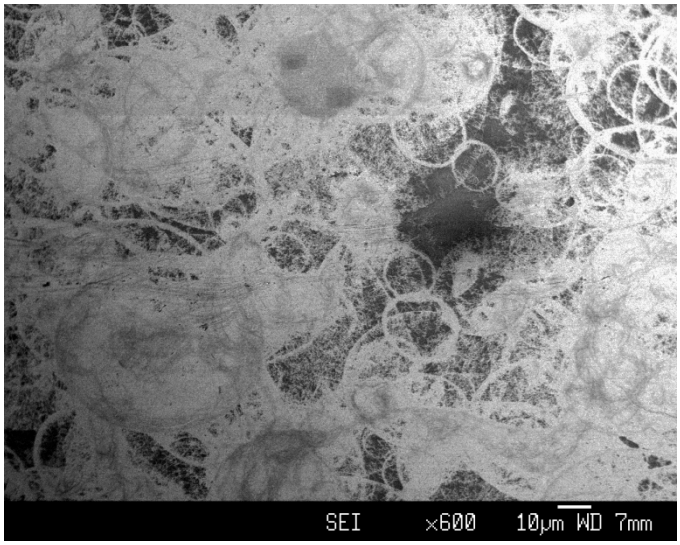

Figure 4-17a. SEM image of coffee ring pattern formed by CNT.

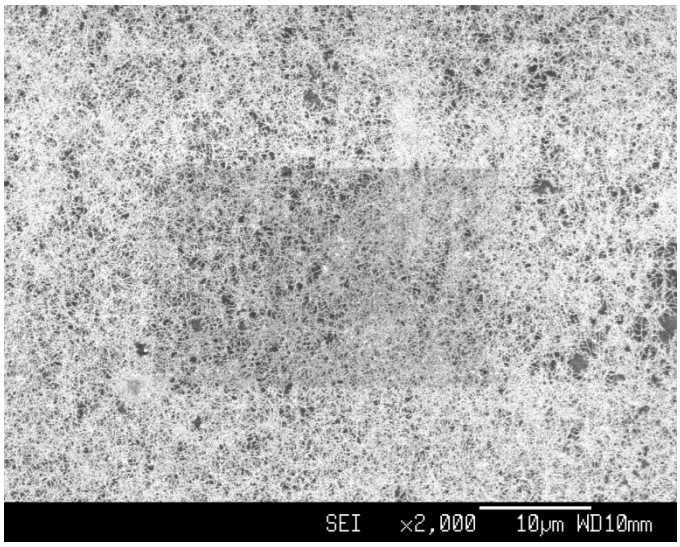

Figure 4-17b. SEM image of sample deposited from ethanol solution.

Another concern of choosing different solvents was the difference in solubility and stability, which in turn affects process yield as well. According to figure 4-16, which shows the absorption graph of CNTs dissolved in various solvents, water could dissolve much more carbon nanotubes compared to ethanol or methanol. The ethanolic solution of carbon nanotubes solution is prone to agglomeration. High temperature heating at 60 degree C as a byproduct of ultrasonic treatment and water contamination caused agglomeration. Even

though the properties of ethanol dissolved carbon nanotube are better, the solution of carbon nanotubes in ethanol is difficult to handle.

In order to enhance carbon nanotube solution stability and also to enable the ethanol solvent to be used for different types of carbon nanotubes other than those with carboxyl functional group, it is necessary to employ surfactants. However the addition of surfactants into carbon nanotube solutions is unable to form a uniform solution due to the lack of solubility of the surfactant in ethanol.

Table 4-6. Observation of alcohol-surfactant formulation

Solvent	Surfactant	Observation
Ethanol	SDBS 0.5%	Surfactant unable to dissolve in ethanol
Ethanol	SDS 0.5%	Surfactant unable to dissolve in ethanol
Ethanol	Triton 0.5%	Surfactant could be dissolved in ethanol however the resulting solution unable to disperse CNT
Ethanol/Water	SDBS 0.5%	Surfactant unable to dissolve in ethanol
Ethanol/Water	SDS 0.5%	Surfactant unable to dissolve in ethanol
Ethanol/Water	Triton 0.5%	Surfactant could be dissolved in ethanol however the resulting solution unable to disperse CNT

Figure 4-18. Suspension of SDBS surfactant in ethanol solvent

An understanding on surfactant behaviour, micelle formation in ethanol or ethanol-water mixture, needs to be obtained beforehand. An effort to use different types of alcohol from methanol to propanol and different mixture ratio was made without success. Unfortunately up to this point, we were unable to obtain a uniform ethanolic solution of carbon nanotubes with surfactants.

4.2.4 Ultrasonic Treatment of Carbon Nanotube Formulation

Ultrasonic treatment is needed to disperse carbon nanotubes in solvents. Solutions made from bath ultrasonication and probe ultrasonication were compared. All the solutions were centrifuged at 6000 g-force after ultrasonication.

There are two phenomena occurring during the ultrasonication, the debundling of CNTs that make it dissolve more into the solution, and the mechanical cutting of nanotubes into smaller length due to the ultrasonic wave power. Bath ultrasonication is milder and is compatible for batch production, so we would expect less damage done to the CNTs. However the lower power might not efficiently disperse carbon nanotubes.

It is shown in the graph figure 4-19a that probe sonication could disperse a much higher concentration of carbon nanotubes in the solution and results in

better conductivity films as shown in figure 4-19b. Thus, it suggested that the debundling of CNTs is more crucial than the length of the CNTs, or perhaps that the length of CNTs is not severely affected at this rate. According to AFM images, the length of the CNT bundles was still about 1 micrometer even after 30 minutes of probe ultrasonication. Also, some agglomeration of CNTs was observed in the bath sonicated solution by the naked eye, which suggests excessive bundling occurs. Excessive bundling is detrimental to CNT film properties because it renders a non-uniform dispersion of CNTs and degrades the transmittance of CNT films.

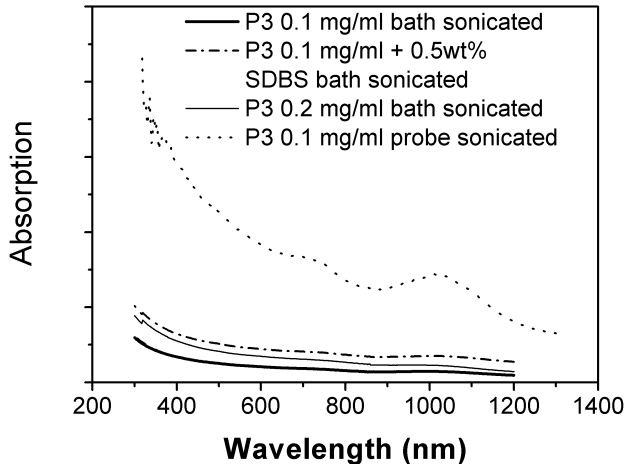

Figure 4-19a. UV-vis absorption of different ultrasound treatment

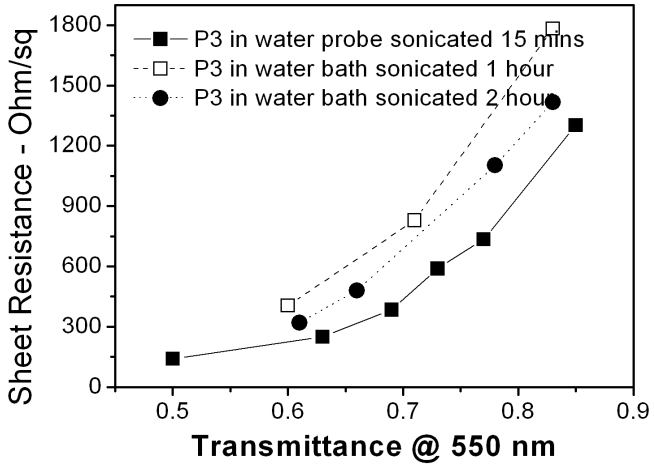

Figure 4-19b. Effect of different ultrasound treatment on film properties.

In conclusion, even though the bath ultrasonic treatment processing is more desirable, its power is not enough to debundle carbon nanotubes to create a good dispersion of it in solvent. Only in small diameter carbon nanotubes, i.e. CoMoCAT 76 it can be seen that the concentration of carbon nanotubse dissolved by bath ultrasonic treatment is comparable to probe ultrasonic treatment, and this concentration is good enough to be used in the airspraying method. Some films are actually fabricated and both methods show similar sheet resistances. However as CoMoCAT 76 is not the best feedstock, study on this matter was not pursued further.

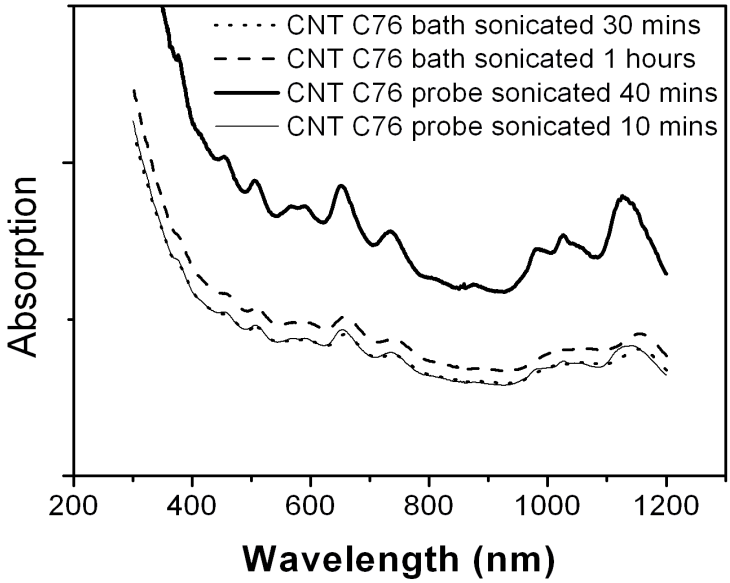

Figure 4-20. Effect of different ultrasound treatment on dissolution of small diameter CoMoCAT

Though probe sonication was shown to give a better result, the duration still needed to be optimized. Even though debundling of CNTs is crucial, that does not mean that a longer ultrasonication duration will give the better solution because, at a certain point, mechanical cutting on carbon nanotubes will eventually take place, and this is surely detrimental to the film properties. Thus it is important to find the optimum ultrasonication time.

Table 4.7 below shows the sheet resistance and transparency of CNT films fabricated from solutions with different probe sonication times.

Table 4-7. Properties of CNT films fabricated from solutions with different sonication time.

Volume sprayed	Time of sonication	Sheet resistance (ohm/sq)	Transmittance at 550 nm
2ml	10 mins	4008	93%
4ml	10 mins	1072	85%
2ml	20 mins	1032	85%
4ml	20 mins	506	75%
2ml	30 mins	556	80%
4ml	30 mins	244	62%
2ml	40 mins	1763	87%
4ml	40 mins	503	71%

It was observed that there was not much difference between solutions sonicated for 20 minutes and 30 minutes. Both solutions yielded similar sheet resistances and transparency films. with a longer sonication time, i.e. 40 minutes of sonication, the film fabricated was not as good as that with a 30 minute sonication, which indicates mechanical cutting start to occur at 40 minutes of ultrasonication. Mechanical cutting could occur after extended periods of time due to the help of heat built-up inside the solution after certain period of time.

The choice for optimum ultrasonication durations should take into account another parameter: the yield of CNT solutions. All the CNT films ultrasonicated for 20 to 30 minutes produced similar properties of films in terms of sheet

resistance and transmittance, however at 30 minutes of ultrasonication duration, a lower amount of CNTs (in terms of ml) is needed to fabricate the films.

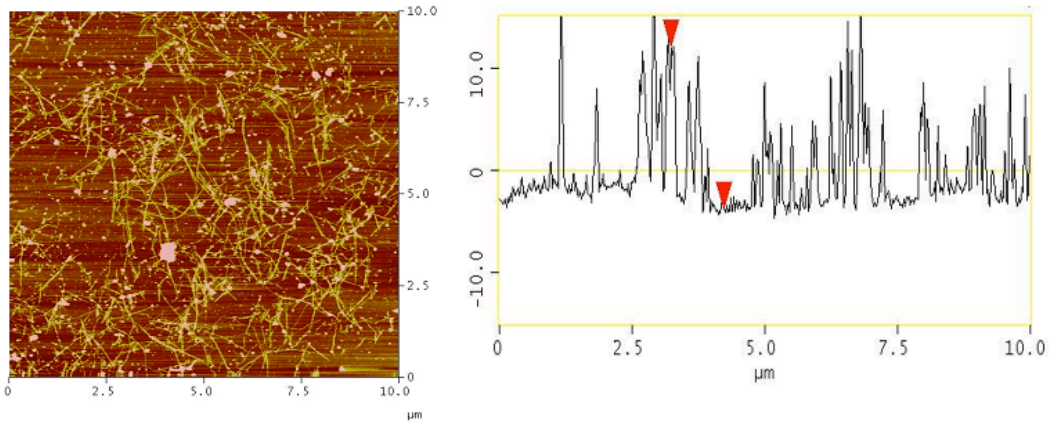

Figure 4-21. AFM image of optimum SWNT solution dropcasted into SIO2 substrate (left) and the section analysis (right).

4.2.5 Centrifugation

The purpose of centrifugation is to filter out large bundles of CNTs, amorphous carbon particles, and other impurities. The principle of centrifugation is to use centrifugal forces during rotation to force heavy mass particles to settle down at the bottom. So in a way centrifugation is a separation method dependent on its mass.

We expect that amorphous carbon particles, other impurities and the large bundles of CNTs possess a higher mass compared to single or small bundles of CNTs, so by centrifugation we would be able to separate them. However, long bundles of CNTs also have heavier mass than shorter ones, so there is a need to compromise in choosing the right centrifugation power.

We carried out a series of centrifugation studies starting with one stock solution of P3-SWNT, ultrasonicated at the same time, but centrifuged at 3 different centrifugation speeds.

Table 4-8. Effect of centrifugation speed on CNT films sheet resistance.

	Centrifugation speed	**Rs average for 3 samples**
P3 0.1 mg/ml in water	2500 G force	378 @ T=74%
P3 0.1 mg/ml in water	5000 G forece	335 @ T=71%
P3 0.1 mg/ml in water	10000 G force	923 @ T=76%

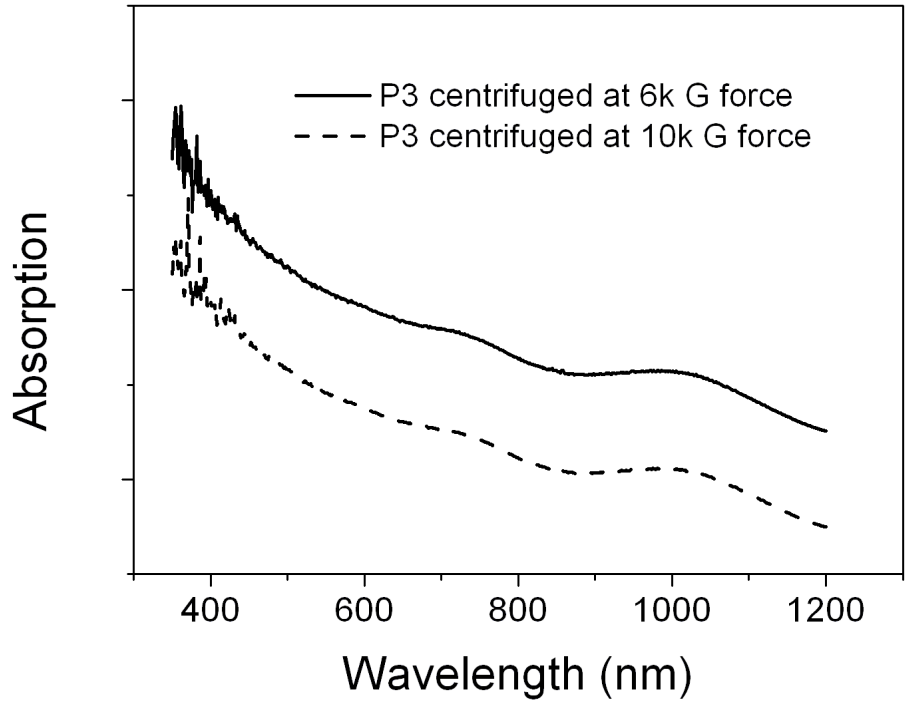

Figure 4-22. UV-vis spectroscopy of CNT centrifuged with different power

According to the data obtained, too high a centrifugation speed is not favorable for conductive thin film fabrication. Some of the possible reasons would be:

- Long length bundles of CNTs settled down as a precipitate, so the supernatant only consists of short CNT bundles.

- The CNT bundles that remain are very small, hence it is less probable to find metallic tubes in each bundles, once this happened, junction resistance between semiconducting and metallic would dominate.
- The concentration of the centrifuged solution becomes very low as shown in figure 4-22. According to previous investigations, if the concentration of CNTs is below a certain threshold, the property of dispersion becomes very poor and is not suitable to be used in conductive film applications.

4.3 Sensitivity and Stability of Carboxylated Carbon Nanotube Solution

Another experiment done in this section was on the stability of carboxylated CNT dispersion, i.e. under what conditions and formulation would the CNTs in the solution stay in a well-dispersed state. Experiments were done on the effect of pH changes, ion concentration changes and presence of co-solvents. Observations would simply be made on whether there is any agglomeration occurring in CNT solution.

Table 4-9. Factors affecting the dispersion of CNTs in solutions.

Carbon Nanotube solution	Chemicals added in	Changes in	Observation
P3- water	Acid (HCl, HNO_3, H_2SO_4)	pH and ion concentration	Agglomeration
P3- water	Salt (NaCl, Na_2SO_4)	Ion concentration	Agglomeration
P3- water	Base (NaOH, KOH)	pH and ion concentration	Agglomeration
P3- water	Ethanol	Solvent interaction	Agglomeration

It is shown from this experiment, that the dispersion of COOH-functionalized CNTs in water is very sensitive to the addition of different chemicals. Changes in pH and ion concentration could significantly affect its stability (a slight change of pH from 5.5 to 4 would cause agglomeration). Thus the solution solubilisation process should be kept free from acids/base and salt contamination. Furthermore the mixed solvents would also cause agglomeration problems. COOH-functionalized CNTs could be solubilised in polar solvents, but not in a mixture of polar solvents.

Changes in ion concentration or pH could easily alter the stability or charge neutrality of the solution, which would in turn reduce the dispersion stability; hence it is reasonable to see agglomeration due to this effect.

However agglomeration caused by mixture of polar solvents is very unusual. COOH-functionalized CNTs could be dissolved in both 100% ethanol and 100% water without any agglomeration. This phenomenon could be explained by interaction changes between two different systems. Initially with COOH functionalized SWNT and water or ethanol, the interaction between the COOH functional group and solvent is favourable, which is why we see a uniform dispersion of CNTs in solvent. However, with the addition of alcohol, the interaction of water and alcohol is stronger than with the COOH functionalized SWNT (water and alcohol would form an azeotropic mixture), which causes these SWNTs to start to agglomerate.

Therefore if some additives were to be added into CNT solutions, those additives will not disturb the solution's stability as long as it does not change the ion concentration or solvent interaction and it dissolves in the same solvent.

4.4 Dispersion Quality of Carbon Nanotube Solution

Dispersion quality of CNT solutions is one crucial aspect that determines the quality of conductive films deposited. However, there is no single method established to characterize the quality of dispersion of the CNT solutions. It was found out that 2-3 days old CNT solutions would show worse result compared to fresh solution in terms of resulting film conductivity. Based on this observation, we investigate and study the dispersion quality by its changes over a period time of 7 days as well as its conductivity.

Two parameters were included in this study: the presence of surfactants and CNT concentration. The surfactant used was 4-dodecylbenzenesulfonic acid (SDBS). CNT concentration could also influence the stability of the dispersion. If carbon nanotubes tend to attract each other, the increase in CNTs content would definitely degrade its stability. But if they repelled one another, the increase in CNT content would increase its stability instead. Surfactants on the other hand stabilize CNTs by having two groups with different polarities. Its long chain carbon will wrap around carbon nanotubes or form a π- π interactions with CNTs, whereas the other group will form permanent dipoles with water molecules. The surfactant stabilization effect is normally perceived to be more stable than carboxyl group stabilization, however the presence of surfactants in carbon nanotube solution is usually undesirable.

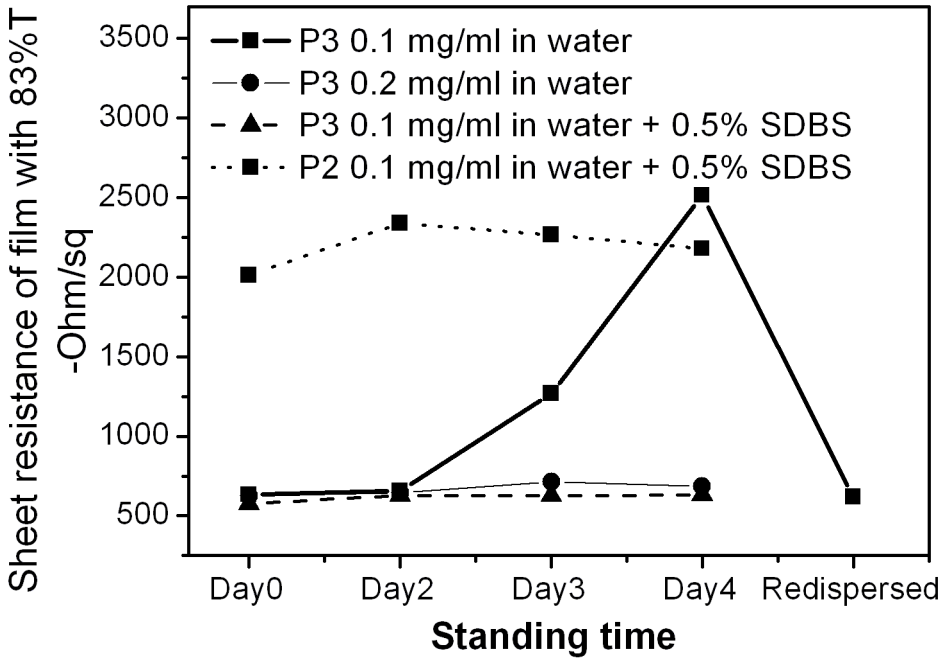

Figure 4-23. Sheet resistance of P3 and P2 CNT films deposited at 83% transmittance from a CNT solution after sonication for a number of days

Observation from figure 4-23, P3 CNT without any surfactant, at 0.1 mg/ml concentration, showed that the quality of the solution degraded after 3 days and required sonication to return to its original state. This piece of evidence clearly showed that the dispersion problem could result in a poor conductivity of the thin film deposited. With the addition of 0.5wt% of surfactant, the stability of the film improved and it remained stable for up to 7 days. Thus, we came to an initial conclusion that surfactants would help to stabilize CNT dispersion. Experiments by increasing and reducing the quantity of carbon nanotubes in the solution were also carried out. At a higher concentration of 0.2 mg/ml, two advantages were achieved. The deposition process was much faster as a lower quantity of solution was consumed and the quality of solution was surprisingly stable for up to 7 days.

The quality of CNT dispersion seems to be affected by the presence of surfactants and the CNT concentration. In the subsequent experiment, we compared P3 carbon nanotubes with concentration of 0.1 mg/ml with and without surfactants by the use of UV-vis spectroscopy on their relative absorbance.

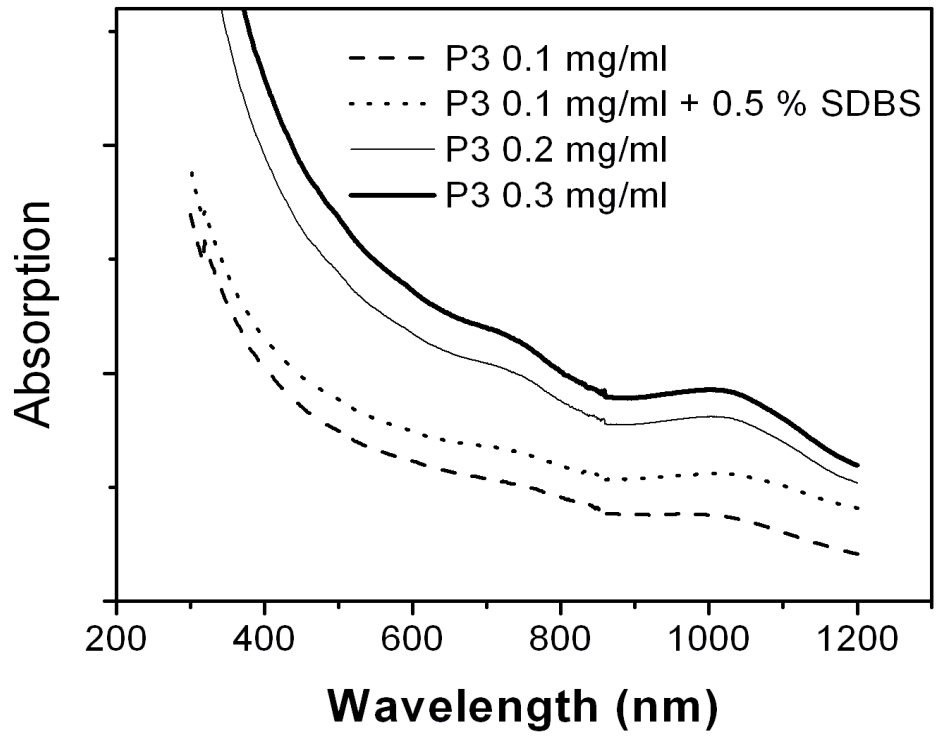

Figure 4-24. Changes in carbon nanotube solution concentration with different formulation

In Figure 4-23, it was observed that addition of 0.5wt% of SDBS surfactants increased the solubility of P3 CNTs. Hence, the final conclusion is that the addition of surfactants in P3 CNT solution increases its dissolved concentration and improves its dispersion. The increase of carboxyl stabilization capability with increasing concentration was due to the presence of –COOH functional groups in P3 CNTs that dissociate partially to form $–COO^-$ ions. These ions repel one another and aid in stabilizing the dispersion. In conclusion, higher

concentrations of such functionalized CNTs would lead to larger repulsion force between the carbon nanotubes and stabilize the dispersion.

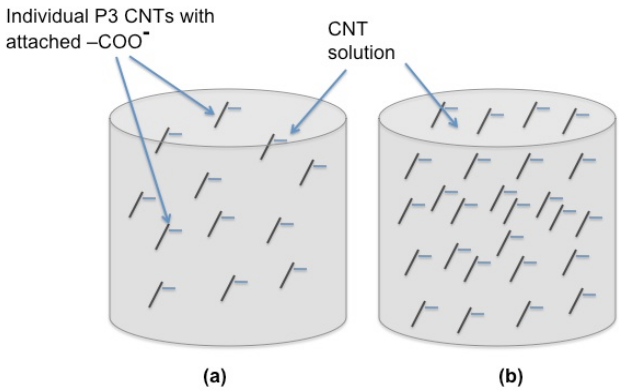

Figure 4-25. Diagrams of varying P3 CNT concentrations that influence the dispersion quality of CNTs. (a) lower CNTs (b) higher CNTs concentration

The best CNT film conductivity was achieved at 0.2 mg/ml concentration with 0.5wt% of SDBS. It was believed that while SDBS wraps around carbon nanotubes, sulfate ions had some contributions to stabilize the dispersion. The effect of CNT concentration on non-functionalized CNT solution was also investigated. CoMoCAT 76 carbon nanotube with different CNT concentrations from 0.1 mg/ml to 0.4mg/ml with 0.5wt% SDBS was fabricated and deposited as CNT thin films. Surfactant concentration was fixed at 0.5wt% as previous experiments suggested that a higher surfactant concentration would give rise to poor CNT solubility due to the difficulty of surfactant removal. The data is shown in figure 4-27. Increasing CNT concentration was shown to increase conductive film performance.

Two possible explanations were suggested for this phenomenon that may both occur at the same time. The first one was that with a higher CNT concentration, the collision probability of nanotubes increased due to higher number of collisions between each tube wrapped by SDBS that formed the sulfate ions in water. The collisions resulted in the repulsion between each tube

that in turn increased its Brownian motion activity and thus stabilized the dispersion and increased its conductive property.

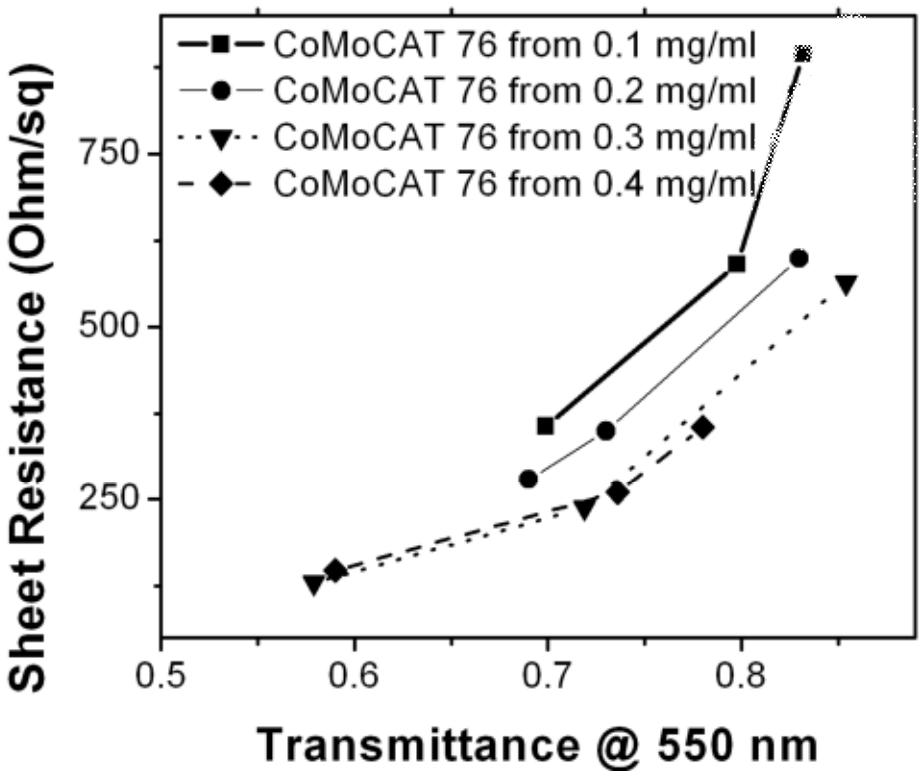

Figure 4-26. Resistance – Transmittance curve for CoMoCAT CNT with increasing CNT contents (fix surfactant content at 0.5wt%)

The second possible mechanism could be the presence of CNT bundles. By increasing CNT concentration and maintaining a certain amount of surfactants, it would raise the possibility of forming small bundles instead of individually dispersed CNTs. At a higher concentration of CNTs with a fixed surfactant amount, CoMoCAT CNT could also resolve into forming bundles. We believe that small bundles might be beneficial in lowering the resistivity because the contact resistance between each strand in the bundles would be lower than the contact resistance of two individual strands, as in Figure 4-27. However, if the

bundles became too large, it would degrade CNT film's light transmittance significantly, which is undesirable.

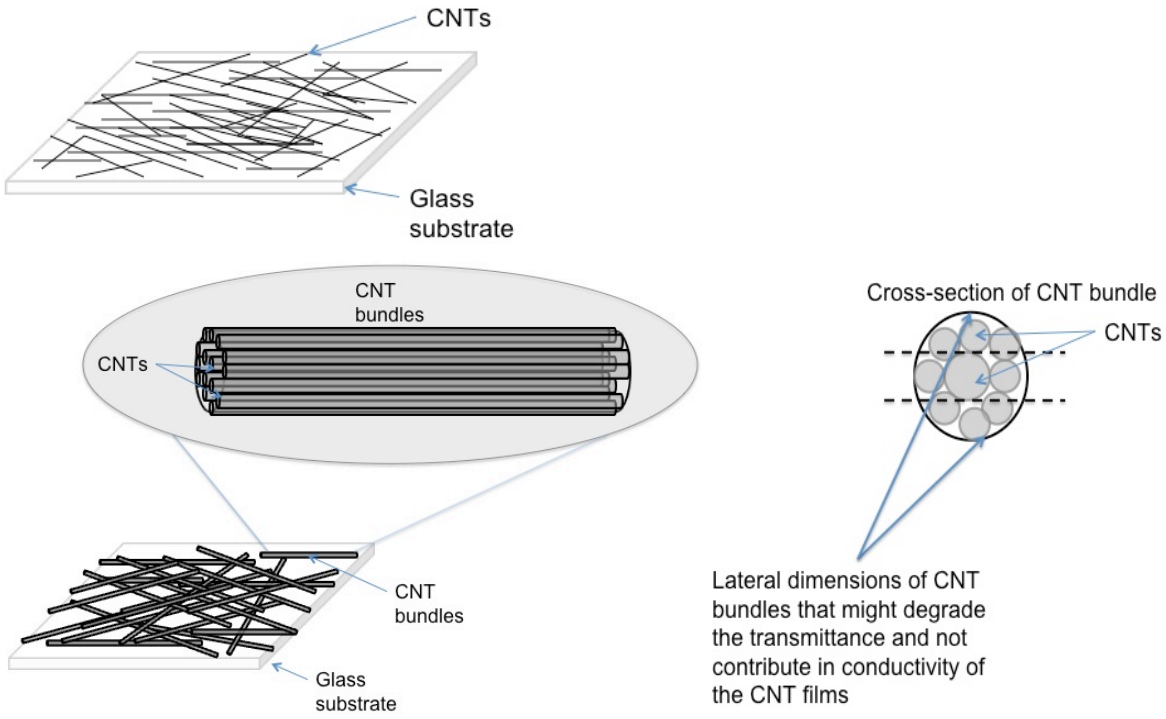

Figure 4-27. Schematic diagram of the assembly of CNT bundles and the effect of bundle size to CNT film conductivity and transmittances

The morphology of surfactants and a carboxyl stabilized carbon nanotube system was observed by Atomic Force Microscopy, and presented in Figure 4-27. Both solutions were made with a 0.2 mg/ml –COOH functionalized carbon nanotube concentration to ensure stability. It can be clearly seen that surfactants together with a carboxyl system could give better surface coverage compared to a carboxyl system.

In carboxyl systems there are uneven clusters of carbon nanotubes formed due to the slow evaporation process that could transport most of the particulates into the edge of droplets. However for surfactant systems, due to the presence of bulky surfactants, the carbon nanotube movement during solvent evaporation is

restricted. In conclusion, surfactants played a big role in carbon nanotube solution.

Firstly, surfactants help to increase the solubility carboxyl functionalized carbon nanotube, secondly, they enhance its stability through wrapping and dispersing the CNT and lastly they enhance carbon nanotube surface coverage by giving them steric hindrance during solvent evaporation.

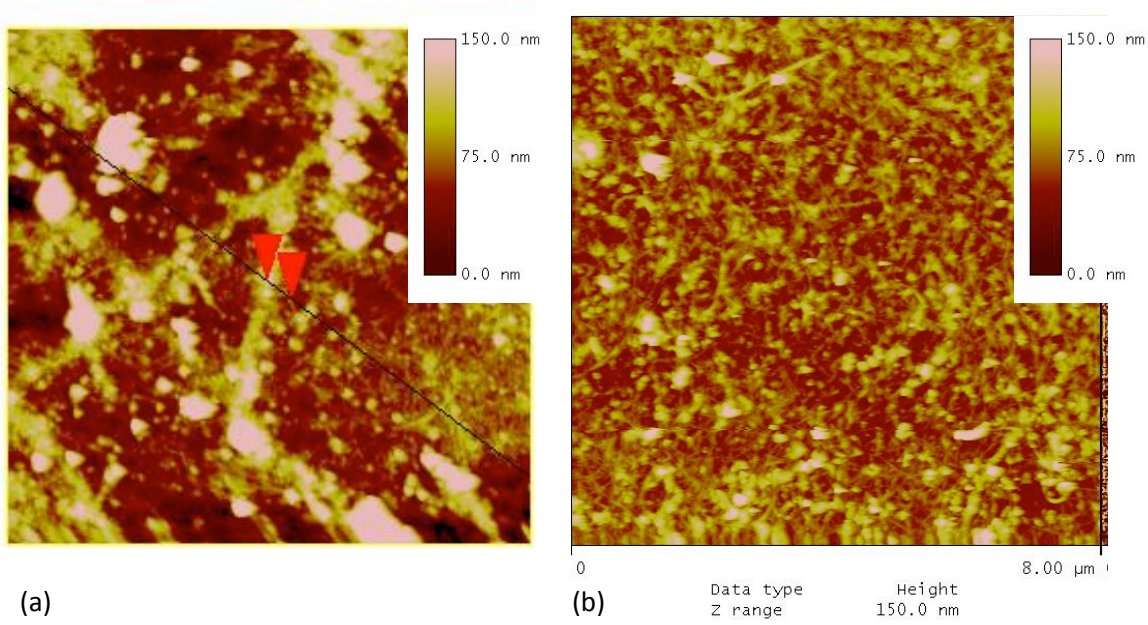

Figure 4-28. AFM Topographic of CNT films deposited from (a) carboxyl stabilized CNT solution and (b) surfactant + carboxyl stabilized CNT solution.

CHAPTER 5 : CONDUCTION MECHANISM OF CARBON NANOTUBE NETWORKS

This chapter studies the correlation between film conductivity and its optical transmittance. The study will start by discussing the basic conductivity equation, followed by the presentation of several models that have been proposed previously, and applying them to our experimental data.

5.1 Basic of Conductivity and Measurement Tools

Electrical conductivity by definition is a material's property that describes how it can conduct electrons. Being a material property, the conductivity of certain materials can be altered with treatment/processing. Conductivity can be best described by the following formula:

$$\sigma = q.n.\mu$$

where

$\sigma : conductivity$

$n : concentration - of - carriers$

$\mu : mobility$

According to the formula, conductivity is dependent on carrier concentration and mobility. Carrier concentration is a measure of how many free electrons or holes a certain material has, and carrier mobility defines how easy it is for a carrier to move about in the material lattice.

All these properties are nanoscopic, which are very difficult to be directly characterized. Hence, we are going to use a macroscopic approach to approximate and compare CNT conductivity.

The resistance (R) or conductance (C) of materials are very easily measured through 4-probes measurement. Four probes Van der Pauw

measurement will give us an output called Sheet Resistance (Rs), which correlates to conductivity as follow:

$$Rs = C_f.R, where$$

Rs = sheet resistance

Cf = correction factors

R = resistance measured between the 4 probe

$$R = \frac{\rho.L}{A} = \frac{\rho.L}{t.x}$$ ……..Equation 5-1

5.2 Models for Conductivity – Transmittance correlation in Carbon Nanotube Films

From the previous section, we understand that conductance/resistance is a function of a material's dimension. In thin films, the conductance/resistance is directly affected by its thickness (t); in equation 5-1, it is shown that resistance is inversely proportional to film thickness (t).

One approach for us to get a very low sheet resistance is to increase its thickness. However, the increased thickness will reduce the film's transparency. Indium Tin Oxide (ITO) can be made 200 nm thick without absorbing much light, but for unsorted carbon nanotube we have to limit the thickness to 40-70 nm (depends on the type of carbon nanotube) to get 85% transmittance at a light wavelength of 550 nm.

For different kinds of carbon nanotubes there are different correlations between thickness and transmittance. Since larger diameter carbon nanotubes have smaller bandgaps, they tend to absorb more photons at lower energy and vice versa. It is logical for us to see a decrease in carbon nanotube film resistance

with decreasing transmittance, but mathematical models that can best describe correlation between sheet resistance and transmittance are still inadequate. With a validated conductivity – transmittance model, from one data point of carbon nanotube films (sheet resistance and transmittance), the properties of any other data point can be predicted, which makes it easier to evaluate the properties of the film. i.e: with a validated model, if we could get a 1000 ohm/sq at 93% transmittance, we can predict what the sheet resistance value at 80% transmittance is, or what transmittance we will get for 200 ohm/sq, and if we are testing using another type of carbon nanotube, and we get 700 ohm/sq at 76% transmittance, we can immediately know whether this carbon nanotube is better or worse by extrapolating it from model without having to prepare samples with exactly the same transmittance. Thus it is important to develop and validate the conductivity- transmittance model for carbon nanotube films.

We are testing different types of carbon nanotubes using three different conductivity-transmittance models. CoMoCAT SWeNT 65, SWeNT 76, SWeNT CG200, and Arc Discharge P3 were tested out for these models. Linear parallel models, "Conductivity of Transparencies" models and "Thin metallic film" models, which were reported on previously, were tested and validated for different types of carbon nanotube film. [101, 102]

Linear Parallel Connection Model

This is the simplest model, and it assumes every 1% absorption of light to be a single thin layer of film with a certain thickness, and the total resistance is calculated by connecting all these thin layers in a parallel manner. This model assumes that layer thickness is linearly proportional with its transmittance, i.e., if

one layer has a thickness of 1 nm and a light absorption of 1%, two layers with a thickness of 2 nm will give a light absorption of 2%. For example if we get carbon nanotube films with 80% transmittance and 800 ohm/sq resistance, it will assume each thin layer with 1% absorption of that film to be 16000 ohm/sq. Hence if this model fits, it could predict the sheet resistance for a 90% transmittance film to be 1600 ohm/sq, and a film with 60% transmittance would have a sheet resistance of 400 ohm/sq.

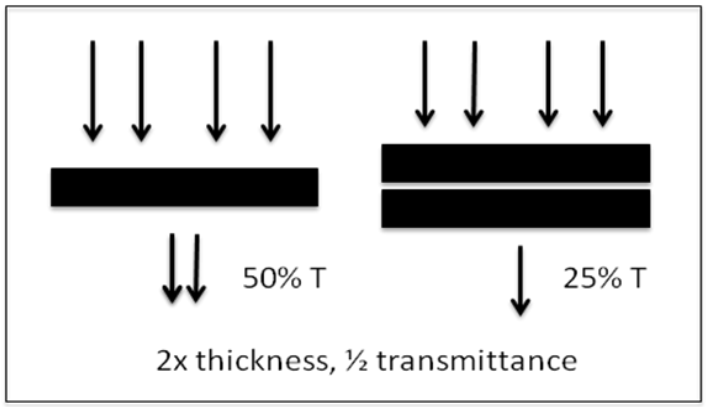

Figure 5-1. Linear Parallel Models

Conductivity of Transparency Models (Beer-Lambert Law)

This model is the refined version of the linear parallel connection model. Instead of assuming the film thickness and light absorption to have a linear correlation, this model uses the Bouguer-Lambert Law to correlate thickness and absorbance.

$$-lg\left(\frac{I}{I_0}\right) = \varepsilon^* cd; \quad \varepsilon^* c = \varepsilon_{graphene}$$ ……..……Equation 5-2

I / I_0 : intensity of transmitted light/ incident light (transmittance percentage)

E : extinction coefficient

C : concentration (proportional to density of film)

d : light pathways (thickness)

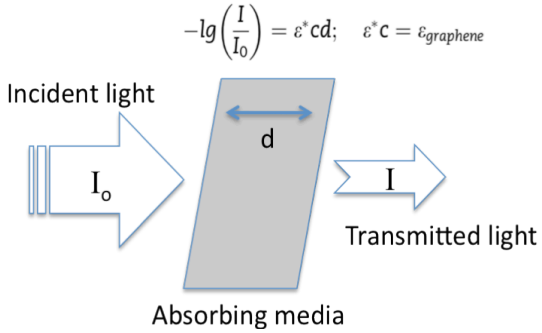

Figure 5-2. Models for Beer-Lambert Law

The Bouguer-Lambert law has been validated for the absorption of liquid / low concentration of solids in liquid. However it has not been validated for thin films with varying transparencies. With this model, it is possible to approximate film thickness from its transmittance once the extinction coefficient is known. Eigler S [101] proposed to use graphene single layer properties to approximate film thickness. Then, from its approximated thickness, the conductivity value can be obtained.

$$\varepsilon_{graphene} = \frac{-lg\left(\frac{I}{I_0}\right)}{d_{graphite}} = \frac{-lg\left(\frac{97.7\%}{100\%}\right)}{3.35^{-8}\ \text{cm}} = 301,655\ \text{cm}^{-1}, \quad d_{ideal} = \frac{-lg\left(\frac{I}{I_0}\right)}{\varepsilon_{graphene}}$$

$$\sigma_{gt} = \frac{\varepsilon_{graphene}}{-lg\left(\frac{I}{I_0}\right)\rho_{sample}} = \frac{301,655\ \text{cm}^{-1}}{-lg\left(\frac{I}{100\%}\right)\rho_{sample}} \quad \text{…….. Equation 5-3}$$

Conductivity is a material property that will not change with the increasing thickness. Hence, the conductivity value is the parameter that needs to be compared against different conductors. The conductivity of the transparency model proposed by Eigler S.[101] calculates film thickness based on film transparencies. Therefore it could act as better comparison parameters between the different carbon based transparent conductive films.

Thin Metallic Film models

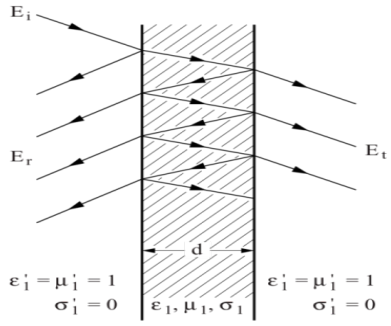

Figure 5-3. Thin Metallic Film Models (Reproduced with permission from ref.[119] Copyrights 2002 Cambridge University Press)

This model is based on the electrodynamic formula that is developed for thin metallic films in air assuming that the thickness is much less than the wavelength (in our case the carbon nanotube film thickness is in the order of 40-70 nm and the optical wavelength is at 550 nm). This model is uses the Maxwell Equation to calculate the interaction between light and matters. With light as electromagnetic waves, there should be a correlation between the material's absorbance and electrical conductivity. A correlation can be represented by equation 5-4. The detailed derivation of this formula is beyond the scope of this project.

$$T = \left(1 + \frac{1}{2R_s}\sqrt{\frac{\mu_0}{\varepsilon_0}}\frac{\sigma_{op}}{\sigma_{dc}}\right)^{-2} = \left(1 + \frac{188(\Omega)}{R_s}\frac{\sigma_{op}}{\sigma_{dc}}\right)^{-2}$$

…….Equation 5-4

Here, σ_{dc} is the DC conductivity, σ_{op} is the optical conductivity, T is film transparency in %, and d is the film thickness. It is assumed that σ_{op}/σ_{dc} remains constant for NTNs of different densities in the measured optical frequency range. And according to previous work by L. Hu [101], the ratio of $\sigma_{op}/$

σ_{dc} is equal to 1 to have a good fit for carbon nanotube networks model. For different types of carbon nanotubes, it is suspected that they would have different value of σ_{op}/σ_{dc}.

5.3 Testing of various Conductivity-Transparencies Models

The various mathematical models for conductivity-transparencies models are constructed from a different theory base. So it would be a useful experiment to compare the accuracy of those mathematical models.

In the first models, using the liner parallel connection models, one data point will be used as a reference (experimental data at ~80% transmittance) and from this data, the sheet resistance value of various transmittance ranges will be predicted and compared with experimental values.

The conductivity of transparency models was also tested in a similar way. One experimental data point will be used as a reference (at ~80%) to calculate σ_{gt} (conductivity of transparencies), with σ_{gt} value obtained, any other sheet resistance value at different ranges of transmittance will be derived. Different carbon nanotubes will be expected to give different σ_{gt} values. For thin metallic film models, we just need to fit the ratio of σ_{op}/σ_{dc} with the experimental data and find the ratio value that fits best. Different carbon nanotubes are expected to have different ratios.

Table 5-1. Experimental data for P3 carbon nanotube

Sheet Resistance	Transmittance
287 Ohm/sq	83%
162 Ohm/sq	73%
103 Ohm/sq	65%
86 Ohm/sq	60%
55 Ohm/sq	45%

In the linear parallel connection models, we first use the value of 282 Ohm/sq at transmittance 83% as the baseline. With this data we got a value of 4,794 Ohm/sq for every 1% light absorbed (we assumed that at 83% transmittance, there are 17 parallel circuit of film that absorb 1% of light).

Table 5-2. Comparison between experimental data and linear parallel connection model for P3 carbon nanotube

Transmittance	*Experimental data*	*Calculated data*	*Deviation*
83%	287 ohm/sq	287 ohm/sq	
73%	162 ohm/sq	177 ohm/sq	9.9 %
65%	103 ohm/sq	136 ohm/sq	19.3 %
60%	86 ohm/sq	119 ohm/sq	26.6 %
45%	56 ohm/sq	87 ohm/sq	55.3%
	Average Deviation		27.8 %

At higher transmittance regions (73%), this model can give a good prediction for P3 carbon nanotubes, however at lower transmittance regions the prediction becomes less accurate. For the 2nd model conductivity of transparencies, we would first need to find the value of σ_{gt}. Using the first experimental value 282 ohm/sq @ 83% transmittance σ_{gt} is found to be 13,218.9 Siemens/cm.

Table 5-3. Comparison between experimental data and Beer-Lambert Law model for P3 carbon nanotube

Transmittance	*Experimental data*	*Calculated data*	*Deviation*
83%	287 ohm/sq	287 ohm/sq	
73%	162 ohm/sq	166.9 ohm/sq	3.7%
65%	103 ohm/sq	122 ohm/sq	7.0%
60%	86 ohm/sq	102 ohm/sq	8.5%
45%	56 ohm/sq	65 ohm/sq	16.1%
	Average Deviation		8.83 %

The 2nd model seems to fit better with experimental data, however at lower transmittance ranges a deviation of more than 10% is still observed, so this model is not suitable for a transmittance of lower than 60%.

The 3rd model is based on thin metallic films in air. For this model we just need to find a suitable σ_{op}/σ_{dc} value, for simplicity we can call it a constant K. By using the first experimental data point, we can get a K value of 0.146. It can be observed from the equation that a smaller K value translates to better film conductivity.

Table 5-4. Comparison between experimental data and thin metallic film model for P3 carbon nanotube

Transmittance	*Experimental data*	*Calculated data*	*Deviation*
83%	287 ohm/sq	287 ohm/sq	
73%	162 ohm/sq	161 ohm/sq	0%
65%	103 ohm/sq	114 ohm/sq	10.8%
60%	86 ohm/sq	94 ohm/sq	10.4%
45%	55 ohm/sq	56 ohm/sq	2.2%
	Av. Deviation		5.85 %

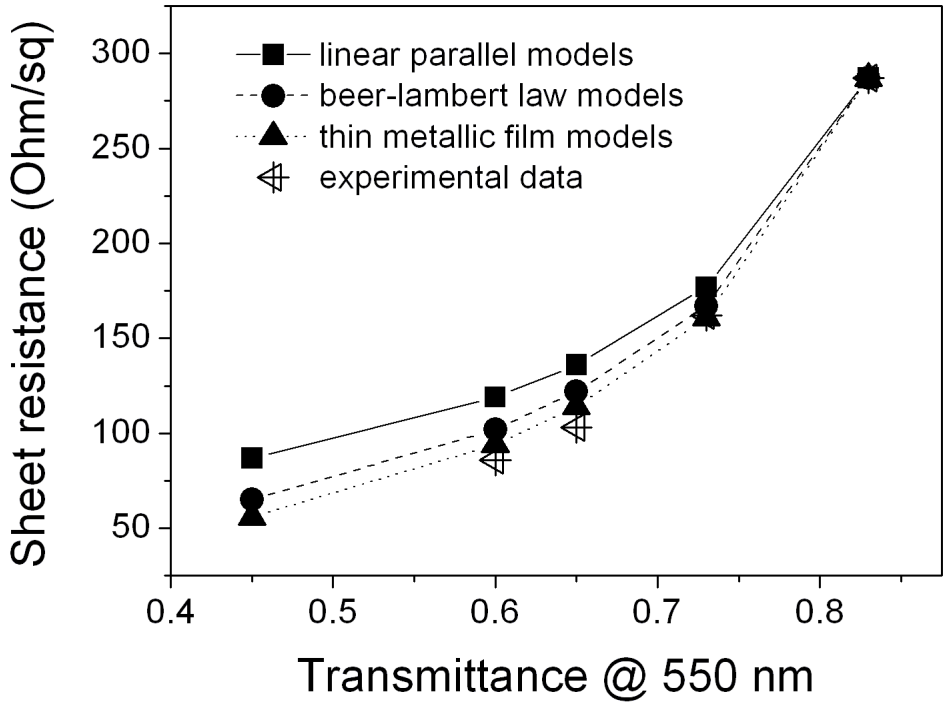

Figure 5-4. Comparison between experimental data and three model for P3 carbon nanotube

The thin metallic film in air model seems to be able to predict very nicely the behaviour of P3 CNTs even in low transmittance regions. CoMoCAT 65 CNT has more than 90% concentration of semiconducting CNTs, which can be shown from the absorption spectra below. The M11/S22 intensity ratio is normally used to approximate the population ratio inside. The metallic nanotubes absorption intensity M11 at around 400 nm was far weaker than S22 intensity at around 570 nm by ratio of 1:10. This proves that there are high semiconducting CNT contents here. Another observation about this CNT is the flat shapes of absorption spectra due to its high semiconducting content. Metallic CNTs possess continuous absorption that is normally reflected in steep background absorption.

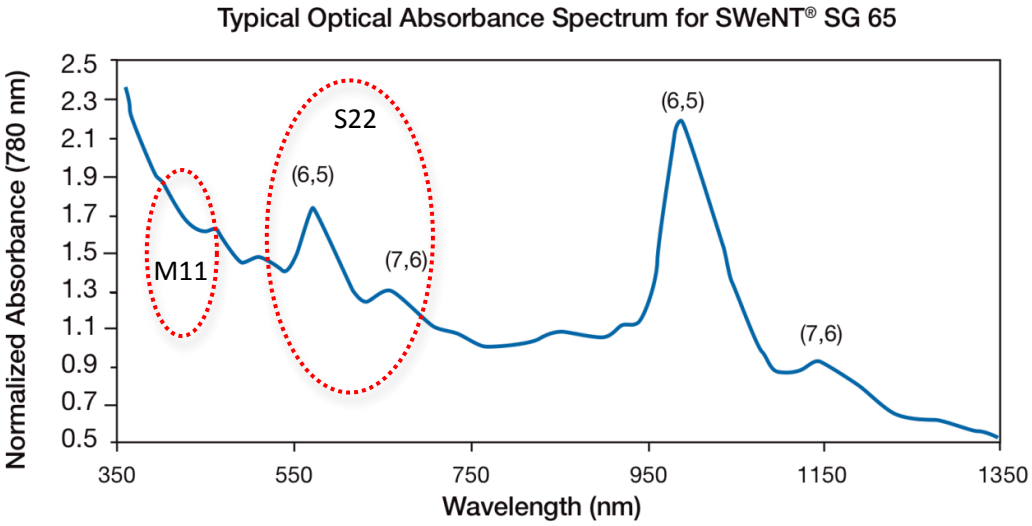

Figure 5-5 Absorption spectra of CoMoCAT SG 65

Table 5-5. Comparison between experimental data and three different resistance-transmittance model for CoMoCAT 65 carbon nanotube

CoMoCAT 65, 1% transmittance 14,351 ohm/sq

Transmittance	*Experimental data*	*Calculated Data*	*Deviation*
88.7%	1264 ohm/sq	1264 ohm/sq	

54%	218 ohm/sq	312 ohm/sq	43.1%
21%	93 ohm/sq	181 ohm/sq	94.6%
	Average Deviation		63.5%

CoMoCAT 65, σ_{gt}=4,561 Siemens/cm

Transmittance	*Experimental data*	*Calculated Data*	*Deviation*
88.7%	1264 ohm/sq	1264 ohm/sq	
54%	218 ohm/sq	247 ohm/sq	13.3%
21%	93 ohm/sq	97.5 ohm/sq	4.8%
	Average Deviation		9.1 %

CoMoCAT 65, K constant = 0.417

Transmittance	*Experimental data*	*Calculated Data*	*Deviation*
88.7%	1264 ohm/sq	1264 ohm/sq	
54%	218 ohm/sq	217.2 ohm/sq	0.4%
21%	93 ohm/sq	66.3 ohm/sq	29%
	Average Deviation		15.2 %

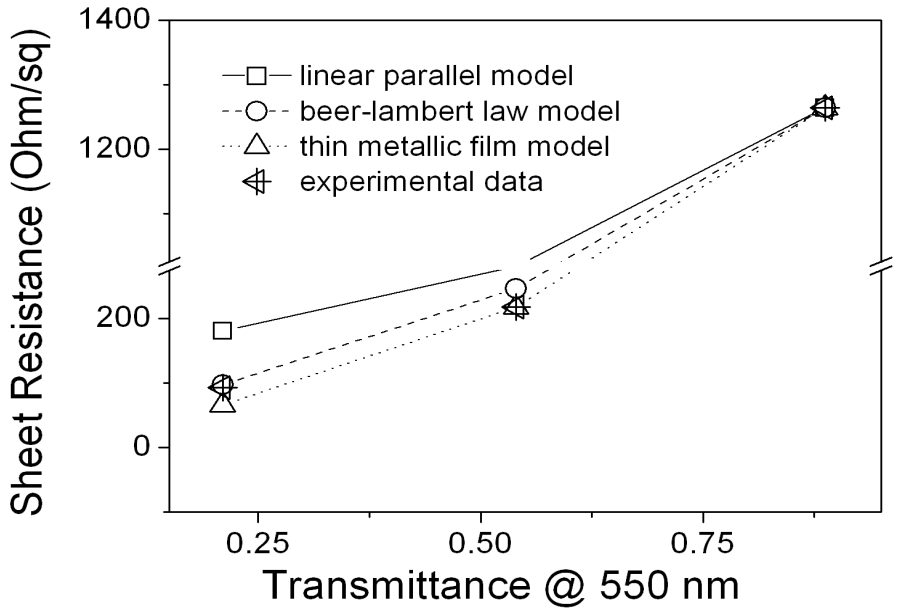

Figure 5-6. Comparison between experimental data and three different resistance-transmittance models for CoMoCAT 65 carbon nanotube.

For CoMoCAT 65, it seems that Beer-Lambert law model fits better compared to other models. The thin metallic film model that normally fits for other CNTs, does not fit the behaviour of CoMoCAT 65. A possible reason behind this perhaps lies on the CNT mixture inside CoMoCAT 65. On manufacturer specification and from UV-vis spectra, it can be seen that there are high percentages of semiconducting carbon nanotubes inside the mixture (more than 90%). Therefore, thin metallic film models cannot describe the behavior of CoMoCAT thin films well.

CoMoCAT SG 76 is another type of carbon nanotube with a preferential content of 7,6 chirality CNTs. It can be seen from the M11/S22 ratio, that it has a higher metallic tube content. There were several metallic peaks observed at M11 intensity around 400 nm, and the observed S22/M11 ratio is more than 2:10.

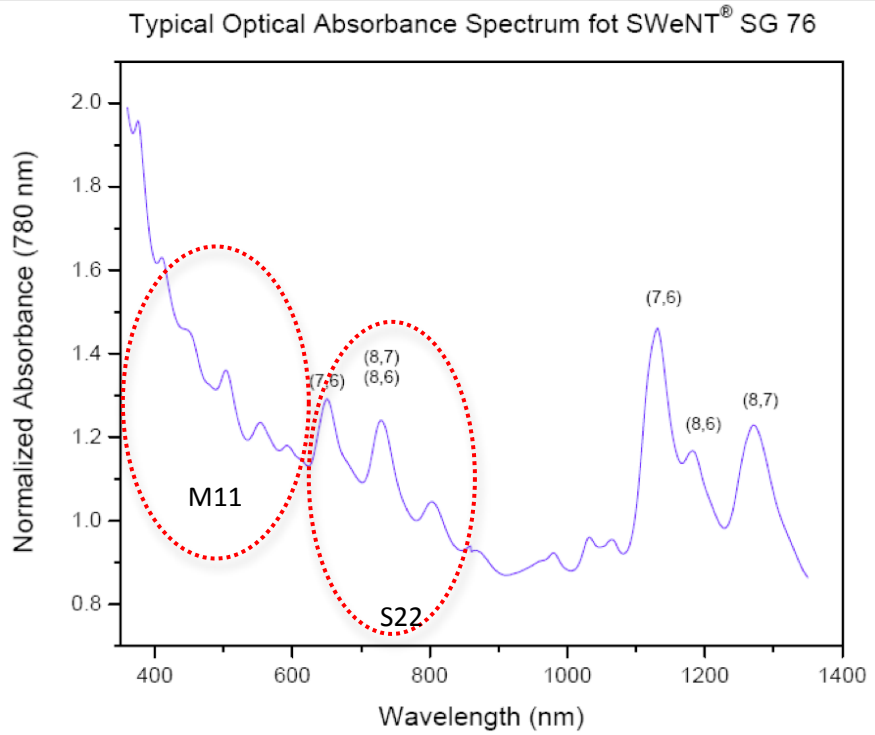

Figure 5-7. Absorption spectra of CoMoCAT SG 76

Table 5-6. Comparison between experimental data and three different resistance-transmittance model for CoMoCAT 76 carbon nanotube

CoMoCAT 76, layer with 1% transmittance = 8,234 Ohm/sq

Transmittance	*Experimental data*	*Calculated data*	*Deviation*
85.4%	564 ohm/sq	564 ohm/sq	
72%	237 ohm/sq	294 ohm/sq	24%
58%	129 ohm/sq	196 ohm/sq	51.9%
29%	53 ohm/sq	155 ohm/sq	188%
	Average Deviation		88 %

CoMoCAT 76, σ_{gt}= 7,803.2 Siemens/cm

Transmittance	*Experimental data*	*Calculated data*	*Deviation*
85.4%	564 ohm/sq	564 ohm/sq	

72%	237 ohm/sq	270 ohm/sq	13.9%
58%	129 ohm/sq	163 ohm/sq	26.3%
29%	53 ohm/sq	71.9 ohm/sq	35.6%
	Average Deviation		21.6 %

CoMoCAT 76, constant K =0.246

Transmittance	*Experimental data*	*Calculated data*	*Deviation*
85.4%	564 ohm/sq	564 ohm/sq	
72%	237 ohm/sq	259 ohm/sq	9.2%
58%	129 ohm/sq	147 ohm/sq	13.9%
29%	53 ohm/sq	53.9 ohm/sq	1.6%
	Average Deviation		8.23 %

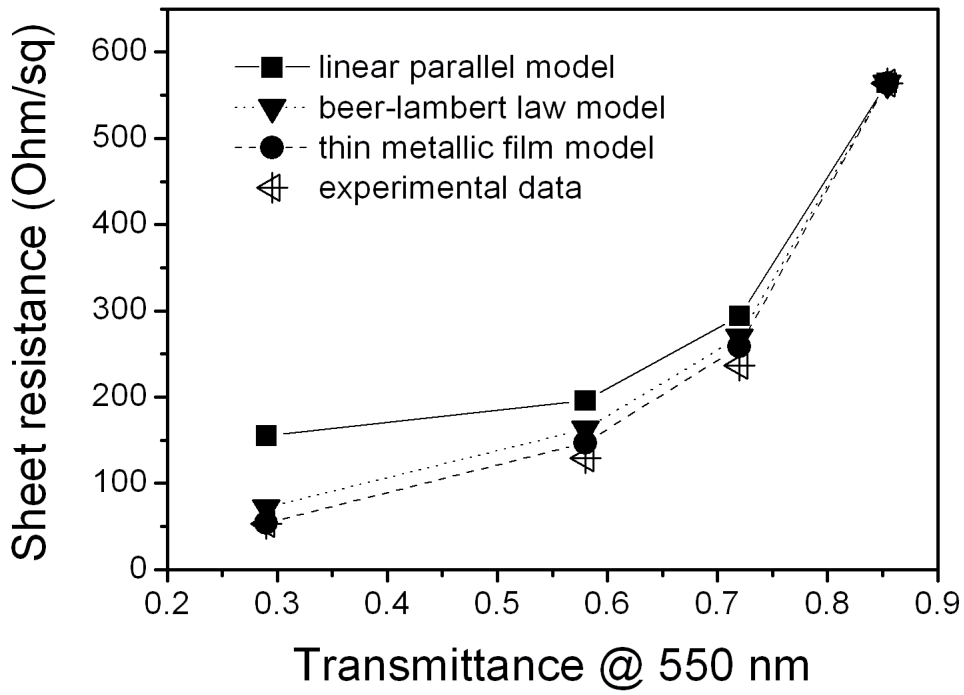

Figure 5-8. Comparison between experimental data and three different resistance-transmittance model for CoMoCAT 76 carbon nanotube

CoMoCAT 76 is another type of carbon nanotube that has a semiconducting carbon nanotube content of around 70% with preferential chirality on (7,6). In terms of semiconducting to metallic ratio, CoMoCAT 76 has a greater metallic carbon nanotube content compared to CoMoCAT 65, and thin metallic film models can describe the film behaviour pretty well.

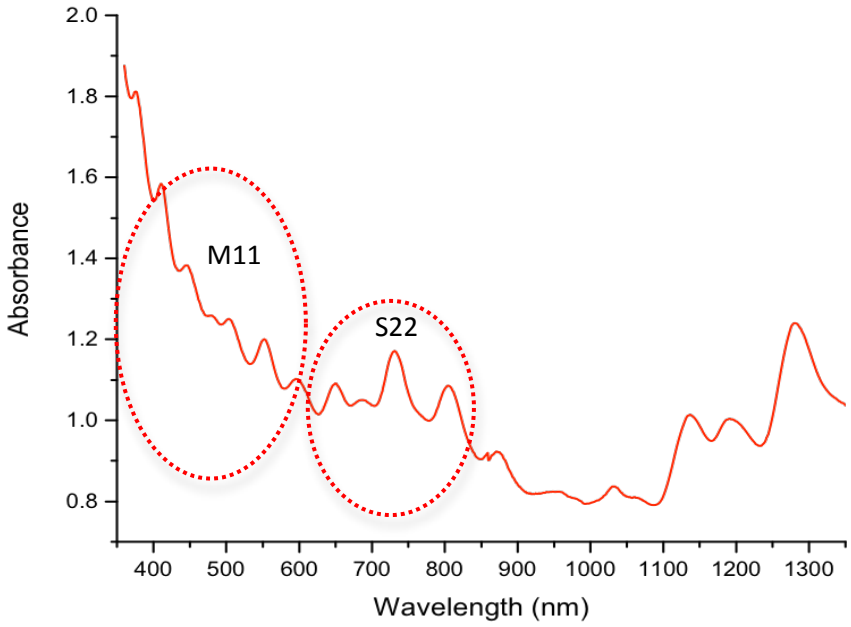

Figure 5-9. Absorption spectra of CoMoCAT CG 200

Figure 5-9 shows the absorption spectra of individually dispersed CoMoCAT CG 200. M11/S22 seems to be larger than CoMoCAT 76, hence it has a higher metallic CNT content than CoMoCAT SG76. CoMoCAT CG200, layer with 1% transmittance = 7,450 Ohm/sq.

Table 5-7. Comparison between experimental data and three different resistance-transmittance model for CoMoCAT CG200 carbon nanotube

Transmittance	*Experimental data*	*Calculated data*	*Deviation*
80.7%	367 ohm/sq	367 ohm/sq	

71.3%	185 ohm/sq	259 ohm/sq	45.4%
64.2%	141 ohm/sq	208 ohm/sq	47.5%
43%	72 ohm/sq	130 ohm/sq	80.5%
	Average deviation		57.8%

CoMoCAT CG200, σ_{gt}= 8,826 Siemens/cm

Transmittance	*Experimental data*	*Calculated data*	*Deviation*
80.7%	367 ohm/sq	367 ohm/sq	
71.3%	185 ohm/sq	232 ohm/sq	25.4%
64.2%	141 ohm/sq	177 ohm/sq	25.5%
43%	72 ohm/sq	93 ohm/sq	29.2%
	Average deviation		26.7%

CoMoCAT CG200, constant K = 0.22

Transmittance	*Experimental data*	*Calculated data*	*Deviation*
80.7%	367 ohm/sq	367 ohm/sq	
71.3%	185 ohm/sq	224 ohm/sq	21%
64.2%	141 ohm/sq	166 ohm/sq	17.7%
43%	72 ohm/sq	78.7 ohm/sq	9.3%
	Average deviation		16 %

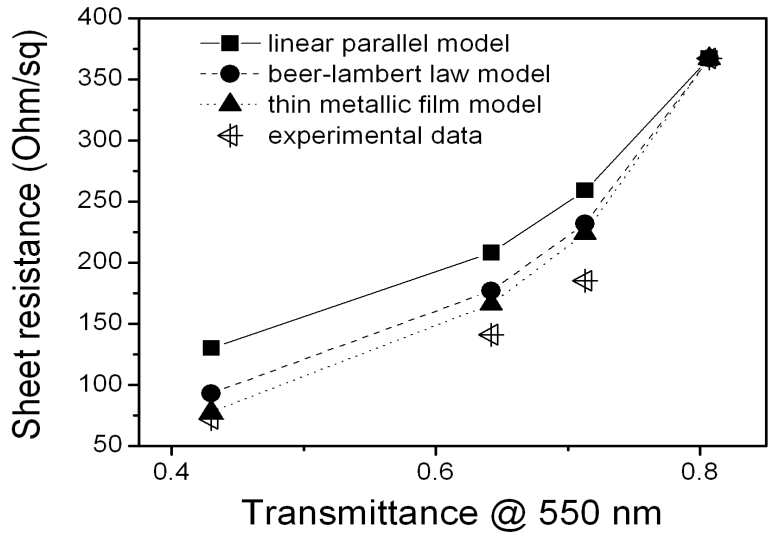

Figure 5-10. Comparison between experimental data and three different resistance-transmittance model for CoMoCAT CG200 carbon nanotube

CG200 carbon nanotubes, according to manufacturer specifications, possess the highest metallic carbon nanotube contents compared to other carbon nanotubes (CoMoCAT 65 and CoMoCAT 76). And as expected, thin metallic film models could best fit the sheet resistance and transmittance series.

In conclusion, several models of resistance-transmittance models were tested for the different types of carbon nanotubes. P3 carbon nanotubes represented carbon nanotubes with random population, and the series of CoMoCAT 65, CoMoCAT 76, and CoMoCAT CG200 represented carbon nanotubes with increasing metallic tube contents.

Carbon nanotubes with no specific preferential population (normally around 1/3 metallic population and 2/3 semiconducting) once made into thin films showed the behavior of thin metallic films and the thin metallic film model fits nicely. At low metallic tube contents in CoMoCAT 65 (metallic tube content approximated to be around 5%), the thin metallic film model does not fit nicely. Instead other models: conductivity of transparencies models could describe the

thin film behavior better. At increased metallic tube content, in CoMoCAT 76 and 200, thin metallic film models could again fit nicely to the resistance and transmittance curve. So overall, among all the other models, the thin metallic film model can provide the best fit on transmittance and sheet resistance of carbon nanotube thin films, just that in the case where the metallic content of carbon nanotubes is less than 10%, the Beer-Lambert law models would be a better to describe carbon nanotube thin film resistance with different transmittances. The reason for this phenomenon perhaps lies in the carbon nanotube network assembly.

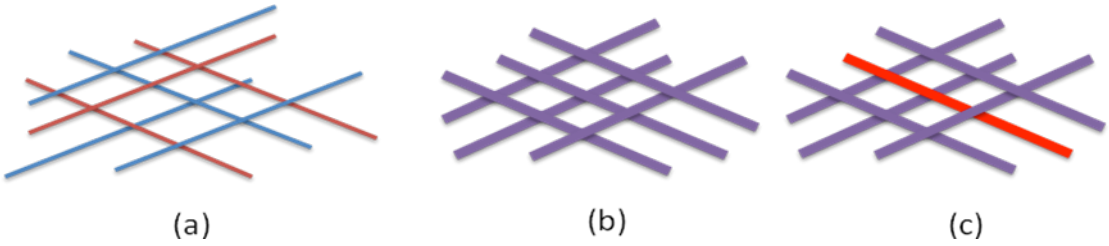

Figure 5-11. Schematic diagram of (a) individual CNT assembly (b) bundles assembly with more than 20% metallic CNT content (c) bundles assembly with less than 10% metallic CNT contents

The components of CNT thin films here are bundles of nanotubes. And it is known that once there ar metallic nanotubes inside a bundle the behaviour of the whole bundle becomes metallic as the resistance between carbon nanotubes in bundles is much less compared to those junctions. Whenever we have 20-30% of metallic nanotube contents in the whole population, it is possible to find 1-2 metallic nanotubes in one bundle. According to the AFM image (Figure 4-21) the bundle size is around 8-15 nm, hence on average there are 5-10 nanotubes in 1 bundle. At 20% probability, there is perhaps one metallic nanotube in every five nanotube bundles, or 2 in 10 nanotube bundles. Therefore, because each bundle has metallic properties, the whole film will have metallic properties as

well. However as the population of metallic nanotube gets smaller ~10% in the case of CoMoCAT 65, it is more difficult to have at least 1 metallic nanotube in every bundle, hence this thin metallic film models will not fit. The percolating pathways for conducting sticks in this case is not as good as those with 20% and above metallic contents, because now not all the bundles are metallic bundles, some of them are semiconducting bundles, which have a large inter-junction resistance with the conducting stick. The summary of this investigation can be seen in table 5-8.

Table 5-8. Correlation between type of carbon nanotube and the suitable mathematical models

Carbon Nanotube	Models	Average Deviation
P3	Linear Models	27.8 %
	Beer- Lambert Law	8.83 %
	Thin metallic film	**5.85 %**
CoMoCAT 65	Linear Models	63.5 %
	Beer- Lambert Law	**9.1 %**
	Thin metallic film	15.2 %
CoMoCAT 76	Linear Models	88 %
	Beer- Lambert Law	21.6%
	Thin metallic film	**8.23 %**

CoMoCAT 200	Linear Models	57.8 %
	Beer- Lambert Law	26.7 %
	Thin metallic film	**16.6 %**

5.3 Understanding Population Mixture in Carbon Nanotube Thin Film

Carbon nanotube thin films are constructed from nets of nanotubes, where each strand of carbon nanotube can be a semiconducting or metallic strand. One strand makes contacts to hundreds and thousands of other strands in the thin film architecture. This morphology makes it difficult to understand what can influence the conductivity of these nets of strands. Individually, the contacts between semiconducting and metallic nanotubes are highly resistive compared to semiconducting-semiconducting or metallic-metallic contact [64]. Some reports have shown that segregating metallic nanotubes from its mixture can improve its conductivity by eliminating metallic semiconducting junctions[90]. However the methods that are used to separate a metallic nanotubes from its mixture have a very low yield, such as density gradient ultracentrifugation. Only 1% or less of the CNTs from the original solution could be used.

So, our investigation in this sub-chapter is dedicated to understanding the contribution of metallic-semiconducting junctions in carbon nanotube thin film conductors. The improvement of conductivity by segregating carbon nanotubes from its mixture could arise from two possible phenomena. First, as proposed in the report, the improvement may come from the elimination of a highly resistive junction of semiconducting – metallic carbon nanotubes. Second, conductivity improvement could just have resulted from the higher metallic nanotube contents

in the thin film (metallic nanotube has higher inherent conductivity compared to semiconducting nanotube). Highly resistive junctions may not contribute significantly in thin film carbon nanotube networks, but with the improvement in the conductivity of the components of thin film, the overall conductivity will be improved as a result.

In order to further understand the role of metallic-semiconducting carbon nanotubes, an experiment involving CoMoCAT 65 CNTs was carried out. CoMoCAT 65 carbon nanotubes have a high content of semiconducting carbon nanotubes (~95%), hence we would expect that in the thin films made by this type of CNTs, the junctions are predominantly semiconducting – semiconducting (S-S) junctions. If we add some other carbon nanotubes such as P3 and 76 into the above-mentioned conductive thin film, more semiconducting-metallic (S-M) junctions would be expected.

So if S-M junctions contribute significantly to film resistance, we would observe an increase in resistivity. Our experimental approach is the opposite of what people have reported. Instead of starting from mixture and separating it, here, we started from separated carbon nanotubes (CoMoCAT 65 with 90+% semiconducting nanotube) and mixed it with other nanotubes with a higher metallic content.

Table 5-9. Sheet resistance and transmittance of different mixture of CoMoCAT 65 and 76

Carbon Nanotube 1	*Carbon Nanotube 2*	*Sheet resistance*	*Transmittance*
CoMoCAT 65 (100%)	CoMoCAT 76	694 Ohm/sq	69%
CoMoCAT 65 (75%)	CoMoCAT 76 (25%)	392 Ohm/sq	74%
CoMoCAT 65 (50%)	CoMoCAT 76 (50%)	263 Ohm/sq	71%
CoMoCAT 65 (25%)	CoMoCAT 76 (75%)	252 Ohm/sq	74%

From the first set of data (Table 5-9), it is apparent that with an increasing CoMoCAT 76 content inside the carbon nanotube solution, the conductivity of the resulting thin film in fact increases, even though mixing CoMoCAT 76 into CoMoCAT 65 will increase the number of metallic and semiconducting junctions.

Thus, the semiconducting – metallic junction might not be the most important factor in carbon nanotube films. The conductivity of individual carbon nanotubes will be the dominant factor in thin film conductivity. As CoMoCAT 76 is more conductive than CoMoCAT 65 due to a higher metallic nanotube content and larger diameter, an increase in CoMoCAT 76 content in carbon nanotube solution would definitely improve the resulting thin film conductivity.

Another set of experiments was then designed to verify this initial finding. Instead of fabricating thin films from a mixture solution of 65 and 76 CNT, a multilayer film of a different sequence is used (65 layer below, 76 layer on top and vice versa). Films fabricated from a mixture of 65 and 76 CNTs are expected to have more S-M contacts compared to the ones with multilayer architecture.

Table 5-10. Sheet resistance and transmittance of different structure of CNT films

Multilayered structure

Mixture structure

Ratio 76 : 65	*Architecture*	*Transmittance*	*Resistance*
50:50	Mixture	71%	263 Ohm/sq

50:50	CoMoCAT 76 on top	67%	276 Ohm/sq
50:50	CoMoCAT 65 on top	67%	378 Ohm/sq

Table 5-10 shows that a multilayer architecture will degrade the thin film conductivity. This is probably due to resistance building up between different layers. With the higher conductivity CNTs (CoMoCAT 7,6) placed on top, a higher thin film conductivity is obtained. Hence, it can be concluded that the resistance of those top layers is more important than those from the bottom ones. However, a single uniform layer will still deliver a better result compared to any multilayer structure.

From the two series of experiments conducted, we can safely conclude that S-M junctions, even though they are highly resistive and play a huge role in transistor devices, are not significant in conductive thin film devices. This evidence is in fact aligned with our findings in chapter 5.2. Most carbon nanotube film conductivity fits well with mathematical models of thin metallic films. In thin metallic films there is no specificity of junctions, the whole component of the film is regarded as a conducting building block.

The reason again lies in the morphology of carbon nanotube films, which consists of carbon nanotube bundles. Inside the carbon nanotube bundles, even though there are semiconducting and metallic nanotubes intact, the resistance is quite low because of the possibility for the carrier to tunnel through as the distance between tubes is very short. When it comes to thin conductive films, obtaining larger diameters, a higher purity, fewer defects and longer lengths of CNTs through fine tuning CNT synthesis is a better direction to pursue than the separation of carbon nanotubes. When we take a closer look at the sheet

resistances of different carbon nanotube mixtures and plot them onto a graph, as shown in Figure 5-13 and 5-14, we observe that the mixture rule of carbon nanotube films follows a linear relationship.

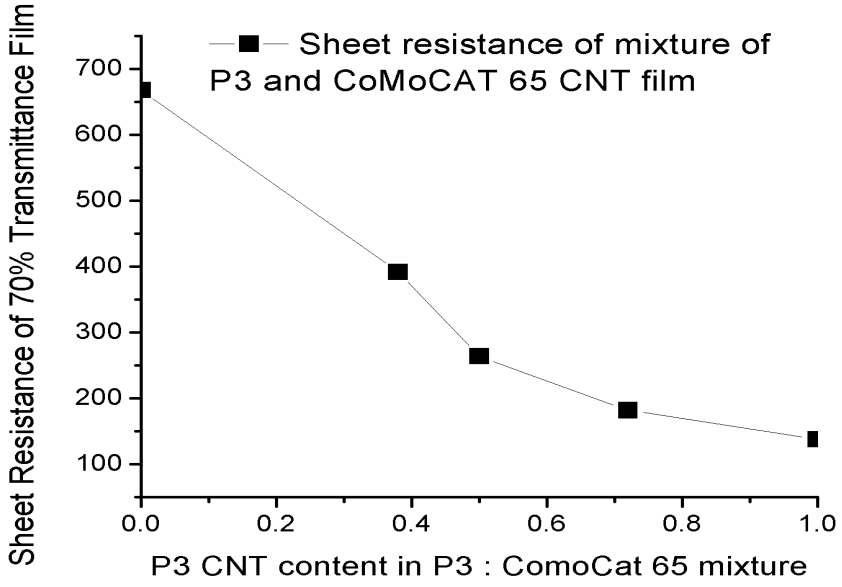

Figure 5-12. Sheet resistance of mixture of arc discharge (P3) and CoMoCAT 65 carbon nanotube film with different mixture ratio

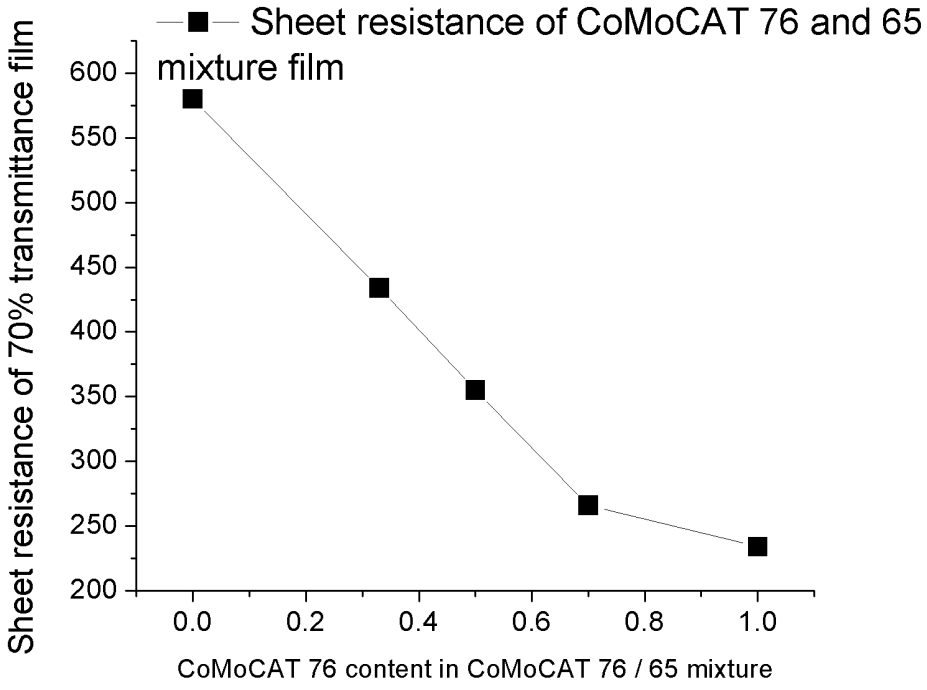

Figure 5-13. Sheet resistance of mixture of CoMoCAT 65 and 76 carbon nanotube film with different concentration

A linear relationship with the conductivity of CNT mixture suggests that it is the conductivity of individual components of the CNT assembly, and not its junctions, that determine network conductivity. Resistive junctions which were observed in individual semiconducting / metallic CNT junctions did not have a significant contribution due to the morphology of carbon nanotubes as bundles. The resistance of carbon nanotubes inside bundles is very low regardless of whether it is a semiconducting or metallic species that is present inside the bundles. Therefore bundles of carbon nanotubes can be regarded as a conducting stick that builds the film assembly.

The results of this chapter tell us that since semiconducting and metallic junctions are not dominant factors in film conductivity, separating CNTs into semiconducting and metallic species is not a wise choice when trying to improve CNT film properties. Therefore, in the next chapter, doping methods will be presented and studied in depth as a method to improve carbon nanotube film electrical properties further.

CHAPTER 6 – DOPING OF CARBON NANOTUBE FILM

After discussing the fabrication of carbon nanotube films, studying the behavior and the correlation between electrical and optical properties, we realized that even the optimized films' electrical and optical properties are still far from Indium Tin Oxide. Hence, an additional post-treatment process or doping is necessary.

There are many approaches that have been used to improve carbon nanotube thin film conductivity, such as the sorting of carbon nanotube solution [75], the fabrication of high purity and less defective carbon nanotubes [91], surfactant removal from carbon nanotube films [60] and the doping of carbon nanotubes [71]. Sorting carbon nanotubes (metallic to semiconducting) has proven to be able to improve film conductivity as it can remove metallic-semiconducting junctions which have much higher electrical resistances [81].

However, the proven sorting method of carbon nanotubes, density gradient ultracentrifugation, has a very low utilisation yield. Only less than 1% of original solution can be used. Fabrication of high purity and less defective carbon nanotubes is a very broad topic and it is beyond the scope of this work. Therefore, the doping of carbon nanotube films was chosen as the topic to study, as it is relatively easy to obtain systematic data, can be scaled and is not comprehensively researched. As mentioned previously in chapter 5, two factors affect the intrinsic conductivity of materials: carrier concentration and mobility. Since the intrinsic mobility of carbon nanotubes is quite high, a possible improvement could lie with increasing the carrier concentration of carbon nanotubes.

6.1 Oxidation Doping

There are many reports that discuss the doping of conductive carbon nanotube thin films. The most common dopants are nitric acid (HNO_3), sulphuric acid (H_2SO_4), and thionyl chloride ($SOCl_2$). However there is still some argument on how these dopants could improve the conductivity of carbon nanotube films. Parekh et. al[71] suggested that the improvement in the conductivity of carbon nanotube films originates from covalent functionalization of carbon nanotubes with the electron withdrawing functional group, his argument is supported by the FTIR data of carbon nanotubes films with C-Cl and C=O and OH vibrational signal as shown in figure 6-1.

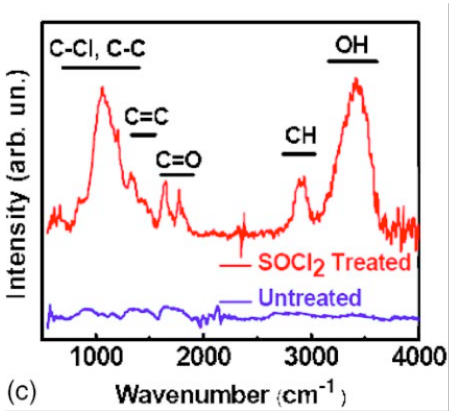

Figure 6-1. FTIR of SOCl treated carbon nanotube film (Reproduced with permission from ref.[82] Copyrights 2007 AIP Publishing)

However another report by Geng et al [71], suggested that no chemical doping happens during the acid treatment. The improvement in conductivity is only due to densification and surfactant removal. His argument is backed by XPS data that shows the removal of sodium peak from SDS surfactant after acid treatment and no shifting in G band in Raman signal as shown in figure 6-2.

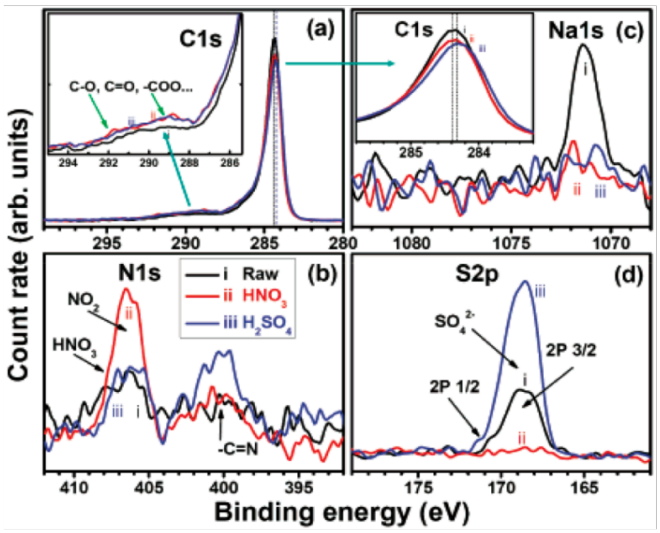

Figure 6-2. XPS and Raman Spectra of nitric acid and sulphuric acid treated carbon nanotube film (Reproduced with permission from ref. [71] Copyrights 2007 American Chemical Society)

Due to these two conflicting arguments sometimes it is difficult to carry on further work, hence the initial step in this chapter is to verify the mechanism of acid treatment doping.

An experiment was carried out using Arc Discharge P2 and P3 carbon nanotubes purchased from Carbon Nanotube Inc. Those SWNTs (0.1 mg/ml) were dispersed in an aqueous solution; sodium dodecyl benzene sulphate (SDBS) surfactant was added for P2 solution. Both solutions were sonicated and then air-sprayed onto the glass substrates and followed by rinsing with distilled water. Various post-treatments for P2 and P3 electrodes were subsequently carried out: exposure to iodine vapor (I_2), immersion in different oxidizing acids such as: HNO_3 (60%), ammonium peroxodisulfate ($NH_4S_2O_8$; 20%) and sulfuric acid (H_2SO_4; 98%) was performed to investigate the effect of oxidation doping. A transmittance (T) measurement was taken at 550 nm of wavelength using a UV-vis spectrophotometer.

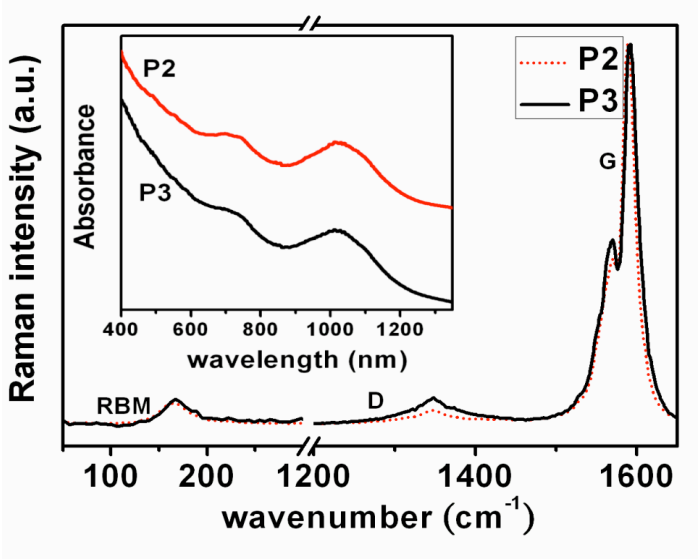

Figure 6-3. Raman Spectra and Absorption Spectra of P2 and P3 films

Figure 6-3 shows the Raman spectra (excited at 488nm and 633 nm) for water-washed P2 electrodes and as-prepared P3 electrodes. The higher Raman D/G peak intensity ratio (D/G ratio) and slightly up-shifted G-frequency for P3 is due to the presence of defects of COOH functional groups. No significant difference is observed in the Raman radial breathing mode (RBM) and in the UV-visible absorption spectra (Inset), suggesting that there are similar SWCNT species (chirality and/or diameter) existing in P2 and P3. The morphology of these two carbon nanotubes i.e. bundling states and length, were found to be similar. Therefore, the observed Rs difference in subsequent comparative measurements is not attributed to the difference of nanotube species content or morphology. Figure 6-5 (a) shows that the as-prepared P2 film exhibits a high Rs (>30000 Ohm/sq. with a 68 % transmittance (T)). After washing with water, the Rs is drastically decreased to ~1700 Ohm/sq, suggesting that the presence of surfactants significantly degrades the conductivity of SWCNT electrodes.

Prior to the treatment of the carbon nanotube film with acid, it is carefully washed with water until the conductivity did not change anymore. A sequential

washing process was adopted to increase the efficiency of the water washing as shown in figure 6-4.

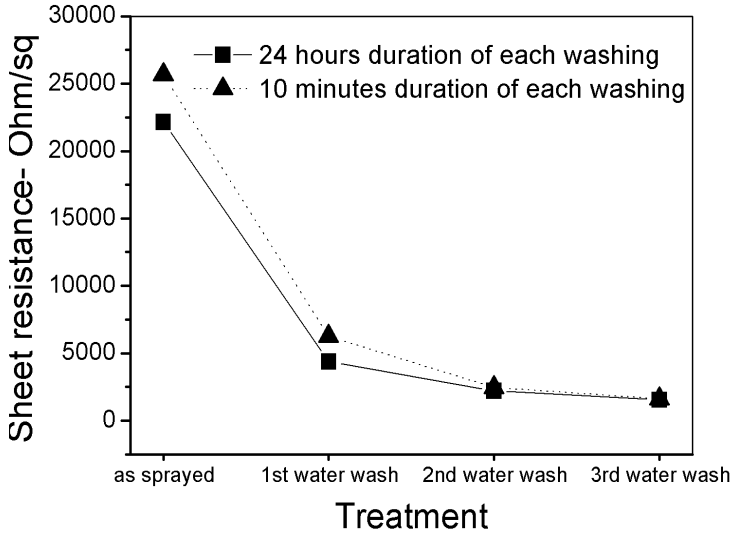

Figure 6-4. Resistivity change with surfactant washing sequence

Subsequent immersion in HNO_3 or H_2SO_4 further reduced their Rs by 5-10 times. From Figure6-6(a) and (b), it can be concluded that H_2SO_4 treatment for P2 or P3 electrodes resulted in a significantly lower Rs and higher stability, compared with the HNO_3 treatment. If the surfactant removal is solely responsible for Rs reduction, no Rs reduction would be observed in surfactant free-P3 thin films. Therefore, other effects resulting from acid treatments, such as hole-doping on SWCNT or chemical functionalization [82] shall be considered.

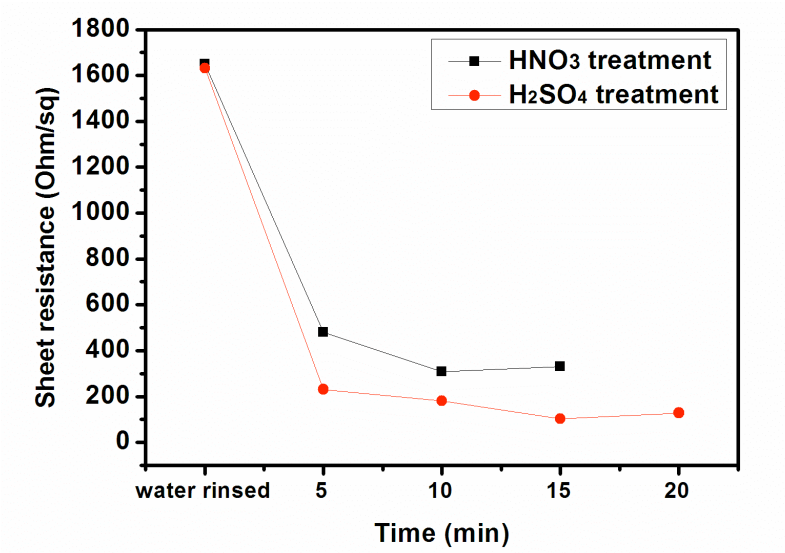

Figure 6-5. Time dependent acid treatment of Carbon nanotube film

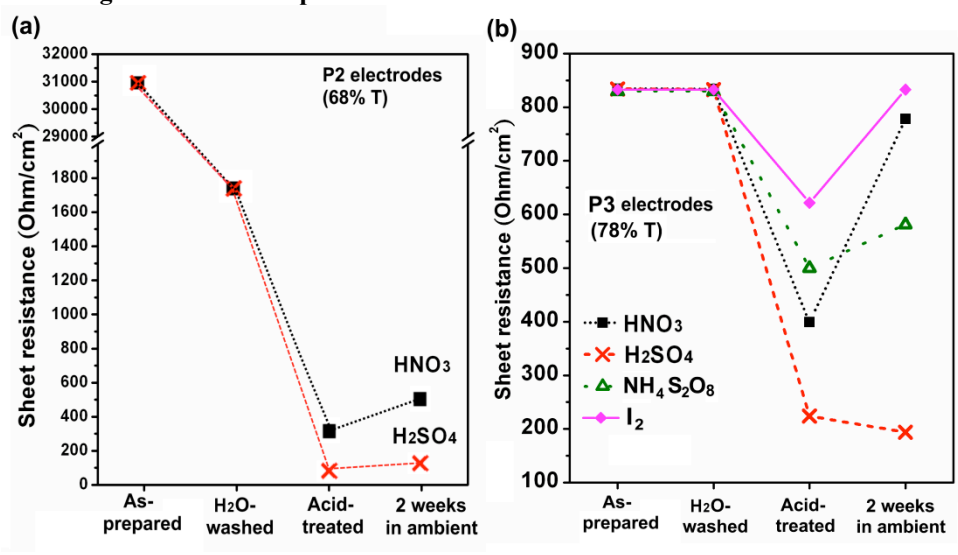

Figure 6-6 (a) Sheet resistance change of P2 carbon nanotube film with acid treatment, (b) Sheet resistance change of P3 carbon nanotube film with acid treatment

The Rs for the as-prepared P3 (Figures 6-6(b)) is almost half of the water-washed P2, suggesting that some residual surfactants are still present in the water-washed P2 electrodes. The Rs reduction of P3 electrodes is likely attributed to the lowering of the Fermi level (or *p*-doping) due to the electron-accepting (or oxidative) nature of these chemicals. The mechanism is supported by other works, where the Brønsted acids such as H_2SO_4 and HNO_3 can cause *p*-doping in SWCNT based on their photoelectron spectroscopy (XPS) results [104].

The results in Figure 6-6(b) showed that I_2, $NH_4S_2O_8$ and even HNO_3 doping are relatively unstable in ambient conditions. The Rs of the I_2-doped film undergoes the de-doping process immediately after the film is taken out from the I_2-vapor environment. This phenomenon is expected as the volatile I_2-vapor could easily detach from the carbon nanotubes to sublime in the air. The Rs for the films doped with HNO_3 also increases significantly after being exposed to the ambient environment for two weeks. These imply that the *p*-dopants, such as I_2, $NH_4S_2O_8$ and HNO_3, are not able to form stable bond with SWCNT and therefore are easily desorbed from SWCNT. In contrast, immersion in H_2SO_4 results in a film with the lowest Rs and a relatively stable doping and this indicates that the coexistence of strong oxidative and acidic properties is crucial for doping stability.

Figure 6-7(a) demonstrates the Rs-transmittance relation for the as-prepared and H_2SO_4-treated P3 electrodes. The typical Rs for the H_2SO_4-treated P3 electrode is comparable (~50 Ohm/sq. at 45% T) to the recent report using $SOCl_2$ for post-treatment [106]. Moreover, we observed that the Rs for P2 electrodes can also be reduced to similar low Rs values after H_2SO_4-treatment as shown in Figures 6-7(a).

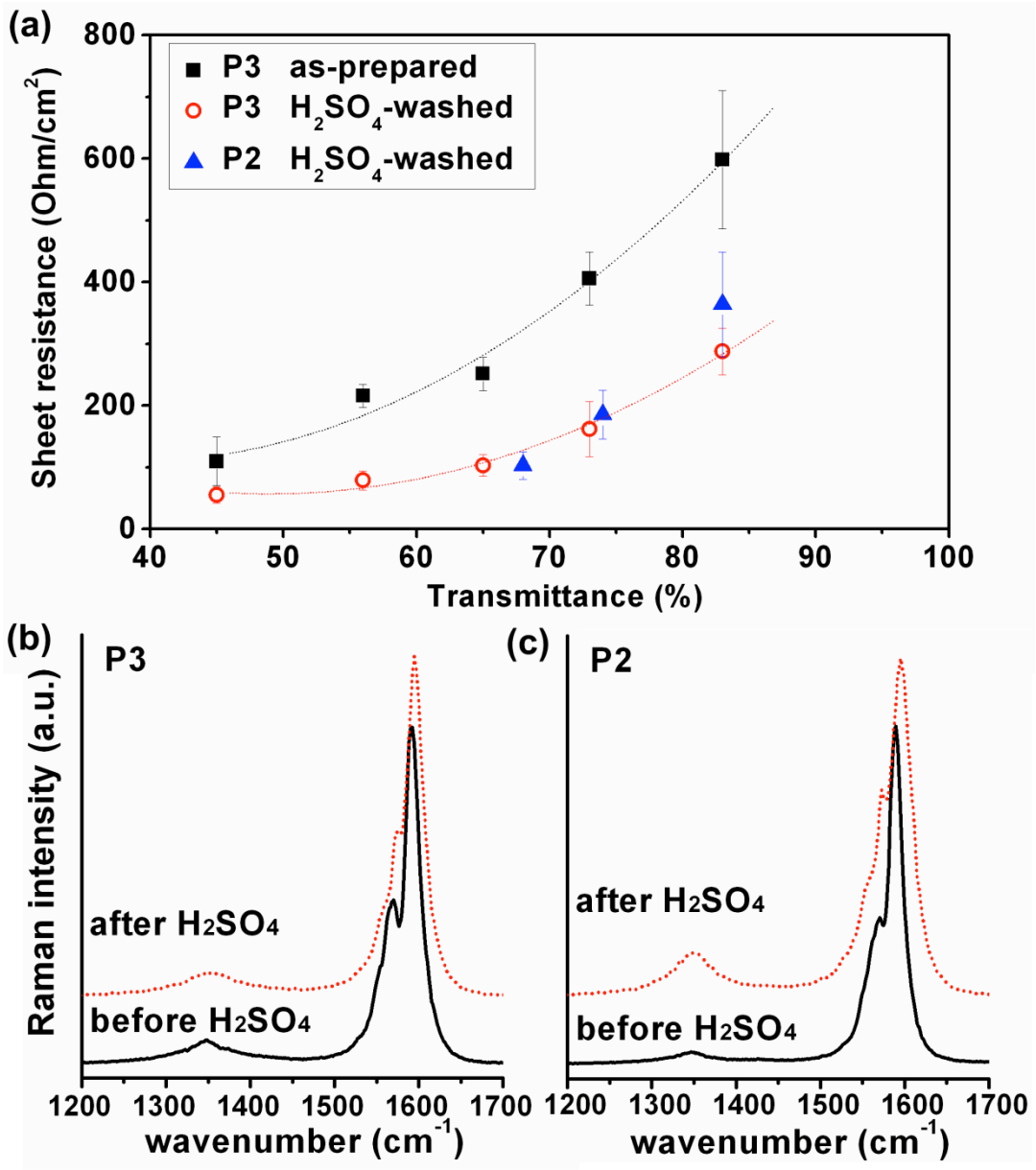

Figure 6-7 (a) Sheet resistance and transmittance of P2 and P3 film with acid treatment (b) Raman Spectra of P3 film with acid treatment (c) Raman Spectra of P2 film with acid treatment

To reveal the effect of oxidative treatments on the structure of SWCNTs, we performed Raman spectroscopic and FTIR measurements for both P2 and P3 after HNO_3 and H_2SO_4 treatments. The intensity ratio of D- to G-bands (D/G ratio) was enhanced and the G-frequency was up-shifted after H_2SO_4 treatment, as shown in Figures 6-7(b) and 6-7(c), thus suggesting an increase in defect concentration. The presence of $–SO_3H$ and –COOH group in these films is

confirmed with a strong FTIR peaks at 1048 and 1710 cm-1 shown in Figure 6-8, which represent the vibrational mode of those functional groups.

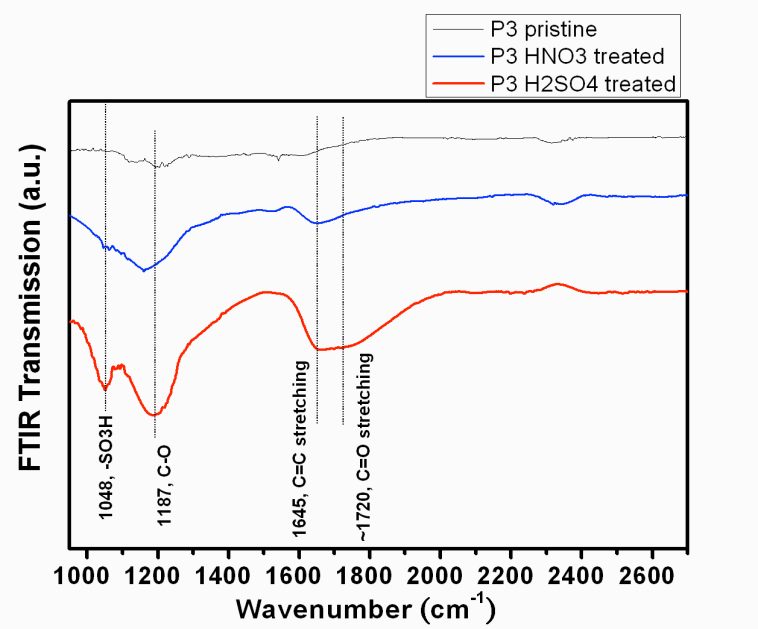

Figure 6-8. FTIR Signal of Carbon nanotube film before and after acid treatment

P3 and P2 carbon nanotube films showed similarities in morphology, in terms of bundles and length as shown in figure 6-9. Therefore, it is reasonable for us to compare these two carbon nanotubes for acid treatment effect. Also, the FESEM picture of the film before and after acid treatment (figure 6-10) shows similar features. Hence the acid treatment does not change CNT film morphology. In conclusion, the conductivity change is not caused by change in film morphology.

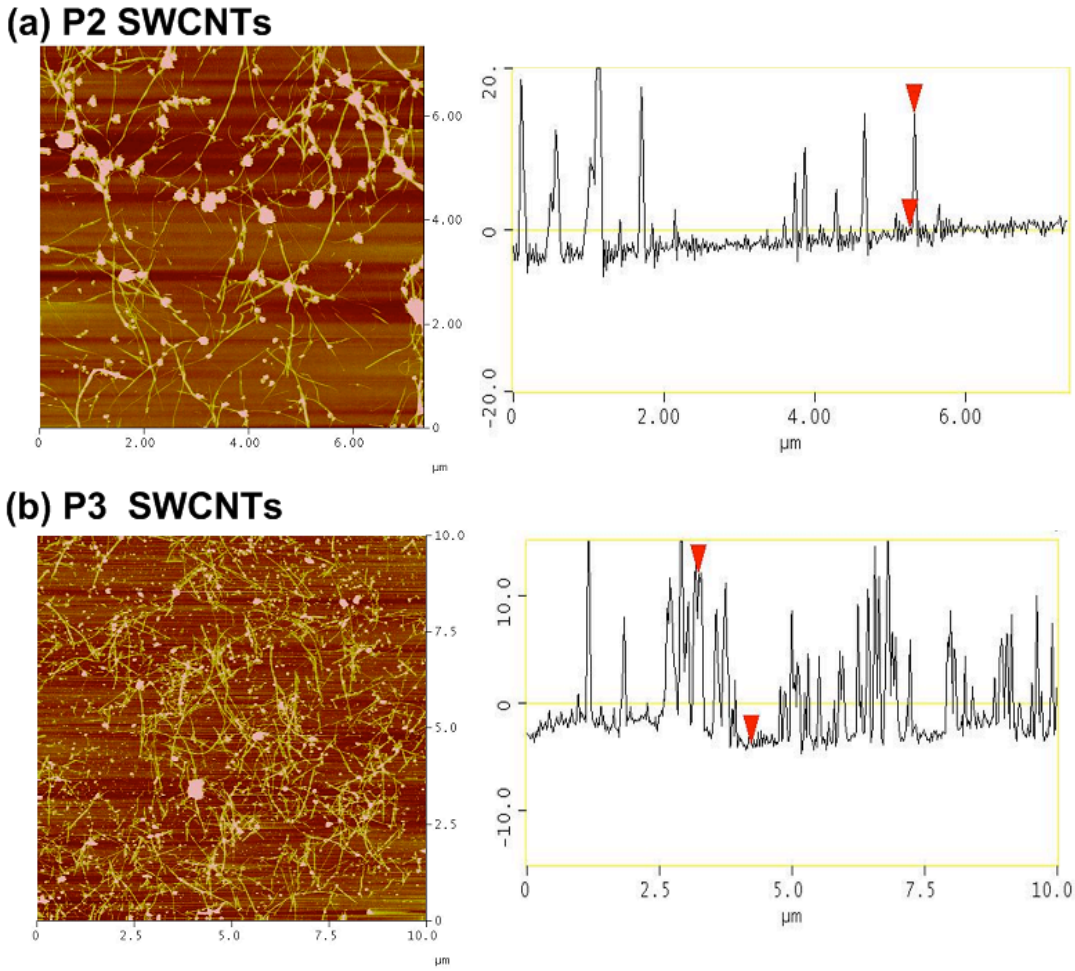

Figure 6-9. AFM picture of P2 and P3 carbon nanotube bundles

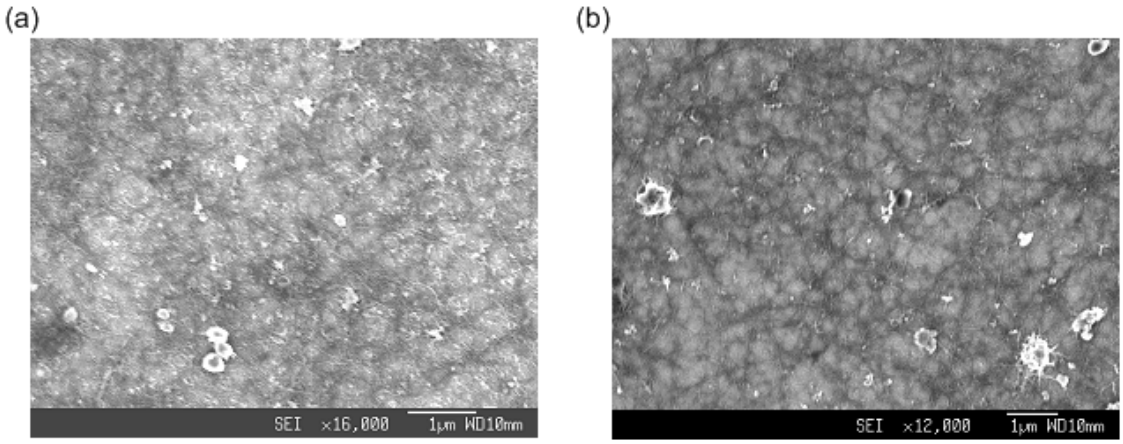

Figure 6-10. FESEM picture of P2 and P3 carbon nanotube film before (a) and after (b) acid treatment

We also noticed that the Rs started to increase if the H_2SO_4 treatment time was longer than 1 day as a result of the deterioration of π-π conjugation structure in SWCNT.

6.2 Protonation Doping

The first set of experiments seems to yield one valid conclusion: the acid treatment not only removes the surfactants, but also provides a doping effect to CNT. With all the data provided, it is still difficult to conclude how the chemical doping actually takes place. In the beginning, it is reasonable to hypothesise that the –COOH group is the origin of conductivity enhancement. [107] However, the FTIR signal also shows $–SO_3H$ peaks that could only come from sulphuric acid oxoanions. This phenomenon could indicate other possibilities. Oxygen containing acids such as sulphuric acid or nitric acid might only physically attach to carbon nanotubes, and protonize it. Protonation is the attachment of protons onto the walls of CNTs. An acid in aqueous solution will release a high concentration of protons, and these protons once attached to CNTs could act as a p-type dopant that would increase CNTs hole concentration.

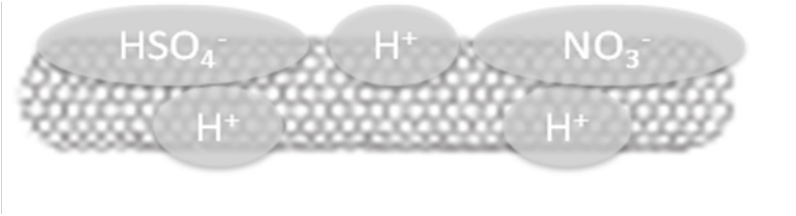

Figure 6-11 Schematic diagram of solid state protonation hypothesis

Protonation and acid treatment (also known as Bronsted treatment) on CNTs have been reported separately. In solution, protonation is detected by the suppression of S_{11} absorption peaks [108] followed by S_{22}. However, no reports of protonation have been made on solid thin films and the subsequent impact on the CNT films properties. Protonation in carbon nanotube solutions is a concentration dependent process. At a low proton concentration (pH close to 7),

metallic and large diameter semiconducting nanotubes will be protonized first and then at high proton concentration small diameter semiconducting nanotube will be protonised last.

In this investigation, the CNT film is prepared with the air-spraying technique described previously. CoMoCAT carbon nanotubes with metallic enriched (SWeNT CG200) and semiconducting enriched (SWeNT 65) was purchased from Southwest Nanotechnology and used without further treatment. These two ranges of carbon nanotubes were a good candidate for protonation study due to their selectivity in metallic / semiconducting contents. Carbon nanotube powder was dissolved in 0.5wt% SDBS solution with concentration of 0.2 mg/ml. Before any treatment, the film was immersed in water to remove the majority of surfactants. Afterwards, the film was further treated to solutions of different acid concentrations. Measurement of sheet resistance and UV-vis absorption of the film was carried out after every treatment. Sulfuric acid with different concentration and hydrochloric acid were used as post-treatment agents in this experiment.

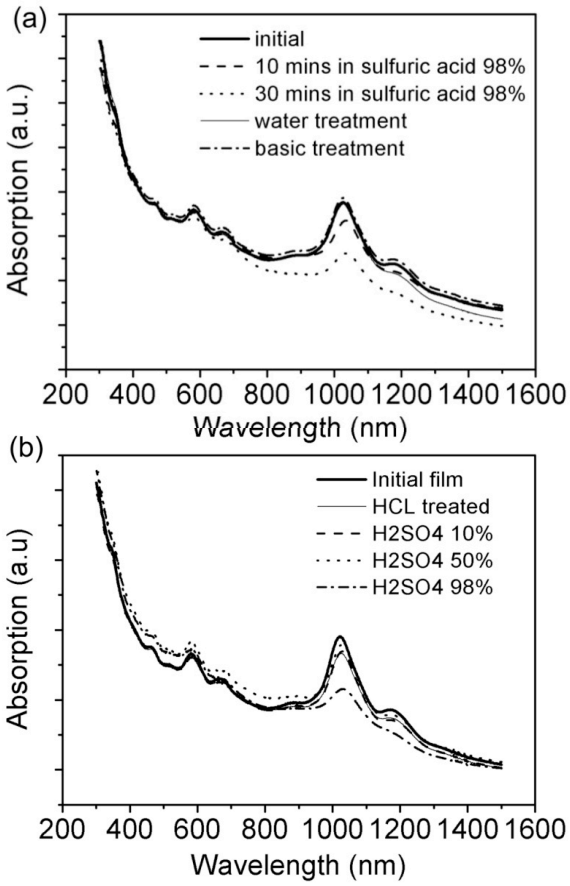

Figure 6-12 (a) Time dependent and (b) concentration dependent protonation of CoMoCAT 65 Carbon Nanotube Film

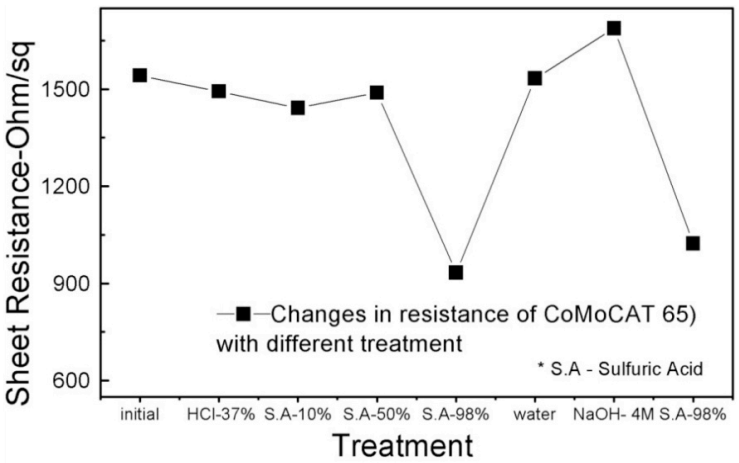

Figure 6-13. Resistance change with acid and basic treatment

From Figure 6-12 and 6-13 it is observed that the effect of acid treatment on UV-vis absorption is very similar to that of protonation [90]. The absorption peak of S11 band transition of carbon nanotubes is suppressed only upon 98% acid treatment, and the absorption peak of S22 is unchanged. This is due to

CoMoCAT 65's small diameter. On small diameter carbon nanotubes, protonation can only happen at a high proton concentration. The suppression of the S11 band transition could be reversed upon immersion in a basic solution.

The acid treatment process and protonation phenomenon share the similarities in their reversibility, time and concentration dependency. It is shown in Figure 6-12 on CoMoCAT 65 experiment for 15 minute and 30 minute immersion in an acid environment, the degree of protonation changes with a further suppression of S11 peaks. An immersion time longer than 30 minutes does not have any effect on the absorption spectra.

For CoMoCAT 65, the changes of conductivity are closely correlated to changes in the UV-vis absorption spectra. With the treatment of acid with low concentration (10-50 wt %), there are no observable changes in the UV-vis absorption peaks and film resistance. At 98 wt% sulfuric acid treatment, the UV-vis absorption spectra showed a S11 peak suppression at around 900-1000 nm, and its film conductivity was correspondingly enhanced. Upon immersion in low proton concentration solvents such as water, film conductivity and absorption spectra reverted to pre-treatment levels.

In Figure 6-13 another type of CNT, CoMoCAT CG200 was used, this product has a higher metallic NT content than CoMoCAT 65 (which can be observed from larger intensity of ratio of M11/S22).

The effect of protonation in CG200 CNTs takes place gradually, due to the larger diameters that are present in the CNTs population. At a lower acid concentration there are only suppressions of the S11 absorption peak at around 1300 nm, followed by S11 at 900 nm with increasing acid concentration. And the recovery also starts from 900 nm to 1300 nm. Its sheet resistance also

changes gradually with acid concentration treatment. Again, this supports the idea that acid treatment is a protonation process; with large diameter CNTs with smaller bandgaps, the protonation process occurs more easily (at 10% concentration peak suppression start to occur compared to CoMoCAT 65 that only experience protonation at 98% acid concentration).

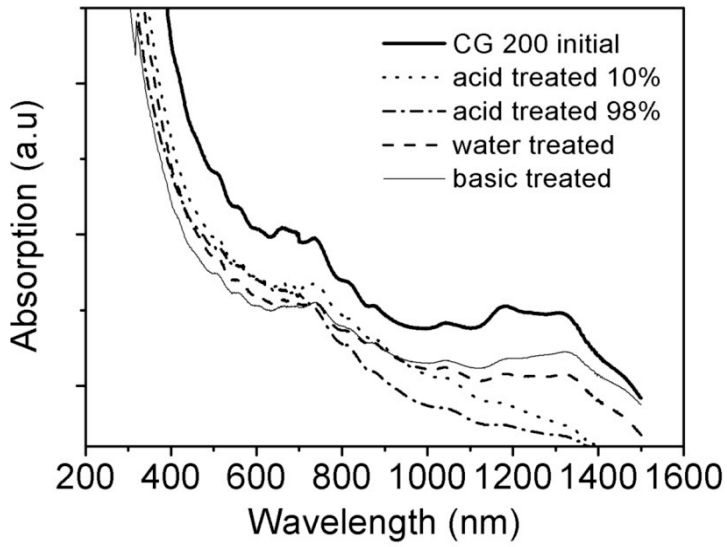

Figure 6-14. UV-Vis absorption spectra of CoMoCAT 200 Carbon nanotube film with different proton concentration treatment

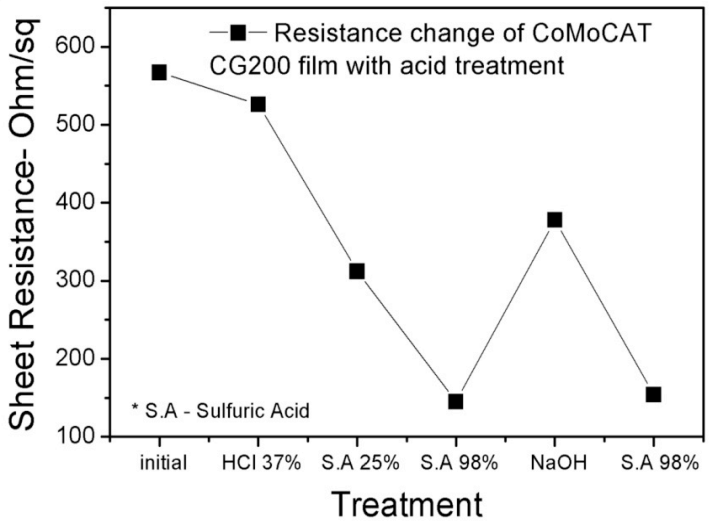

Figure 6-15. Sheet Resistance changeon different proton concentration treatment

For stability testing one sample was left to sit for two months after the acid treatment and followed by deprotonation to show that the protons attached to the

carbon nanotubes were still present and could only be removed upon deprotonation in a basic solution or water (figure 6-16).

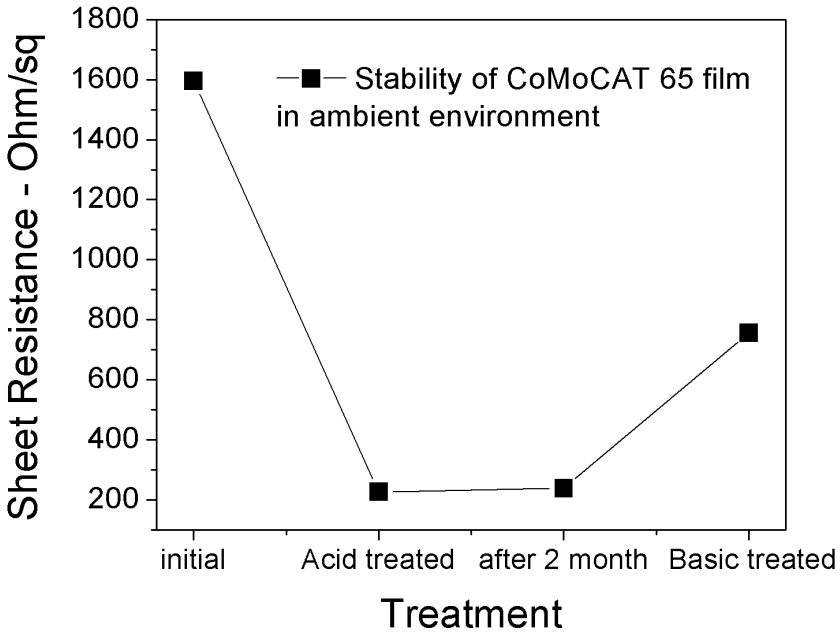

Figure 6-16. Sheet Resistance stability at ambient environment

However for CoMoCAT 65, due to its larger bandgaps, the protonation effect could only be observed at high acid concentrations. Our observations are in accordance with earlier reports of protonation by Strano et al. [108], smaller bandgap carbon nanotubes were protonised first followed by larger bandgap carbon nanotubes. If acid treatment were a chemical functionalization process or solely surfactant removal process, carbon nanotube conductivity would not change upon immersion in water, as water will not induce any chemical reaction in carbon nanotubes. However carbon nanotube properties seems to change in accordance with the proton concentration of the environment.

The protonation of carbon nanotube films can only be performed by using acid with oxygen containing anions such as HNO_3, H_2SO_4, H_2O_2. Trying protonation on carbon nanotube film by using HCl has shown no effect on both

conductivity and UV-vis absorption peaks. This evidence shows that the oxoanion plays an important role in enabling the protonation to take place.

There are many reports that observe the formation of crystalline layer by sulfate anion surrounding carbon nanotube wall [109] by-SAXS (Small Angle X-ray Scattering) . One report mentioned that after acid treatment the oxoanions XPS signal such as SO_4 and NO_3 was still found on the CNT film.[72]

From previous reports and current experimental data, a hypothesis on protonation mechanism can be constructed.

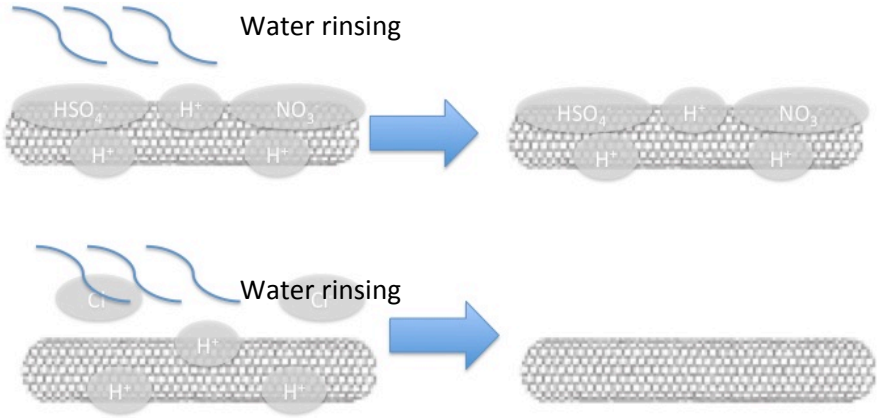

Figure 6-17. Schematic Mechanism for Solid State Protonation.

The acid oxoanion, which has been reported to stay stable on carbon nanotube walls, are believed to have some interaction with protons, and hence enable protonation to take place using H_2SO_4 or HNO_3 oxoacids. Ionic attraction between proton (positively charged) and oxoanion (negatively charged) could be the interaction that binds protons to CNT walls. HCl, which does not possess any oxoanions, has chlorine ions instead and cannot form a crystalline layer on CNT walls, and is unable to stabilize protons on CNT walls, and hence cannot protonize CNT films. Other possibilities such as using sodium ions (Na^+) and

hydroxyl ion (OH^-) to protonize CNTs were attempted but did not result in any change in absorption spectra or sheet resistance.

CNT films immersed in Na_2SO_4 for sodium protonation and NaOH for hydroxylation however, show no changes in UV-vis absorption and sheet resistance. The size of sodium ions is perhaps too big to allow interaction with the carbon nanotube electronic structure. It perhaps takes a strong implantation voltage to force the ion in and modify the CNT electronic structure. Hydroxyl ions, without a good stabilizer would not be able to hydroxylate CNTs. So, protons (H^+), due to its inherent properties, is able to play the role as dopant. By having a small size to let them easily interact with the CNT electronic structure as p-dopant. By having strong ionic interaction with oxoacid anions, it can stay stable on CNT sidewalls.

Further evidence on protonation can be observed with Raman spectroscopy. For semiconducting carbon nanotubes, protonation can be easily observed by the peak's suppression in the UV-vis spectra. In metallic tubes, it is difficult to monitor the electron near the Fermi level by spectroscopy, so the shifting of the BWF (Breit-Wigner-Fano) line in Raman spectroscopy is used to observe it. For CoMoCAT 65 carbon nanotubes none or very little shifting in the BWF upon protonation due to the lower content of metallic nanotubes was observed. However for CoMoCAT CG200, an obvious BWF peak shifting was observed, similar to those observed by Strano et al [108] in solution protonation of carbon nanotubes.

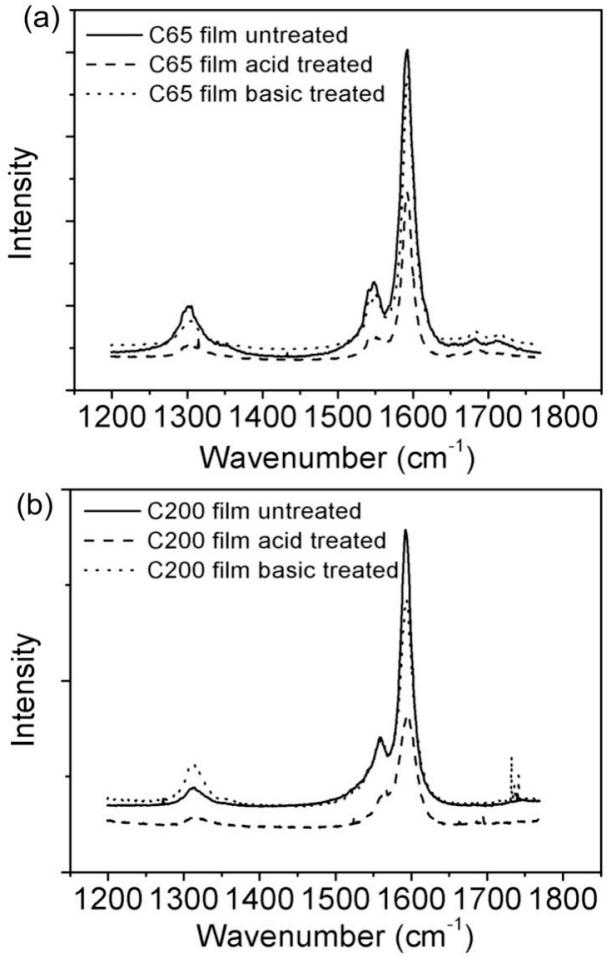

Figure 6-18. Raman spectra change of CoMoCAT 65 film (a) and CoMoCAT CG200 (b) with protonation

Protonation in solution phase would be a more efficient practice. However there are some factors that could hinder the practicality of solution protonation. Sodium dodecyl sulphate (SDS) is the only surfactant that gives us a protonated carbon nanotube solution as shown in Figure 6-19. As previously discussed, SDS is not a suitable surfactant to use for film deposition (unless it is on flexible PET substrate). The protonation of a solution with SDS could only be performed on low concentrations of carbon nanotubes, which is too low for conductive films fabrication by airspraying. At high concentrations agglomeration would occur. The protonation of carboxyl stabilized carbon nanotube solutions without the presence of a surfactant always leads to agglomeration problem, as the protons

disturbs the stability of carbon nanotubes, which originated from repulsion of the $–COO^-$ functional group. Protonation of SDBS stabilized carbon nanotube solution could not be performed due to strong binding forces between SDBS and carbon nanotubes which could prevent the carbon nanotubes from being protonized. No change in UV-vis absorption was observed from this system. Protonation in solution phase in fact was not very practical due to its exclusivity to the Sodium Dodecyl Sulphate (SDS) surfactant, which later on still needs to be removed via acid post-treatment. Hence, even if a CNT-SDS system could be protonized effectively in solution phase, an acid post treatment would still be necessary to remove the SDS. Only a surfactant free protonation in solutions, would be a remarkable development that could enhance process scalability, since it would eliminate the need for the post-treatment process.

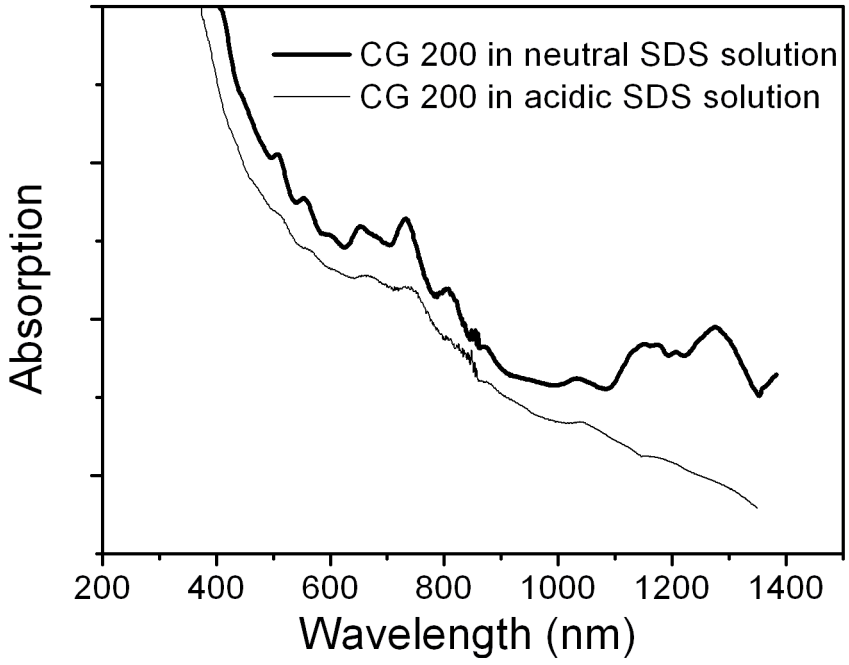

Figure 6-19. Protonation in Solution phase of CoMoCAT CG 200 with SDS surfactant

The solid state protonation can act as a very stable doping for CNTs. Protonated carbon nanotubes at different degrees can be explored for many

different applications such as sensing or Fermi energy engineering of carbon nanotubes.

6.3 Peroxides for enhanced protonation

The CNTs used in this work were purchased from Carbon Solution Inc. (denoted as P2 and P3) and Southwest Nanotechnologies (denoted as CG200)and used without further purification. CNTs produced by Carbon Solution Inc. by arc discharge process are a large diameter carbon nanotubes (could be observed from the S11 peak), whereas CNTs produced by Southwest Nanotechnologies by CVD process are a smaller diameter carbon nanotubes. CNT powder with a concentration of 0.2 mg/ml was dissolved in surfactant/water mixture. In our case the Sodium Dodecylbenzenesulfonate (SDBS) surfactant with 0.5wt% was used. P3 CNTs could be dissolved without addition of any surfactant, but later on it was discovered that a surfactant could enhance its morphology by restricting CNT movement during solvent evaporation, and in turn result in better conductivity. Hence even for P3 carbon nanotubes with a –COOH group, a 0.5wt% surfactant was still used. A solution of CNTs was obtained after 30 minutes of 20 Hz 120 watt probe sonication and 6000 rcf centrifugation. Thin film fabrication was done by air spraying on to a glass substrate (Badger equipment). The film is then soaked in water to remove the majority of the surfactant. Characterization of the film was carried out by 4-point probe measurement for conductivity, UV-vis spectroscopy for transmittance and absorption, Raman spectroscopy and Atomic force microscopy for morphology.

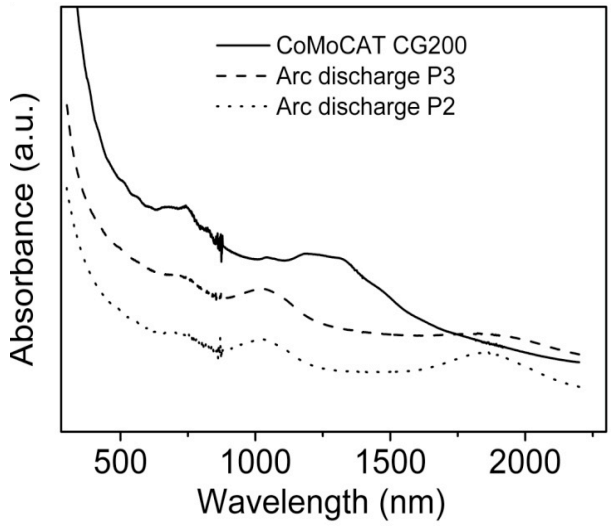

Figure 6-20. UV-Vis Absorption Spectra of Arc discharge (P2 and P3) and CoMoCAT Carbon nanotube

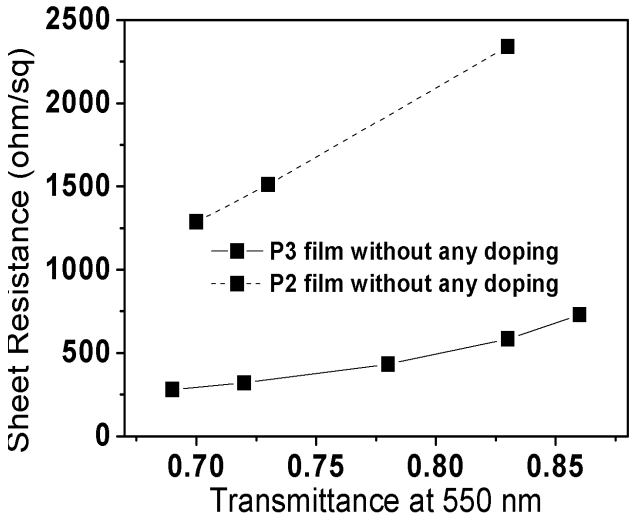

Figure 6-21. Sheet Resistance of Pristine Carbon Nanotube Film

The UV-vis characterization of initial pristine CNT film can be observed in Figure 6-20 Arc discharge CNTs by Carbon solution has S11 peaks at 1800 nm whereas CoMoCAT carbon nanotubes by Southwest Nanotechnology have it at 1300 nm. It shows that Arc discharge CNTs have larger diameters. Between P2 and P3 CNTs it is observed that S11 peaks on P3 are not as strong as P2, and in turn as observed in Figure 6-21 the pristine film of P3 has a higher conductivity than P2. Suppression of S11 peaks observed in P3 is possibly due to p-doping of

CNTs due to its –COOH functional group, and p-doping could result in increased conductivity.

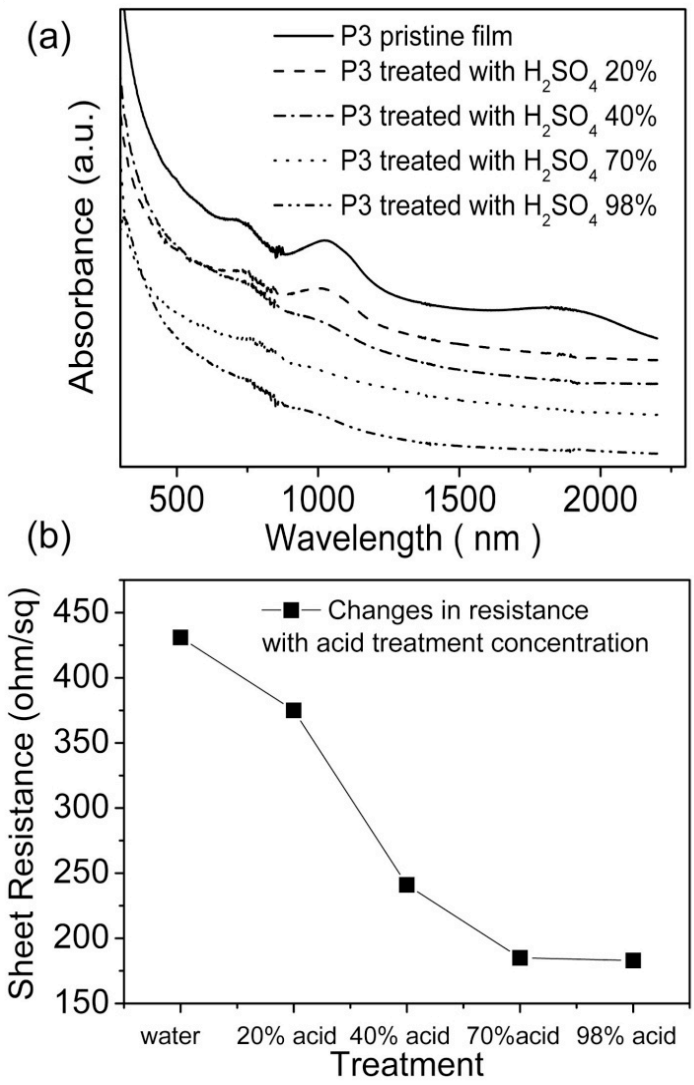

Figure 6-22 (a) UV-Vis-NIR absorption and (b) sheet resistance of P3 carbon nanotube film with increasing acid treatment

Subsequently, the CNT films were doped step-by-step by sulphuric acid until most of the peaks were suppressed due to acid protonation. The film was immersed in acid solution for 15 minutes and washed with water before testing. As seen in Figure 6-22(b) conductivity of carbon nanotubes increases with increasing acid concentration from 20-98%. Further increase of the acid concentration from 70% does not have an additional effect on carbon nanotube

absorption peaks and conductivity. In this situation, it means the doping by acid has reached its limit.

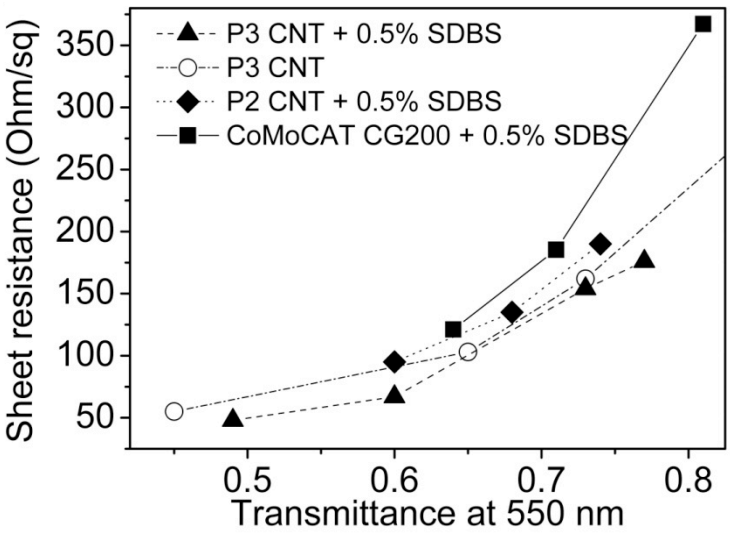

Figure 6-23. Sheet resistance of different carbon nanotube film formulation

In figure 6-23, P3 with 0.5wt% SDBS shows better conductivity compared to P3 without SDBS. It is initially confusing to see that an addition of SDBS in the solution could affect the conductivity of the resulting films. Therefore the morphology of both films are check using AFM. An AFM characterization in Figure 6-24 shows that SDBS surfactants could help carbon nanotubes attain favorable morphology. The CNTs from SDBS solution were evenly distributed in the substrate (Figure 6-24 b), whereas we observed many non uniform clumps of CNTs from P3 solution without SDBS (Figure 6-24 a).

CoMoCAT CG200 by Southwest Nanotechnology showed the best morphology among all the films (less particle and impurity), however its conductivity is not as high as P2 and P3 CNTs.

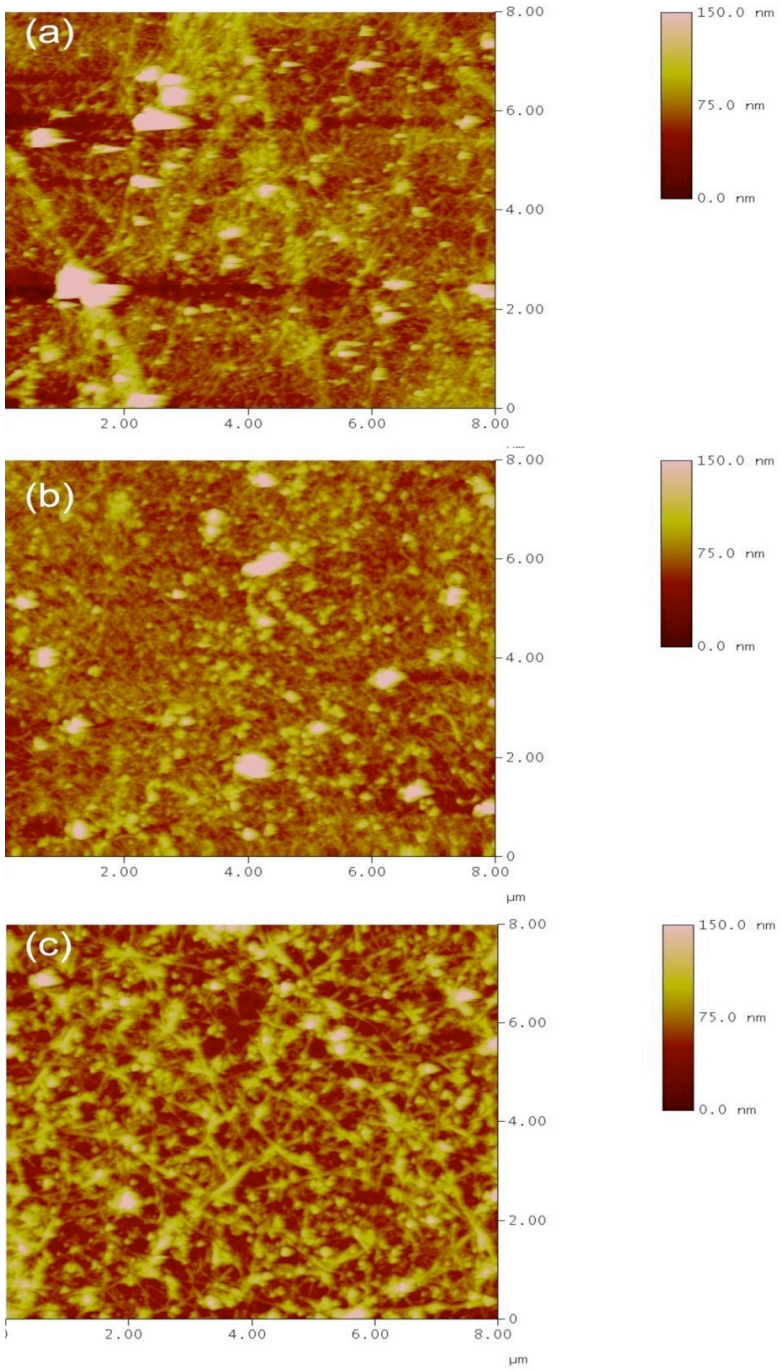

Figure 6-24. AFM image of carbon nanotube films (a) P3 without SDBS (b) P3 with 0.5wt% SDBS; (c) CG 200 with 0.5wt% SDBS

So in conclusion, morphology does play a role in attaining high conductivity films, but CNT diameter is the more important parameter. Large diameter CNTs will provide higher carrier concentration that could improve overall film conductivity.

In this present state, CNT film conductivity is still insufficient as an Indium Tin Oxide replacement (sheet resistance is still in the range of ~280 ohm/sq @ 85% transmittance). A new dopant that has very high reduction potential (strong oxidator) is needed to inject even more protons into carbon nanotubes. Hydrogen Peroxide is used as one of the candidates. Hydrogen peroxide / water shows a high reduction potential E^0 of 1.8 V. H_2O_2 would need an acidic condition to initiate its reaction, therefore a mixture of H_2O_2 and H_2SO_4 is used, this mixture is normally called the Piranha mixture. The reaction in piranha solution with carbon materials is as followed :$C + H_2O_2 + 2H^+ \rightarrow C^+ + 2\ H_2O$.

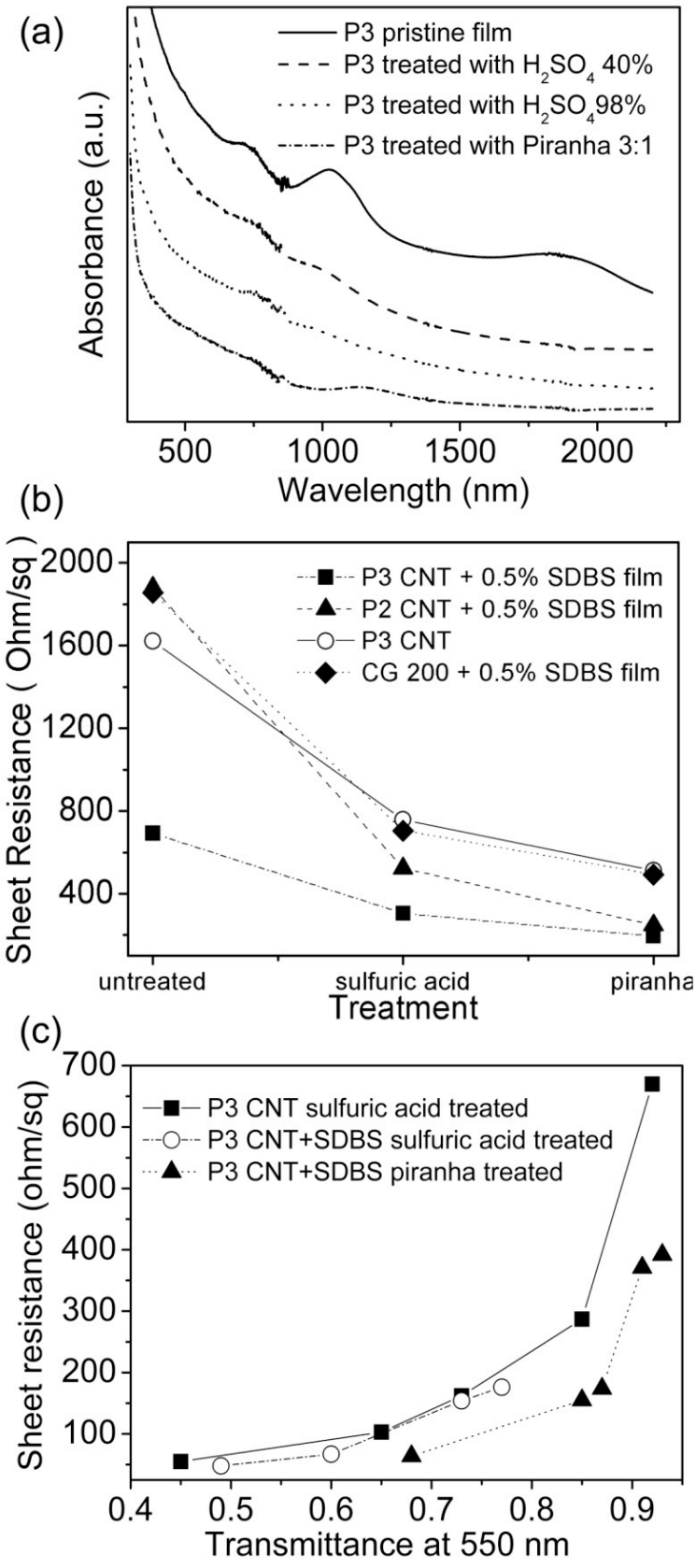

Figure 6-25. The effect of piranha treatment on (a) Sheet resistance change (b) UV-Vis-NIR absorption spectra (c) Resistance and transmittance curve of different doping of carbon nanotube

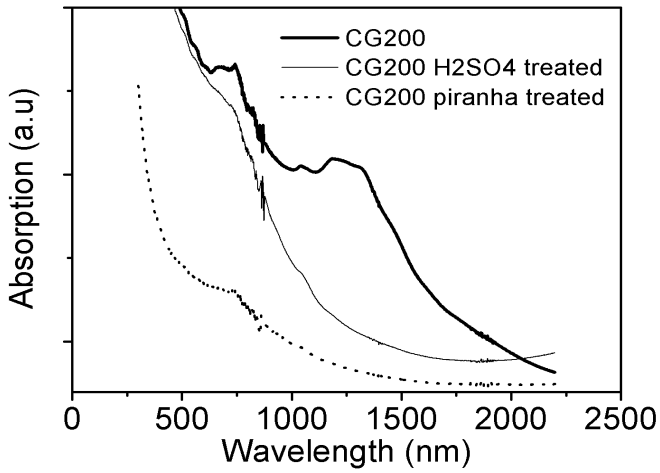

Figure 6-26. UV-Vis Absorption spectra of Piranha treatment of CG 200 film

With a subsequent treatment of Piranha mixture, the P2, P3 and CG200 carbon nanotube film conductivity could be further lowered . The best result was achieved by the P3 + 0.5% SDBS film, where the sheet resistance could be further lowered from ~280 ohm/sq @ 85% transmittance to ~150 ohm/sq @ 85% transmittance as shown in figure 6-25. The UV-vis spectroscopy measurement shows a further suppression on most CNT peaks. This highly conductive carbon nanotube film was stable for weeks in an ambient environment. However immersion in water and/or basic solution could decrease its conductivity to its original state. This phenomenon clearly indicates that the doping mechanism of peroxides is by protonation. Peroxides could give better protonation compared to normal acids due to its higher reduction potential.

The Raman spectroscopy on P3 carbon nanotube films (figure 6-27) shows there is up-shift in the G band that indicates hole doping to the carbon nanotube film. The shift (around 20 wavenumber) is much more pronounced than normal sulphuric acid treatment (10 wavenumber).

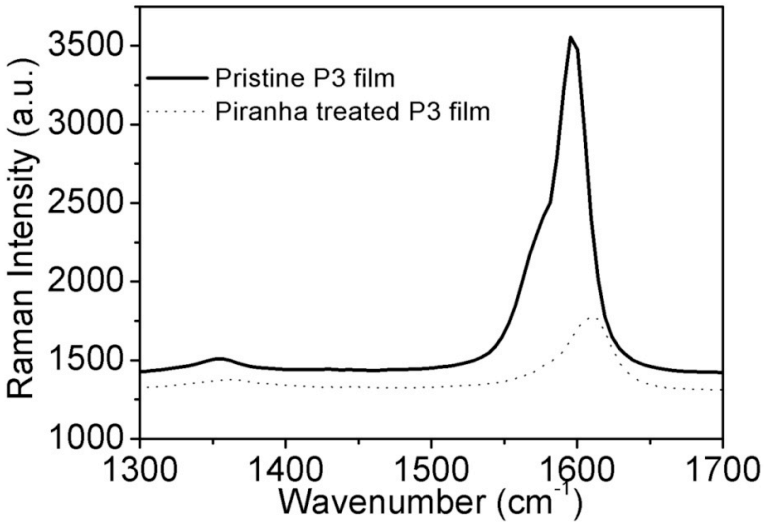

Figure 6-27. Effect of piranha treatment on Raman Spectra shift of Carbon Nanotube

The highly conductive film by piranha treatment is the main accomplishment of this research. Even though this value of ~150 ohm/sq @ 85% transmittance at 550 nm wavelength has been seen in other reports, the main point highlighted here is that we are using commercially available carbon nanotubes without further purification or separation and a low cost chemical as dopant. Our process is also scalable with a high yield. 1 miligram of carbon nanotube powder (cost 0.4 USD) could be used to fabricate 5 pcs of 2.5 cm x 2.5 cm carbon nanotube film in 20 minutes. Hence the material cost for each thin film would be only 0.08 USD.

CHAPTER 7 – APPLICATION OF CARBON NANOTUBE CONDUCTIVE FILM ON DEVICES

After carrying out comprehensive experiments on carbon nanotube film fabrication and able to fabricate CNT films with good electrical and optical properties, it is important for us to test these CNT films in devices. It is common to have integration issues when using new conductive films components. Hence this chapter is a proof of concept to show that our CNT films can be integrated into some devices with or without processing modification.

CNT-based transparent conductive films, as mentioned in the introduction chapter, have numerous potential applications. As a replacement for Indium Tin Oxide, carbon nanotube films could be used in light emitting diodes, solar cells, touch screens, etc. In this research, two types of devices: dye sensitized solar cells and transistors, have been fabricated using our carbon nanotube conductive films. Both devices show promising performance compared to the traditional types.

The dye-sensitized solar cell uses carbon nanotube films as its photo-anode and counter electrodes, whereas the transistor uses carbon nanotube films as its electrodes, making it an all-carbon based transistor.

7.1 Dye Sensitized Solar Cell (DSSC)

The DSSC, is a type of 3rd generation that uses dyes as its light harvesting components. Its schematic diagram can be shown in the Figure 7-1 below. According to the diagram, there are four components that comprise the solar cell: the photo anode (conducting glass – normally Fluorine doped Tin Oxide –FTO),

Titanium Dioxide (TiO_2) with dyes as an active layer, electrolytes, and the counter electrodes (platinum coated FTO).

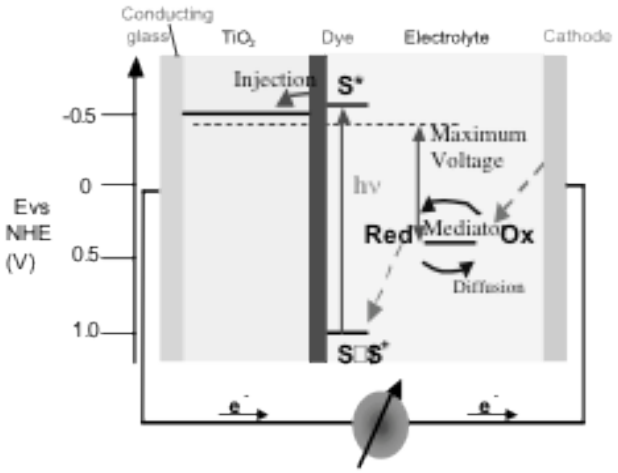

Figure 7-1. Dye Sensitized Solar Cell (Reproduced with permission from ref. [113] Copyright 2009 Wiley-VCH)

The working principle starts from the dye. When light shines on the cell, the electron in the dyes was excited to higher energy state and become a configuration called excitons. This exciton will separate into electrons and holes. Electrons will be injected into Titanium dioxide and holes will transport into the electrolytes. After receiving holes, the electrolyte will be reduced and diffuse to counter electrodes. In counter electrodes, the electrolyte will transfer its hole to the electrodes and be oxidized back to its original state.

DSSC have several advantages compared to other 3rd generation solar cells because of its high efficiency. DSSC power conversion efficiency can reach 11% [107]. However, the real problem of DSSC is its stability and cost. The usage of Fluorine-doped Tin Oxide and Platinum liner as the photo anode and counter electrodes is very costly, and the Ruthenium-complex dyes may degreade under ambient environment. Despite all these drawbacks, DSSCs are still one of the

most promising solar cell structures that can attain such a high power conversion efficiency. Organic solar cells that make use of polymers or small molecules can only attain a 4-5% power conversion efficiency and are unstable in ambient environments.

Currently, research on DSSCs is still actively ongoing in two directions: stabilizing the cell and decreasing its cost. The first direction is to find a stable dye with a suitable bandgap for light absorption. A common problem in organic dye is its versatility. It tends to decay after a few days of operations. The second direction is to search for a cheaper alternative to replace the current component. Carbon nanotube transparent conductive films could help to replace the usage of Fluorine doped tin oxide (FTO) for photo anodes or Platinum coated FTO for counter electrodes.

Figure 7-2 below shows the fabrication process of dye sensitized solar cell :

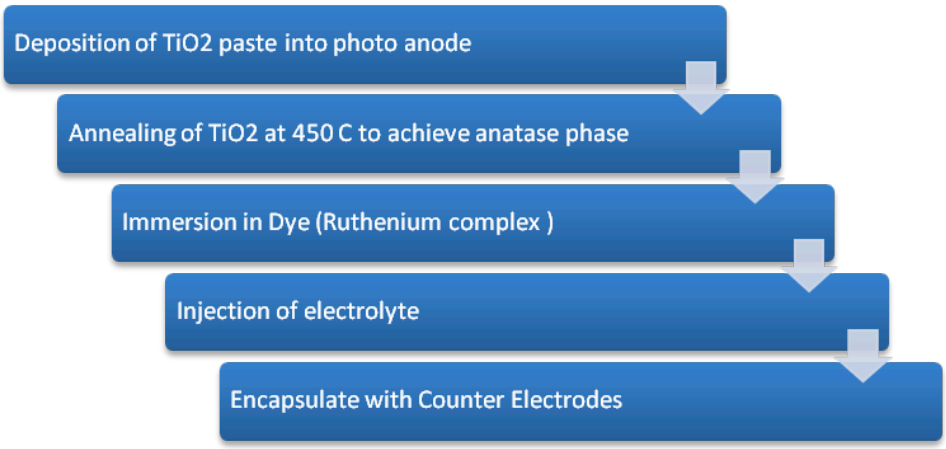

Figure 7-2. Dye Sensitized Solar Cell Fabrication Step

For usage of CNTs electrodes as working electrodes / photoanodes, there are some fabrication problems caused by the subsequent process of high temperature annealing. Formation of a TiO2 anatase phase would need annealing in 450 ^{o}C for 3 hours in an ambient environment. At this temperature carbon nanotubes will

be partially oxidized to carbon dioxides, hence a lower temperature process needs to be adopted. Secondly the mesoporous morphology of the TiO2 layer may cause a shorting with carbon nanotube film electrodes. CNT films, naturally would have rough morphology due to its tubular geometry. The spikes from CNT films once connected to the electrolyte would cause the whole solar cell to short circuit and become unable to produce any power. The short circuit and oxidation problems have been solved in our works by introducing a dense protective layer of TiOx on top of the CNTs electrodes before the deposition of mesoporous TiOx. The structure of DSC with CNT working electrodes is shown in Figure 7-3.

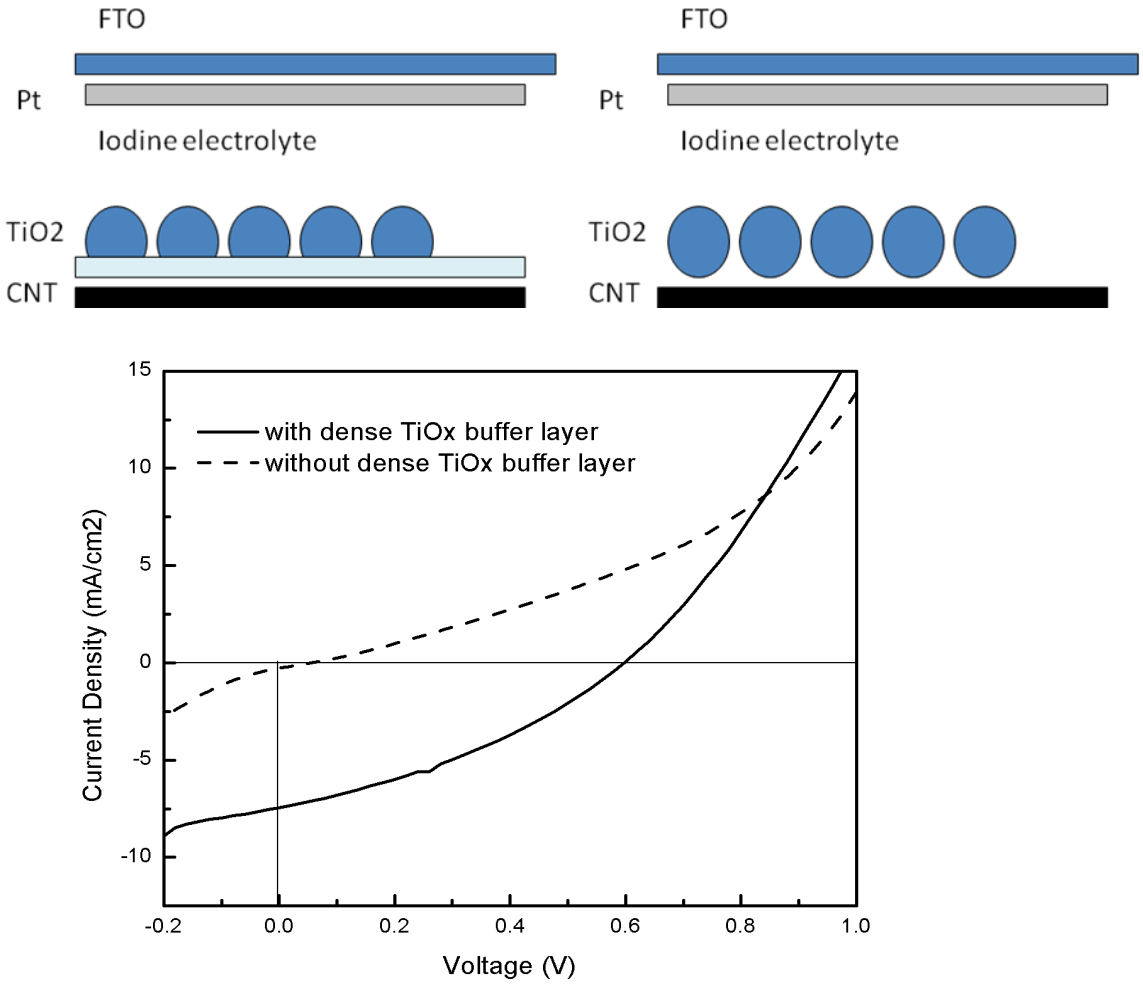

Figure 7-3 Schematic diagram and Performance of Dye Sensitized solar cell with FTO-Pt counter electrodes and P3 CNT working electrodes.

The dense layer of Titanium oxide has been shown to be able to prevent shorting between CNT electrodes and the iodine electrolyte. Without the dense layer of TiOx, the cell did not show any photovoltaic effects due to shorting.

Apart from that, the dense TiOx buffer layer also played a role in protecting the CNT electrodes from oxidation during annealing at 450 ^{o}C. The performance of the CNT electrodes as DSC photo-anodes are summarized in the table below (under 100 mW/cm2 light).

Table 7-1. Performance of Carbon Nanotube Working Electrodes

Electrodes	Buffer layer	Isc	Voc	FF	Efficiency
CNT electrodes	Yes	7.441 mA	0.598 V	0.34	1.53 %
CNT electrodes	No	0.281 mA	0.057 V	-	-

As to the usage of CNTs as counter electrodes, there is no fabrication issue. According to some reports[114], carbon paste can be coated onto FTO glass to replace Platinum as counter electrodes. However a thick film is required (around 200 micron) in order to achieve a similar performance to platinum. The role of platinum in dye sensitized solar cells is to catalyze the electron transfer to the electrolyte, this electron transfer is by redox reaction of iodide to triodide and vice versa. Non-catalyzed electrons transferring from the electrolyte to control electrodes have shown to adversely affect solar cell performance. Only a 0.02% efficiency can be achieved if FTO is used without any deposited Pt layer [116]. Even though FTO has good conductivity, it is still not a good electron transfer catalyst. Carbon nanotubes are expected to have a better performance than Carbon black due to its higher catalytic activity and better conductivity. Clearly, the

conductivity of carbon nanotube films is good enough to be used as the electrodes and it also possesses good catalytic properties for redox reaction between triiodide and iodide.

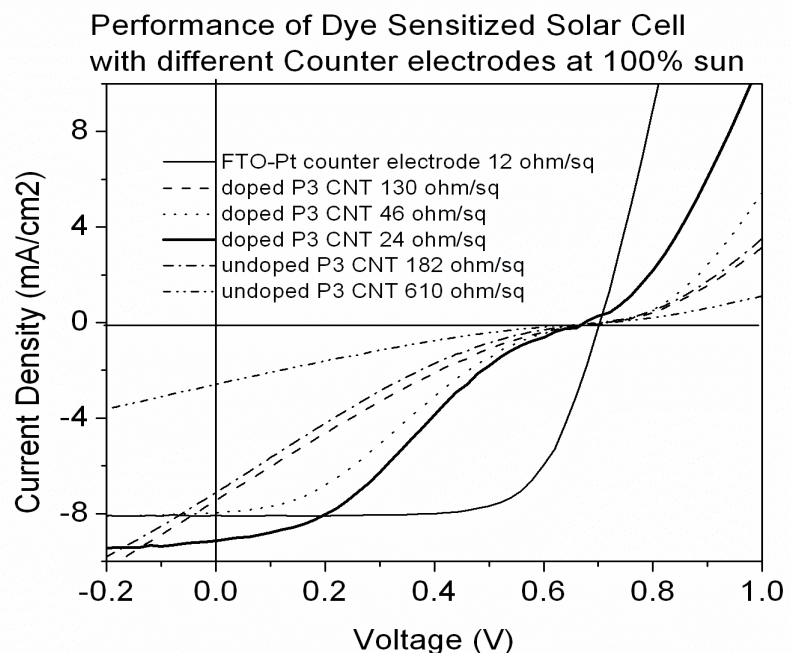

Figure 7-4. Performance of Dye Sensitized solar cell with P3 Carbon Nanotube Counter Electrodes

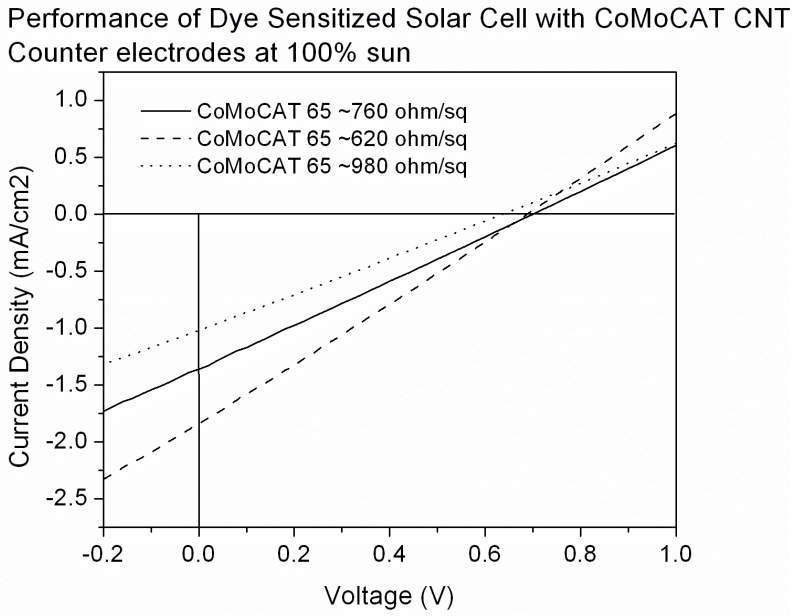

Figure 7-5. Performance of Dye Sensitized Solar Cell with CoMoCAT CNT counter electrodes

Table 7-2 Performance of Carbon Nanotube Counter Electrodes

Device	Counter Electrodes	Voc	Jsc	FF	Eff.
1	FTO-Pt ~12 ohm/sq	0.703	-8.079	0.7	3.95 %
2	**CNT- P3 ~ 24 ohm/sq**	**0.679**	**-9.136**	**0.3**	**1.88 %**
3	CNT- P3 ~ 46 ohm/sq	0.717	-7.958	0.27	1.53 %
4	CNT- P3 ~ 130 ohm/sq	0.714	-7.452	0.19	1.00 %
5	CNT- P3 ~ 162 ohm/sq (undoped)	0.711	-7.114	0.17	0.88 %
6	CNT- P3 ~ 610 ohm/sq (undoped)	0.711	-2.584	0.19	0.35 %
7	CNT- CoMoCAT 65~ 620 ohm/sq	0.688	-1.835	0.26	0.32 %
8	CNT- CoMoCAT 65 ~ 980 ohm/sq	0.637	-1.019	0.26	0.17 %

From table 7-2, it can be observed that the sheet resistance of carbon nanotube films is closely proportional to its short circuit current density. Doping of CNT with the piranha solution did not reduce the CNT performance. In fact, it improved the carbon nanotube conductivity and helped to increase short circuit currents. Sample 4 and 5 compare two different counter electrodes, sample 4 is doped with piranha, with transmittance of 85%, and sample 5 is undoped, with transmittance of 60%. The performance of these two counter electrodes was

found to be similar. Hence the thickness and doping level of carbon nanotubes did not really affect the performance of counter electrodes significantly.

Even though the performance of carbon nanotube counter electrodes in our lab is lower than FTO-Pt standard electrodes, this result is better than other reports on CNT counter electrodes. Definitely there is still room for further improvement of device performance. The fill factor of carbon nanotube counter electrodes seems to be quite low, and further study needs to be focused on this topic.

7.2 All Carbon Based Field Effect Transistor

Transistors were one of the extensively explored applications of CNTs due to theoretical ballistic transport of CNT. The separation of semiconducting carbon nanotubes from metallic one has been a popular topic for the past 5-10 years, and currently we can comfortably get 98-99% semiconducting carbon nanotubes, which eases the fabrication of transistors. Nano Integris Pte Ltd currently sells carbon nanotubes of this quality. This makes it much more convenient to fabricate field effect transistors from carbon nanotubes compared to few years ago when the technique had not been perfected and there were no commercially available separated CNTs. The structure of carbon nanotube transistors is as follows:

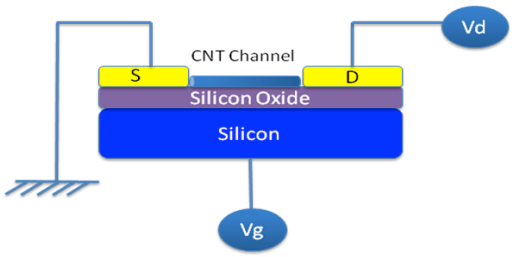

Figure 7-6. Bottom Gated All Carbon Nanotube Transistor

However, not many people actually study the effects of using carbon nanotubes as electrodes. Although a few reports [117,118] have developed carbon nanotube devices, there is no detailed study on the effect of different carbon nanotubes as electrodes, or what are the properties that needed for a good electrode in field effect transistors. The use of carbon nanotubes on both electrodes and channels would allow a fully printable field effect transistor. The fabrication method of this device is as shown in Figure 7-7

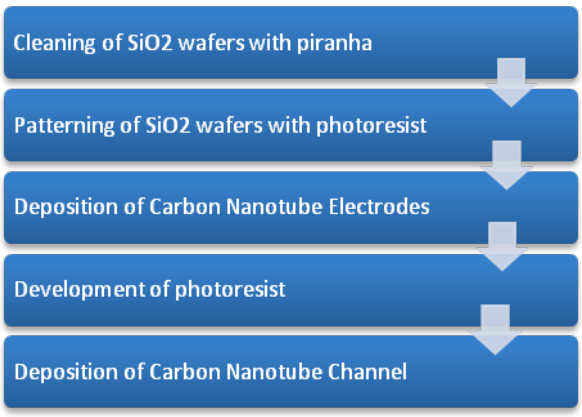

Figure 7-7 Fabrication step of All Carbon Nanotube Transistor

In this study, three different types of carbon nanotubes are used: CoMoCAT 65, CoMoCAT 76, and Arc Discharge P3. These three different carbon nanotubes were deposited into patterned photoresist, and followed with a photoresist lift off process to obtain patterned carbon nanotube electrodes. The channel of this carbon nanotube transistor used 98% Semiconducting Carbon Nanotube (Isotubes) purchased from Nano-Integris Inc.

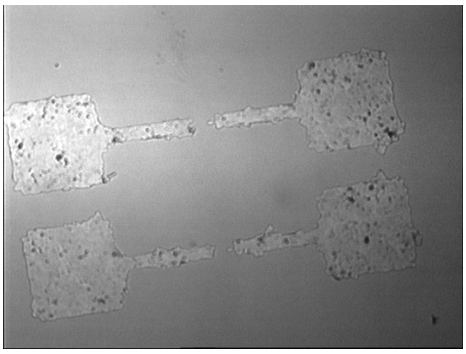

Figure 7-8. Optical Microscope Image of Carbon Nanotube Electrodes

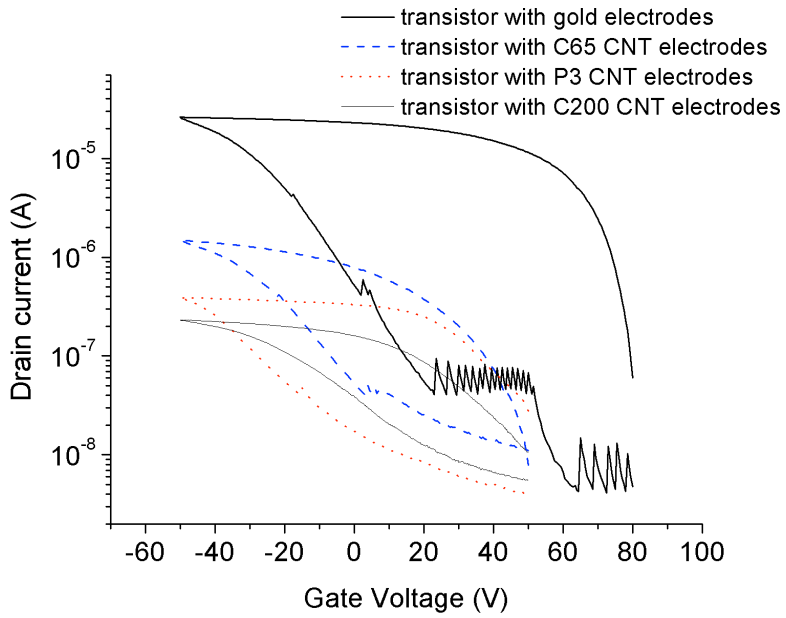

Figure 7-9 Performance comparisons between gold electrodes and carbon nanotube electrodes

Table 7-3 Mobility of Bottom Gated Transistor with Carbon nanotube electrodes

Electrodes	Channel	Dimension	On/Off	Mobility
Gold	NanoIntegris 99% semiconducting	25 um (W) x 50 um (L)	2 order	13.9
P3 CNT	NanoIntegris 99% semiconducting	25 um (W) x 50 um (L)	2 order	1.25
CoMoCAT 65 CNT	NanoIntegris 99% semiconducting	25 um (W) x 50 um (L)	2 order	1.91
CoMoCAT 200 CNT	NanoIntegris 99% semiconducting	25 um (W) x 50 um (L)	1.5 order	0.33

In figure 7-9, it can be concluded that CNT electrodes can be used as electrodes in bottom gated transistors. This would allow an all solution-based fabrication of bottom gated transistors. However, the overall performance of the bottom gated transistors with carbon nanotube electrodes is still inferior to those

with gold electrodes. There are many possible reasons for this phenomenon. For example, lower conductivity of carbon nanotubes may limit the on current of the transistor. Charge trapping in carbon nanotube thin films may also induce another resistance. CoMoCAT CNTs with higher semiconducting contents show better transistor performance, and this could be due to a lower schottky barrier between semiconducting CNT (in channel and in electrodes). Further research is needed to optimize this bottom gated transistor device and finally to scale up the device fabrication by integrating this solution process to inkjet printing system.

CHAPTER 8 – CONCLUSION AND FUTURE WORK RECOMMENDATION

8.1 Conclusion

In this work, the use of a carbon nanotube network film as a transparent conductor was thoroughly investigated. The CNT film was fabricated by an airspraying method - a fast, high yield and scalable method that can be easily implemented in industrial application.

8.1.1 Fabrication of Carbon Nanotube Thin Film

The fabrication technique for CNT thin films by airspraying was first studied and optimized in order to fully understand the process. There are many different parameters involved in this process, starting from solution formulation (CNT type, concentration, surfactants type and concentration), the solubilization process (ultrasonication duration, intensity, centrifugation), the time dependent property of the carbon nanotube solution, and properties of the CNT solution. An ideal solubilization process would be able to solubilize as many CNTs into the solution and create a stable dispersion. Arc discharge CNTs with functional groups have been found to possess the highest conductivity, and can be dissolved without the addition of surfactants. However the dispersion stability and solubility of CNTs in water can be enhanced with the addition of surfactants, which in turn it can enhance CNT film conductivity even more by having a better dispersion. Probe ultrasonication has been shown to be a better process compared to bath ultrasonication, as it can provide sufficient power to debundle and solubilize CNTs better than bath ultrasonication. Probe ultrasonication at 20 Hz 120 watts was also

shown to not induce much damage to CNTs. The length of CNTs after ultrasonication is still more than one micron. Centrifugation at 6000 RCF is sufficient to remove some impurities, but at a higher centrifugation speed of 10,000 RCF, the conductive long length bundles would be precipitated due to its higher weight. Hence, we observed the quality of the supernatant solution is not as good for conductive film fabrication. A low boiling point solvent such as ethanol is favored for conductive film fabrication due to its quick evaporation and uniform deposition pattern (no coffee ring pattern). However, a low boiling point solvent suffers from a lack of CNT solubility, as surfactants are unable to solubilize CNTs in alcohol-based solvents. Thus, the basic fabrication parameters for CNT films were thoroughly investigated and a solid understanding of the process was gained.

8.1.2 Conduction Mechanism of Carbon Nanotube Networks

The conduction mechanism of CNT networks was also carefully studied. Different models that have been used by different researchers in modeling the resistance and transmittance of CNT film were tested against the different types of CNT. CNT with a metallic content starting from 10% to 50% were tested with three different models: the linear parallel connection model, the Beer-Lambert law models (conductivity of transparency), and thin metallic film models.

Carbon nanotubes with metallic contents of more than 20% thin metallic film models could fit better compared to the other models. However, for carbon nanotubes with less than 10% metallic content, the conductivity of transparencies model would fit better. This implies that a 20% metallic content is enough to make the carbon nanotube bundles behave like metallic films.

Further study of carbon nanotube mixtures suggested that the properties of CNT mixture depend on the proportion of its individual components similar to the rule of mixture of metallic materials. Thus, this study suggested that the junction resistance between metallic and semiconducting nanotubes is no longer important in the assembly of CNT bundles. Films fabricated from carbon nanotube bundles with more than 20% metallic content will behave exactly like metallic materials. Only the intrinsic conductivity of carbon nanotube bundles will affect its film conductivity.

8.1.3 Doping of Carbon Nanotube Thin Films

The most significant scientific contribution of this work in this chapter is the new doping method that has been proposed together with a new dopants species. The mechanism of acid post treatment is revealed. There are many arguments proposed for this process. Some suggested that it is a surfactant removal process and others suggested a chemical functionalization. Our results indicated that neither of the proposed arguments is correct. The fact that acid treatment on surfactant free film shows an enhancement in electrical conductivity eliminates the first argument. The other fact is that the post treatment effect was easily reversed by immersion in water or a basic solution, suggesting that chemical functionalization does not occur in acid treatment.

Acid protonation is indeed the real mechanism in acid treatment. It is concentration and time dependent. In order to optimize the doping effect, a dopant with high redox potential was needed. Piranha was chosen as the best dopant due to its high redox potential. Piranha doping could further enhance film conductivity that has been treated previously by nitric acid or sulfuric acid.

8.1.4 Application of Carbon Nanotube Thin Films in Solar Cells and Transistors

After the successful fabrication of CNT transparent conductive films, the next step was to incorporate these films into devices. CNT films were used to replace the electrodes of DSSCs and bottom gated transistors. The devices with carbon nanotube electrodes have been shown to work perfectly. The performance of dye-sensitized solar cells fabricated with carbon nanotube electrodes is similar to Platinum coated FTO counter electrodes at low light intensities, but its efficiency drops at higher light intensities.

The performance of bottom gated transistors with carbon nanotube electrodes is still inferior compared to those using gold electrodes, perhaps due to its lower conductivity. All carbon nanotube transistors can easily be scaled up by inject-printing technology.

8.2 Outlook

Since the film fabrication process has been optimized, further research needs to be done on the carbon nanotube synthesis. From this work, we understand that the feedstock quality of carbon nanotubes is important to achieve high electrical conductivity. Minimizing defects and impurities would be a good direction to take to further improve carbon nanotube conductivity. Having an even larger diameter (around 1.8 nm and above), carbon nanotubes are also another alternative to further improve film conductivity. Fine-tuning of carbon nanotube fabrication and purification to achieve lower defects concentration, larger diameter, and higher

yield would be the next direction with which to push carbon nanotube film conductivity higher.

Apart from the CNT components, there is a lot of room for improvement in device integration. The integration of carbon nanotube films into several devices still faces several problems that need to be solved. The decline in fill factors at high light intensities in CNT based dye sensitized solar cells still puzzles many researchers. The efficiencies of CNT based dye sensitized solar cells still need to be improved.

The performance of all carbon nanotube transistors is also still inferior compared to carbon nanotube transistors with metal electrodes. A complete series of study needs to be carried out on the key parameters on transistor electrodes that could improve transistor performance. Finally, a printing technique could be established for the large-scale fabrication of carbon nanotube transistors.

References

1 G. Kawachi, E. Kimura, Y. Wakui, H. Yamamoto, Y. Matsukawa, A. Sasano, A Novel Technology for a-Si TFT-LCD;s with Buried ITO Electrode Structure, IEEE Trans. Electron Devices, 41, 1120-4 (1994)

2 C.-H. Moon, , The Effect of ITO Structure on the Luminous Characteristic of Plasma Display Panel, IEEE Trans. Plasma Sci., 38, 2445-50 (2010)

3 J. H. Lee, Characteristics of ITO Thin Films for the Plasma Display Panel Prepared by a MF Dual Magnetron Sputtering in the Oxygen Atmosphere, Mol. Cryst. Liq. Cryst., 499, 178-84 (2009)

4 Y. J. Lee, J. H. Kim, J. N. Jang, I. H. Yang, S. N. Kwon, M. P. Hong, D. C. Kim, K. S. Oh, S. J. Yoo, B. J. Lee and W. G. Jang, Development of Inverted OLED with top ITO Anode by Plasma Damage-Free Sputtering, Thin Solid Films, 517, 4019-4022 (2008)

5 K. Noda, K. Tanimura, Production of Transparent Conductive Films with Inserted SiO2 Anchor Layer and Application to Resistive Touch Panel, Electron. Commun. Jpn. 2, Electron. , 84, 39-45 (2001)

6 M. Zhu, C. Xiong, and Q. Lee, Research on ITO Transparent Electromagnetic Shielding Coatings for E-O System, Proceedings of the SPIE – The International Society for Optical Engineering, 6722, 67223Y-1-7 (2007).

7 S. Y. Lien, Characterization and Optimization of ITO Thin Films for Application in Heterojunction Silicon Solar Cells, Thin Solid Films, 518, S10-13.

8 A. Tolcin, 2006 Minerals Yearbook "Indium", U.S. Department of the Interior, U.S. Geological Survey, p. 35.1 (2008).

9 R. Miles, G. Zoppi, L. Forbes, Materials today **10**, 20 (2007).

10 T. Hamaguchi, K. Omae, T. Takebayashi, Y. Kikuchi, N. Yoshioka, Y. Nishiwaki, A.Tanaka, M. Hirata, O. Taguchi, T. Chonan, Occup. Environ. Med. **65**, 51 (2008).

11 T. Minami, MRS Bull. **25** , 38 (2000).

12 T. Minami, Semicond. Sci. Technol. **20** , S35 (2005).

13 T. Minami, Thin Solid Films **516,** 1314 (2008).

14 T. Minami, Thin Solid Films **516,** 5822 (2008).

15 R. A. J. Jansen, J. C. Hummelen, and N.S. Sariciftci, MRS Bull. **30**, 33 (2005)

16 L. S. Schadler, S.C. Giannaris and P.M. Ajayan, Appl. Phys.Lett. **73**, 3842 (1998).

17 M. W. Rowell, M. A. Topinka, H. J. Prall, G. Dennler, L. Hu, G. Gruner and M. D. McGehee, Appl. Phys. Lett. **88**, 233506 (2006).

18 J. M. Zhou, "Indium Tin Oxide (ITO) Deposition, Patterning and Schottky Contact Fabrication", Master Thesis, Rochester Institute of Technology, December 2005.

19 L. Gupta, A. Mansingh and P.K. Srivastava, Thin Solid Films **176**, 33 (1989).

20 S. A. Bashar, "Study of Indium Tin Oxide (ITO) for Novel Optoelectonic Devices", Ph. D. Thesis, 1997.

21 S. H. Brewer and S. Franzen, J. Phys. Chem. B **106**, 12986 (2002).

22 S. H. Brewer and S. Franzen, Chem. Phys. **300**, 285 (2004).

23 A. Salehi, Thin Solid Films **324**, 214 (1998).

24 K. R. Zhang, F. R. Zhu, C. H. A. Huan and A. T. S. Wee, J. Appl. Phys. **86**, 974 (1999).

25 K. R. Zhang, F. R.Zhu, C. H. A. Huan, A. T. S. Wee and T. Osipowicz, Surf. and Interface Anal. **28**, 271 (1999).

26 J. K. Sheu, Y. K. Su, G. C. Chi, M. J. Jou and C. M. Chang, Appl. Phys. Lett. **72**, 3317 (1999).

27 S. Major and K. L. Chopra, Solar Energy Materials and Solar Cells **17**, 319 (1988).

28 J. Hu and R. G. Gordon, Journal of Applied Physics **72**, 5381 (1992).

29 Y. Takahashi, S. Okada, R. B. H. Tahar, K. Nakano, T. Ban and Y. Ohya, J. Non-Cryst. Solids **218**, 129 (1997).

30 K. Nishio, T. Sei and T. Tsuchiya, J. Mater. Sci. **31**, 1761 (1996).

31 H. S. Kwok, X. W. Sun and D. H. Kim, Thin Solid Films **335**, 299 (1998).
32 H. Kim, A. Pique´, J. S. Horwitz, H. Mattoussi, H. Murata, Z. H. Kafafi and D. B. Chrisey, Appl. Phys. Lett. **74**, 3444 (1999).
33 C. May and J. Stru¨mpfel, Thin Solid Films **351**, 48 (1999).
34 S. Honda, M. Watamori and K. Oura, Thin Solid Films **281**, 206 (1996).
35 T. Minami, Thin Solid Films **517**, 1474 (2008).
36 T. Minami, S. Ida, T. Miyata, Thin Solid Films **416**, 92 (2002).
37 T. Miyata, Y. Honma, T. Minami, J. Vac. Sci. Technol.A **25**, 1193 (2007).
38 S. Shirakata, T. Sakemi, K. Awai, T. Yamamoto, Superlattices Microstruct. **39**, 218 (2006).
39 J. Uramoto, Res. Rep. Inst. Plasma Phys. IPP **406** (1979).
40 T. Minami, T. Miyata, Y. Ohtani, T. Kuboi, Phys. Stat. Sol. (RRL) **1**, R31 (2007).
41 T. Minami, T. Kuboi, T. Miyata, Y. Ohtani, Phys. Stat. Sol., **A 205**, 255 (2007).
42 T. Miyata, Y. Ohtani, T. Kuboi, T. Minami, Thin Solid Films **516**, 1354 (2008).
43 C. N. Hoth, S. A. Choulis, P. Schilinsky, C. J. Brabec, Adv. Mater. **19**, 3973 (2007).
44 F. C. Krebs, J. Alstrup, H. Spanggaard, K. Larsen, E. Kold, Sol. Energy Mater. Sol. Cells **83**, 293 (2004).
45 S. S. Kim, S. I. Na, J. Jo, G. Tae, D. Y. Kim, Adv. Mater. **19**, 4410 (2007).
46 J. S. Huang, P. F. Miller, J. S. Wilson, A. J. de Mello, J. C. de Mello, D. D. C. Bradley, Adv. Funct. Mater. **15**, 290 (2005).
47 B. L. Groenendaal, F. Jonas, D. Freitag, H. Pielartzik, J.R. Reynolds, Adv. Mater. **12**, 481 (2000).
48 L. A. A. Pettersson, S. Ghosh, O. Inganäs, Org. Electron. **3**, 143 (2002).
49 F. Zhang, M. Johansson, M. R. Andersson, J. C. Hummelen, O. Inganäs, Adv. Mater. **14**, 662 (2002).
50 W.H. Kim, A.J. Makinen, N. Nikolov, R. Shashidhar, H. Kim, Z.H. Kafafi, Appl. Phys. Lett. **80**, 3844 (2002).
51 J.Y. Kim, J.H. Jung, D.E. Lee, J. Joo, Synth. Met. **126**, 311 (2002).
52 S.K.M. Jönsson, J. Birgerson, X. Grispin, G. Greczynski, W. Osikowicz, A.W.D. van der Gon, W.R. Salaneck, M. Fahlman, Synth. Met. **139** , 1 (2003).
53 J. Quyang, C.W. Chu, F. C. Chen, Q. Xu, Y. Yang, Adv. Funct. Mater. **15**, 203 (2005).
54 E. Ahlswede, W. Mühleisen, M.W. bin Moh Wahi, J. Hanisch, M. Powalla, Appl. Phys. Lett. **92**, 1433307 (2008).
55 Y. M. Chang, L. Wang and W. F. Su, Org. Electron. **9**, 968 (2008).
56 A. Oberlin, M. Endo and T. Koyama, J. Cryst. Growth, 32, 335 (1976).
57 S. Iijima, Nature, 354, 56-58 (1991).
58 S. Iijima, Mater. Sci. Eng. B, 19, 172-178 (1993).
59 S. Iijima, P. M. Ajayan, T. Ichihashi, Phys. Rev. Lett., 69, 3100-3 (1992).
60 J. E. Fischer, *Nanomaterials Handbook*, Taylor & Francis Group, LLC (2006).
61 R. Saito, M. S. Dresselhaus, G. Dresselhaus, A. Jorio, A. G. Souza Filho and M. A. Pimenta, *Encyclopedia of Nanoscience and Nanotechnology*, Marcel Dekker, Inc. (2004).
62 M. S. Fuhrer, J. Nygard, L. Shih, M. Forero, Y.-G. Yoon, M. S. C. Mazzoni, H. J. Choi, J. Ihm, S. G. Louie, A. Zettl, P. L. McEuen, Science **288**, 494 (2000).
63 M. Kaempgen, G. S. Duesberg and S. Roth, Applied Surface Science **252**, 425 (2005).
64 Z. Li, H. R. Kandel, E. Dervishi, V. Saini, Y. Xu, A. R. Biris, D. Lupu, G. J. Salamo and A. S. Biris, Langmuir **24**, 2655 (2008).
65 Y. I. Song, C.-M. Yang, D. Y. Kim, H. Kanoh and K. Kaneko, J. Col. Int. Sci. **318**, 365 (2008).
66 J. L. Bahr, E. T. Mickelson, M. J. Bronikowski, R. E. Smalley and J. M. Tour, Chemical Communications **2**, 193 (2001).
67 K. Ghosh, "Electronic Band Structure of Carbon Nanotubes", 2005, Project work, Stanford University.

68 J. H. Yim, Y. S. Kim, K. H. Koh and S. Lee, J. Vac. Sci. Technol. B **26**, 2 (2008).
69 Y. Zhou, L. Hu and G. Gruner, App. Phys. Lett **88**, 123109 (2006).
70 N. Saran, K. Parikh, D.-S. Suh, E. Munoz, H. Kolla and S. K. Manohar, J. Am. Chem. Soc. **126**, 4462 (2004).
71 H. Z. Geng, K. K. Kim, K. P. So, Y. S. Lee, Y. K. Chang and Y. H. Lee, J. Am. Chem. Soc. **129**, 7758 (2007).
72 M. H. A. Ng, L. T. Hartadi, H. W. Tan and C. H. P. Poa, Nanotechnology **19**, 205703 (2008).
73 M. D. Lima, M. J. De Andrade, C. P. Bergmann and S. Roth, J. Mater. Chem. **18**, 776 (2008).
74 M. J. De Andrade, M. D. Lima, V. Skákalová, C. P. Bergmann and S. Roth, Phys. Stat. Sol. (RRL) **1**, 178 (2007).
75 D. H. Zhang, K. M. Ryu, X. L. Liu, E. Polikarpov, J. Ly, M. E. Tompson and C. W. Zhou, Nano Letters **6,** 1880 (2006).
76 R. Ulbricht, S. B. Lee, X. Jiang, K. Inoue, M. Zhang, S. Fang, R. H. Baughman, A. A. Zakhidov, Sol. Energ. Mat. Sol. C. **91**, 416 (2007).
77 M. Kaempgen and S. Roth, AIP Proc. **CP685**, 554 (2003)
78 Z. C. Wu, Z. Chen, X. Du, J. M. Logan, J. Sippel, M. Nikolou, K. Kamaras, J. R. Reynolds, D. B. Tanner, A. F., Hebard and A. G. Rinzler, Science **305**, 1273 (2004)
79 N. Ferrer-Anglada, M. Kaempgen, V. Skakalova, U. Dettlaf-Weglikowska and S. Roth, Diamond Relat. Mater. **13**, 256 (2004).
80 CERAC, inc. – ITO, Indium Tin Oxide for Optical Coatings, accessed on 5th March 2010, from http://www.cerac.com/pubs/proddata/ito.htm
81 S. B. Yang, B. S. Kong, J. Geng and H. T. Jung, J. Phys. Chem. C **113**, 13658 (2009).
82 B. B. Parekh, G. Fanchini, G. Eda and M. Chhowalla, Appl. Phys. Lett. **90**, 121913 (2007).
83 S. B. Yang, B. S. Kong, D. W. Kim, Y. K. Baek and H. T. Jung, J. Phys. Chem. C **114**, 9296 (2010).
84 K. K. Kim, J. J. Bae, H. K. Park, S. M. Kim, H. Z. Geng, K. A. Park, H. J. Shin , S. M. Yoon, A. Benayad, J. Y. Choi and Y. H. Lee, J. Am. Chem. Soc. **130** , 12757 (2008).
85 Y. Miyata, K. Yanagi, Y. Maniwa and H. Kataura, J. Phys. Chem. C **112**, 3591 (2008).
86 A. Green and M. C. Hersam, Nano Lett. 8, 1417 (2008).
87 J. L. Blackburn, T. M. Barnes, M. C. Beard, Y.-H. Kim, R. C. Tenent, T. J. McDonald, B. To, T. J. Coutts and M. J. Heben, ACS Nano **2**, 1266 (2008).
88 A. Green and M. C. Hersam, Nature Nanotechnology **4**, 64 (2008).
89 A. Du Pasquier, H. E. Unalan, A. Kanwal, S. Miller and M. Chhowalla, Applied Physics Letters **87**, 203511 (2005).
90 S. D Bergin, Z. Sun, D. Rickard, P. V. Streich, J. P. Hamilton and J. N. Coleman, ACS Nano, 3, 2340-2350 (2009).
91 J. Wang and W. J. Blau, J. Phys. Chem. C, 112, 2298-303 (2010).
92 M. Monajjemi, M. Khaleghian, N. Tadayonpour, F. Mollaamin, Int. J. Nanosci., 9, 517-29 (2010).
93 D. MacKernan and W. J. Blau, Europhys. Lett., 83, 66009 (2008).
94 B. Krause, G. Petzold, S. Pegel and P. Potschke, Carbon, 47, 602-612 (2009).
95 T. J. McDonald, J. L. Blackburn, W. K. Metzger, G. Rumbles and M. J. Heben, J. Phys. Chem. C, 111, 17894-17900 (2007).
96 J. Loos, J. Yi, N. Grossiord, C. E. Koning, Carbon, 45, 618-623 (2007).
97 H. A. Becerril, J. Mao, Z. Liu, R. M. Stoltenberg, Z. Bao and Y. Chen, ACS Nano **2**, 463 (2008).
98 S. M. Bachilo, M.S. Strano, C. Kittrell, R.H. Hauge, R. E. Smalley, R.B. Weisman, Sciencexpress **298**, 2361 (2002).
99 J. Wei, B. Jiang, D. Wu and B. Wei, J. Phys. Chem. B **108**, 8844 (2004).

100 C. Richard, F. Balavoine, P. Schultz, T. W. Ebbesen and C. Mioskowski, Science **300**, 775 (2003).

101 O. Matarreadona, H. Rhoads, Z. R. Li, J. H. Harwell, L. Balzano and D. E. Resasco, J. Phys. Chem B **107**, 13357 (2003).

102 S. Eigler, Carbon **47**, 2936 (2009).

103 L. Hu, D. S. Hecht and G. Gruner, Nano Lett. **4**, 2513 (2004).

104 R. Graupner, J. Abraham, A. Vencelova, T. Seyller, F. Hennrich, M. M. Kappes et al. Phys. Chem. Chem. Phys. **5**, 5472 (2003).

105 S. Osswald, E. Flahaut and Y. Gogotsi, Chem. Mater. **18**, 1525 (2006)

106 C. Wang, G. Zhou, J. Wu, B. L. Gu, W. Duan, Appl Phys Lett. **89**,1731301 (2006).

107 H. Tantang ,J.Y. Ong, C. L. Loh, X. Dong, P. Chen, Y. Chen, X. Hu, L. P. Tan, L. J. Li, Carbon **47**, 1867 (2009**)**.

108 M. S. Strano, C. B. Huffman, C. V. Moore, M. J. O'Connell, E. H. Haroz, J. Hubbard, M. Miller, K. Rialon, C. Kittrell, S. Ramesh, R. H. Hauge, R. E. Smalley, J. Phys. Chem. B **107**, 6979 (2003).

109 W. Zhou, J. E. Fischer, P. A. Heiney, H. Fam, V.A Davis, M. Pasquali, R. E. Smalley, Phys. Rev. B **72**, 045440 (2005).

110 Y. Wang, C. Di, Y. Liu, H. Kajiura, S. Ye, L. Cao, Adv Mater **20**, 1 (2008).

111 Burghard M. Electronic and vibrational properties of chemically modified single-wall carbon nanotubes, Surf. Sci. Rep., **58**, 1–109 (2005).

112 Rakov EG, Chemistry of carbon nanotubes. In: Gogotsi Y, editor. Nanomaterials handbook, Boca Raton: Taylor & Francis; p. 105 (2006).

113 Y. Luo, D. Li, and Q. Meng, Adv. Mater. **21,** 1 (2009).

114 T. N. Murakami, S. Ito, Q. Wang, M. K. Nazeeruddin, T. Bessho, I. Cesar, P. Liska, R. H. Baker, P. Comte, P. Pechy and M. Gratzel, J. Electrochem. Soc. **153**, A2255 (2006).

115 Y. Chiba, A. Islam, Y. Watanabe, R. Komiya, N. Koide and L. Han, Jpn. J. Appl. Phys. **45**, L738 (2006).

116 K. Aitola, A. Kaskela, J. Halme, V. Ruiz, A. G. Nasibulin, E. I. Kauppinen and P. D. Lund, J. Electrochem. Soc. **157**, B1831 (2010).

117 M. Shiraishi, T. Takenobu, Y. Iwasa, T. Iwai, H. Kataura, and M. Ata, Fullerene Nanotube and Carbon Nanostruct. **13**, 485 (2005).

118 T. Takenobu, N. Miura, S.Y. Lu, H. Okimoto, T. Asano, M. Shiraishi and Y Iwasa, Appl. Phys. Express **2,** 025005 (2009).

119 M. Dressel and G. Gruner " Electrodynamics of solids : optical properties of electrons in mater" Cambridge University Press (2002)